

# **“Multidisciplinary approach to karstwater protection strategy”**

**UNESCO «Erdélyi Mihály» School of Advanced Hydrogeology, Eötvös Loránd University (ELTE)**

**Short Course, 22-27 August 2005, Budapest (Hungary)**

## **A brief introduction to modeling groundwater flow in karst aquifers**

**(or how to talk back to models and to modelers...)**

**Laszlo KIRALY**

**CHYN, University of Neuchâtel**

**E-mail: [Laszlo.Kiraly@unine.ch](mailto:Laszlo.Kiraly@unine.ch)**

## **Preliminary remarks**

**In this short introduction we will not have time to deal with many important technical details. The “absolute beginner” is advised to read the old, but excellent book of Wolfgang Kinzelbach: Groundwater Modelling (Elsevier 1986).**

**For the more interested persons I put a few papers and some PhD theses on an anonymous ftp site: <ftp://sitelftp.unine.ch/Kiraly/Papers> Missing references, figures, etc. will be put onto the same site. If you cannot download the files, ask your assistant for a CD-Rom.**

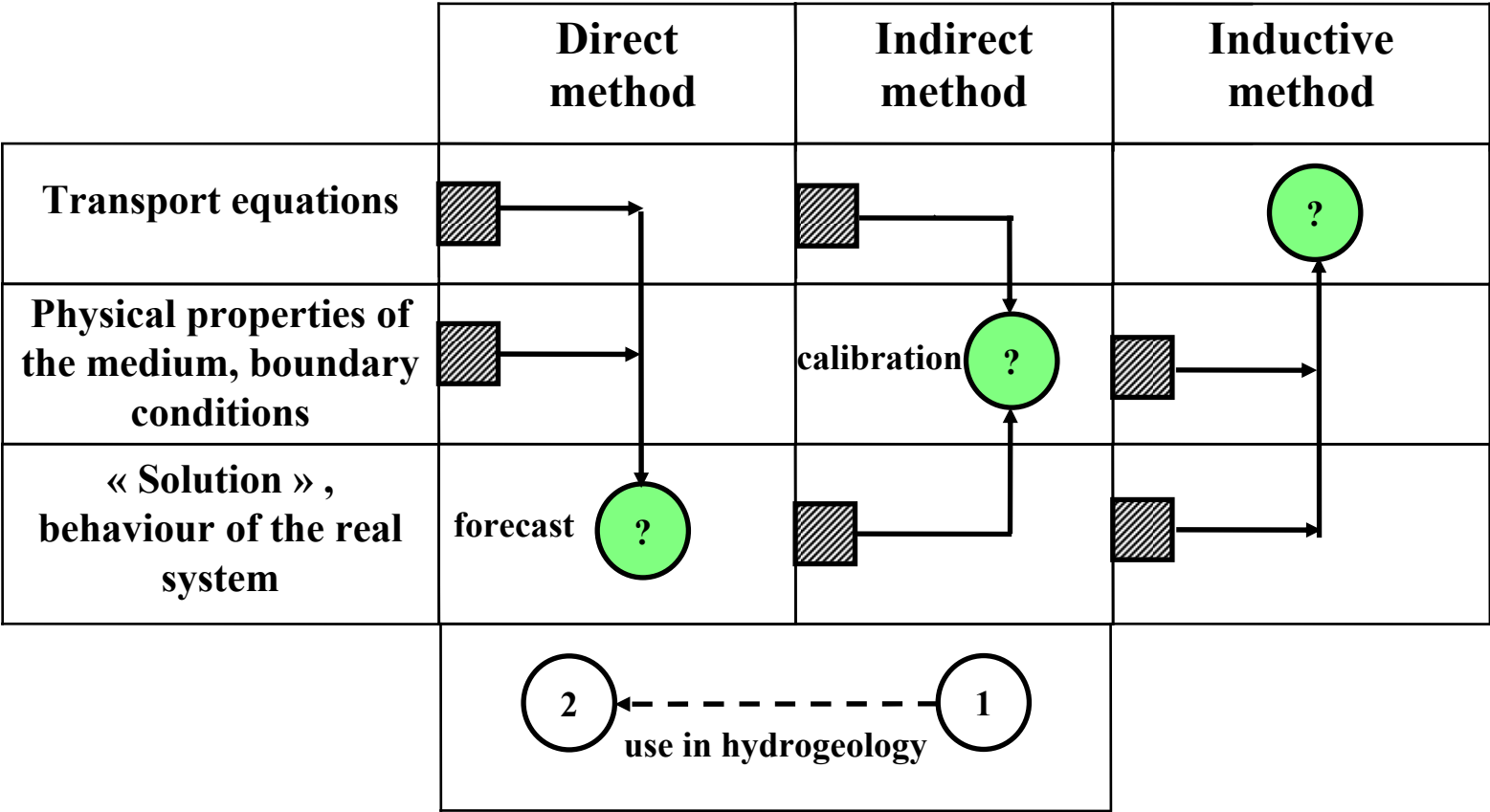
**Some interesting papers can be found on the speleogenesis website: <http://www.speleogenesis.info>**

**Use of hydrodynamic models from a pragmatic point of view**

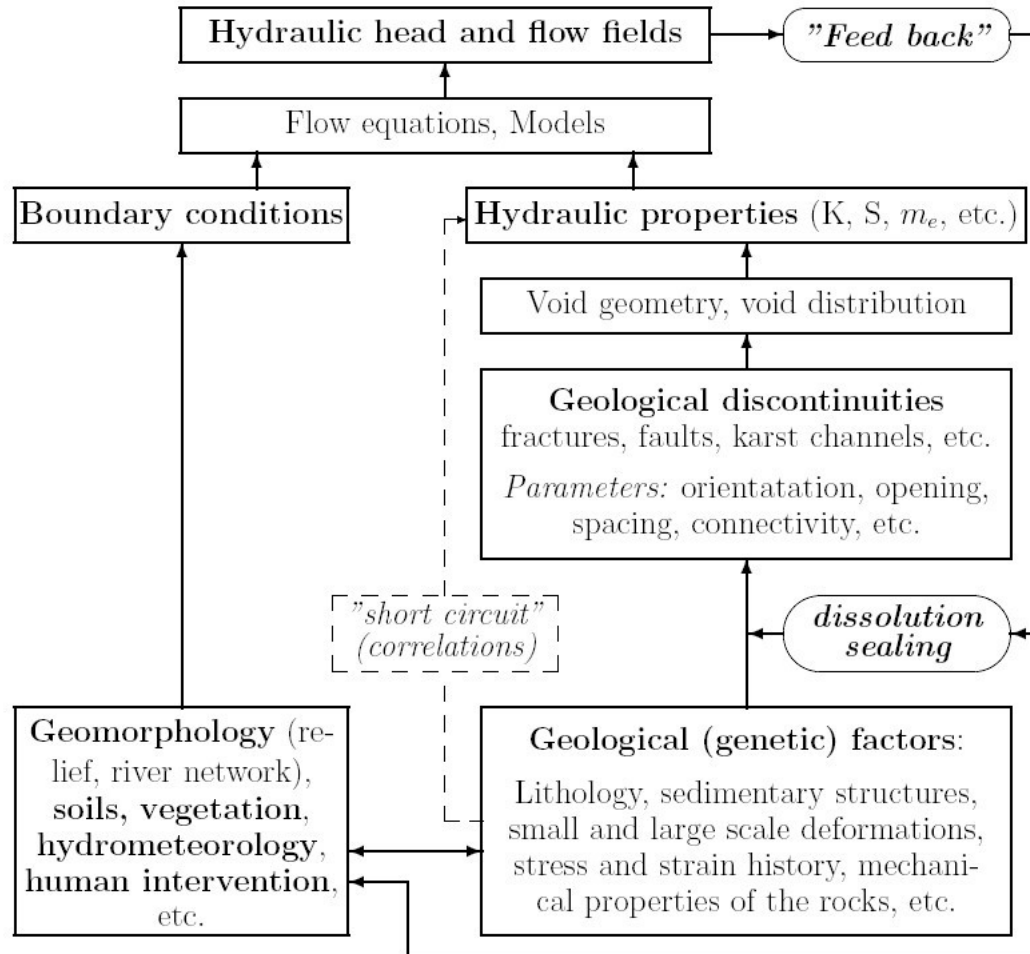
<b>« TEACHING »</b>	<b>COMMUNICATION OF THE KNOWLEDGE IN A SYNTHETIC, NON-VERBAL FORM; DEMONSTRATION OF THE CONSEQUENCES OF HYDRAULIC LAWS</b>
<b>« RESEARCH »</b>	<b>« UNDERSTANDING » THE BEHAVIOR OF HIGHLY HETEROGENEOUS AQUIFERS (KARST, FRACTURED ROCKS); CHECKING HYPOTHESES ON FLOW, TRANSPORT OR KARST GENETIC PROCESSES</b>
<b>« PRACTICE »</b>	<b>FORCASTING FLOW AND TRANSPORT UNDER NATURAL CONDITIONS AND UNDER HUMAN INTERVENTION; SOLVING GROUNDWATER MANAGEMENT PROBLEMS</b>

**« Karst models » are used mainly in teaching and research. Lack of information on the real karst channel network greatly hinders their use for real-world problems**

**Direct, indirect and inductive use of models (after Szűcs E. 1971)**

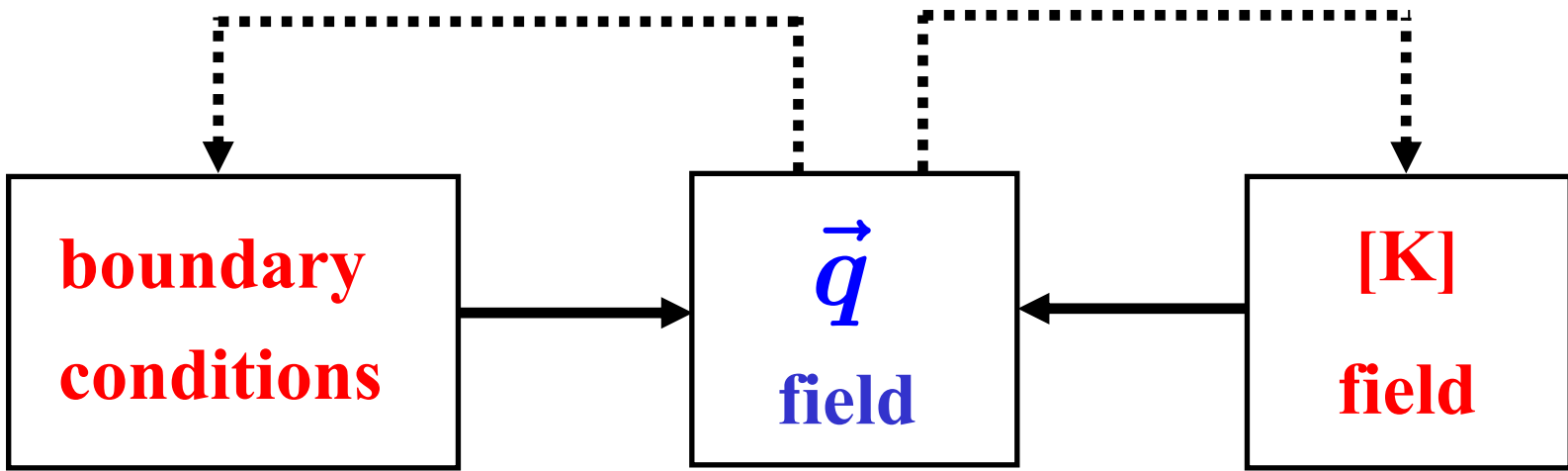


 = information given     
  = result sought for



**Karst aquifer as a partly self-organizing system: feed-back of the flow field on the hydraulic parameter fields and the boundary conditions**

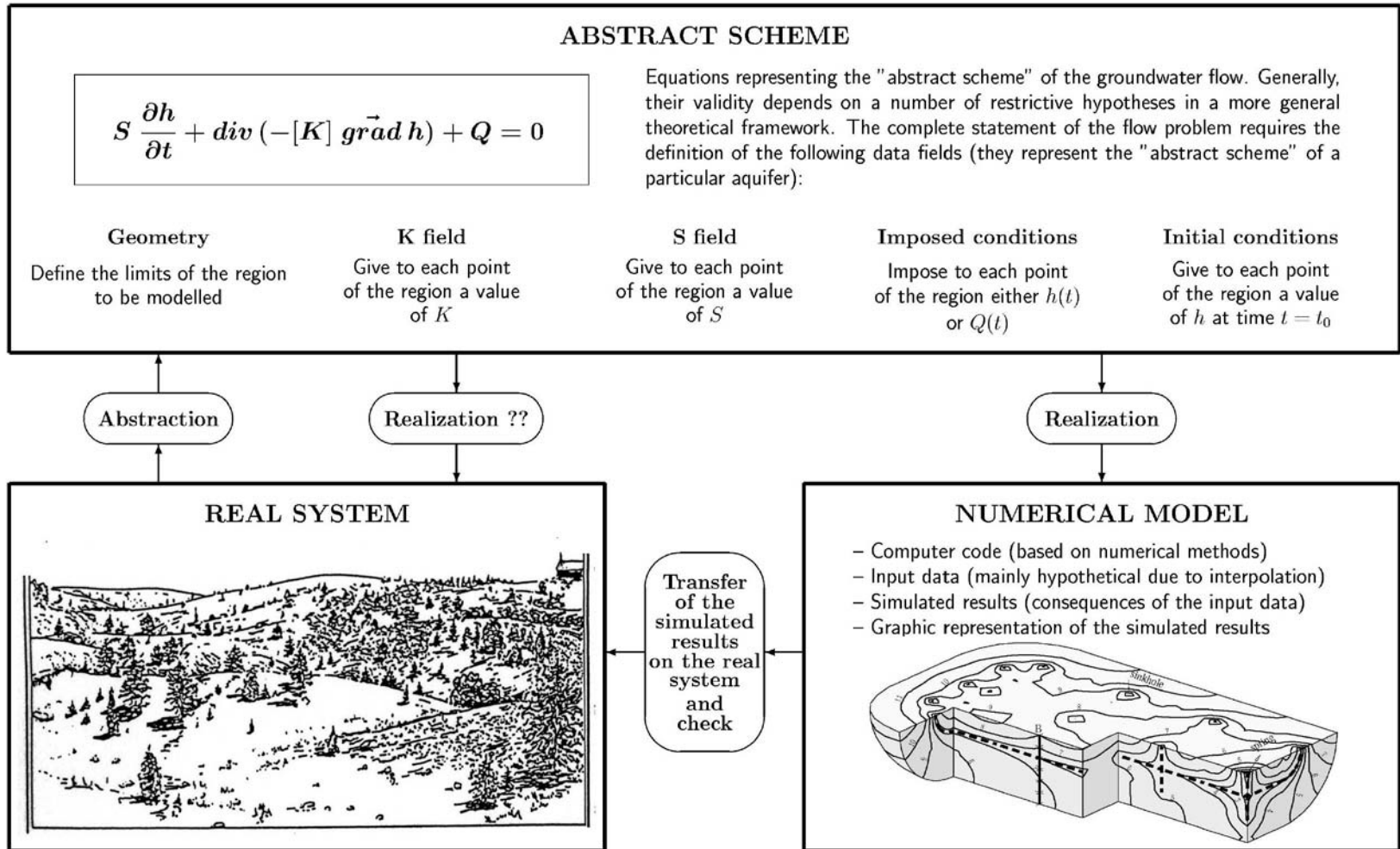
# « Selfregulation » in karst aquifers



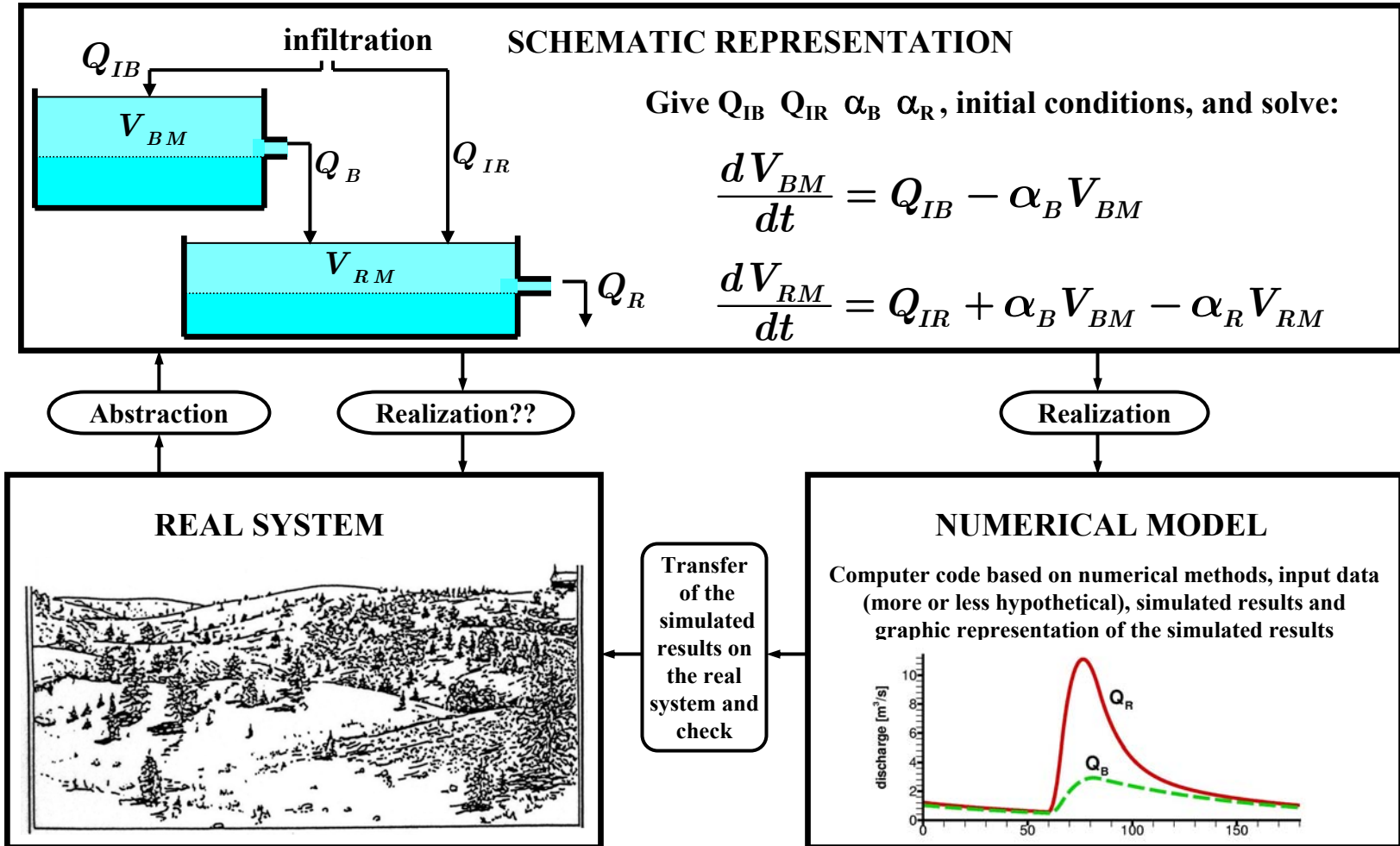
—————> Short-term effect

.....> Long-term effect

## Representation of the principal problems in modelling groundwater flow



## Representation of the principal problems in modeling groundwater flow



Depending on the problem to solve, **the same real system** may be **represented by very different schematic representations**

We are **free to invent** any inevitably hypothetical and schematic representation of the real system, which helps to solve a problem (this a question of **inspiration**)

But then we have to:

1. Deduce the **verifiable consequences** of the assumed hypotheses
2. Check the **consistency** of the schematic representation in a larger theoretical framework (do learn physics and some math!)
3. Check by **direct or indirect experimental methods** whether the real system may (or may not) be considered as a realization of the proposed scheme (do not forget the field work!)

(this requires **perspiration**)

## Transfer of the simulated results onto the real system

Strictly speaking, the simulated results are not "valid" but in the highly simplified numerical model. Their meaningful transfer onto the real system requires that simplifying assumptions and uncertainties on the data explicitly do appear as uncertainties on the results. This could help to avoid such ridiculous situations as trying to simulate observed piezometric heads to within a few centimeters, even though the simplified hydraulic conductivity field in the model "ignores" the strong local heterogeneities existing in the real system.

The transfer is possible if both the numerical model and the real system may be considered as being, to some extent and from a certain point of view, the realizations of the same schematic representation. The central role played by the schematic representation might seem surprising, but it is the only thing we really know, because we have created it.

**Modelling is not just curve fitting!!**

**FOR A GOOD MATHEMATICAL MODEL IT IS  
NOT ENOUGH TO WORK WELL**

**IT MUST WORK WELL FOR THE RIGHT  
REASONS!!**

(V. Klemes, 1986)

**What are the « right reasons » a model should respect when simulating flow  
and transport in karst aquifers?**

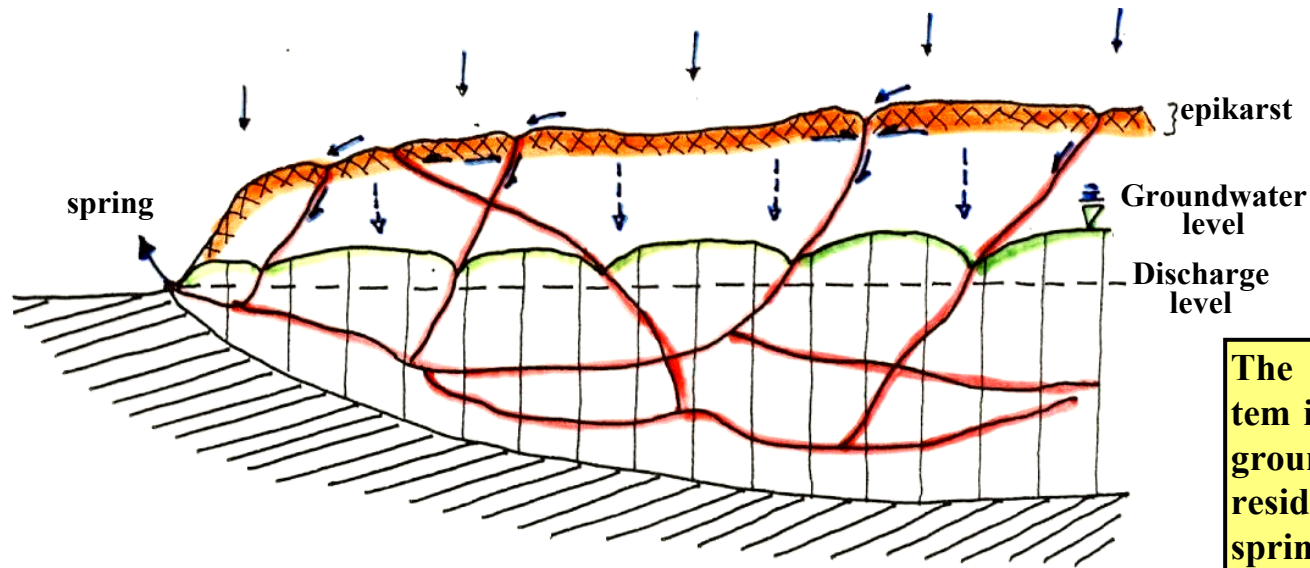
The **DUALITY** of karst (effect on permeability, infiltration, discharge)

The **NESTED STRUCTURE OF DISCONTINUITIES** with « meshes » of different order of magnitudes.

The **SCALE EFFECT** on the **HYDRAULIC CONDUCTIVITY**

The typical **KARSTIC HYDROGRAPHS** of karst springs

## « DUALITY » OF KARST



The behaviour of the whole system is determined by this duality: groundwater level, flow velocities, residence times, head distribution, spring hydrograph, chemistry, etc.

### PERMEABILITY

- 1 High permeability karstic network « immersed » in
- 2 Low permeability fractured rock volumes

### INFILTRATION

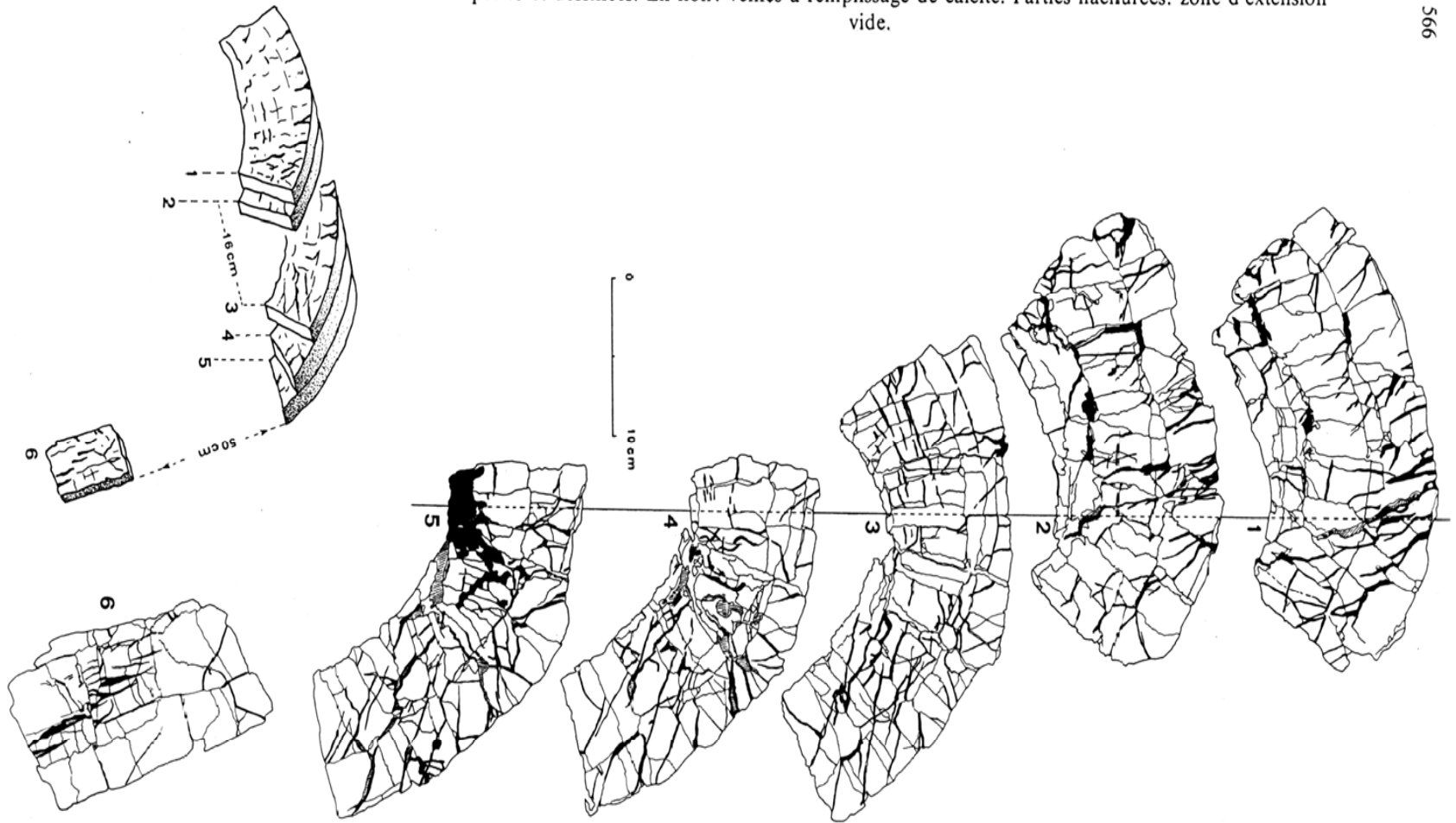
- 1 High intensity (« concentrated ») input into the karstic network (dolines, drainage in the epikarst zone)
- 2 Low intensity (« diffuse ») percolation through the low permeability fractured volumes

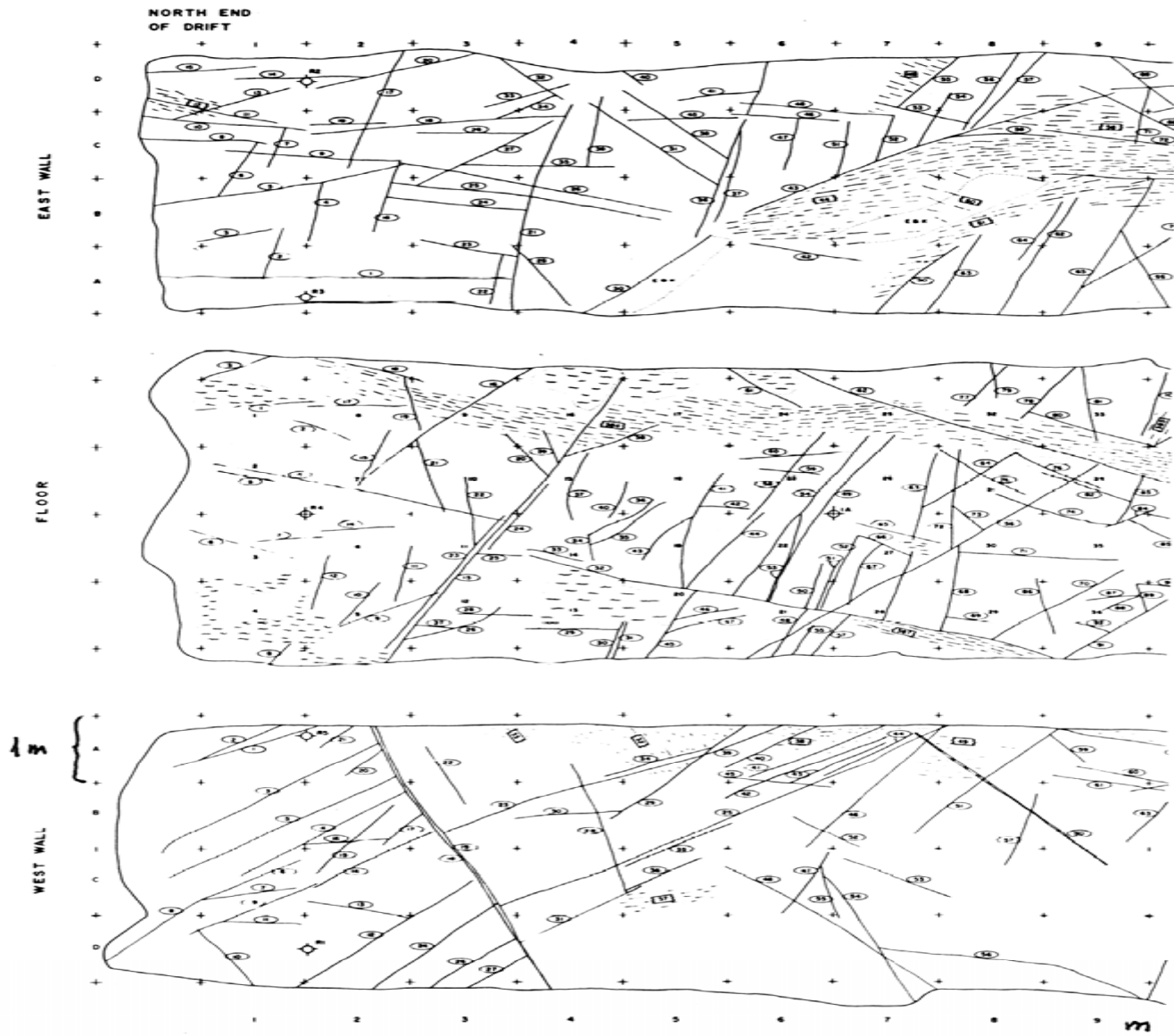
### DISCHARGE

- 1 « Concentrated » from the channel network at karst springs
- 2 « Diffuse » from the low permeability volumes

## Nested network of discontinuities of different magnitude

Fig. 13. Plis dans calcaire micritique de la base de l'Argovien, région «Vorpet» (coord. 544.975/212.780).  
Le pli d'entraînement a été scié en tranches de 2 à 3 cm d'épaisseur. Un certain nombre de surfaces furent polies et dessinées. En noir: veines à remplissage de calcite. Parties hachurées: zone d'extension vide.





XBL 833-8646

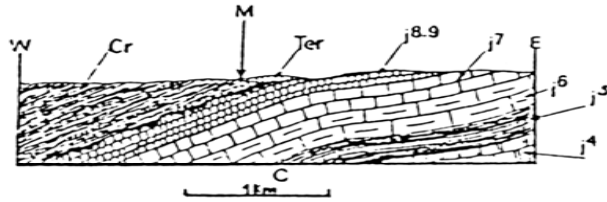
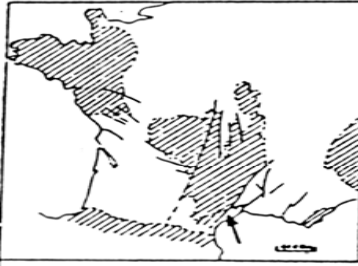
Fig. 2.1 Fracture map B - north end of drift

1/1500°



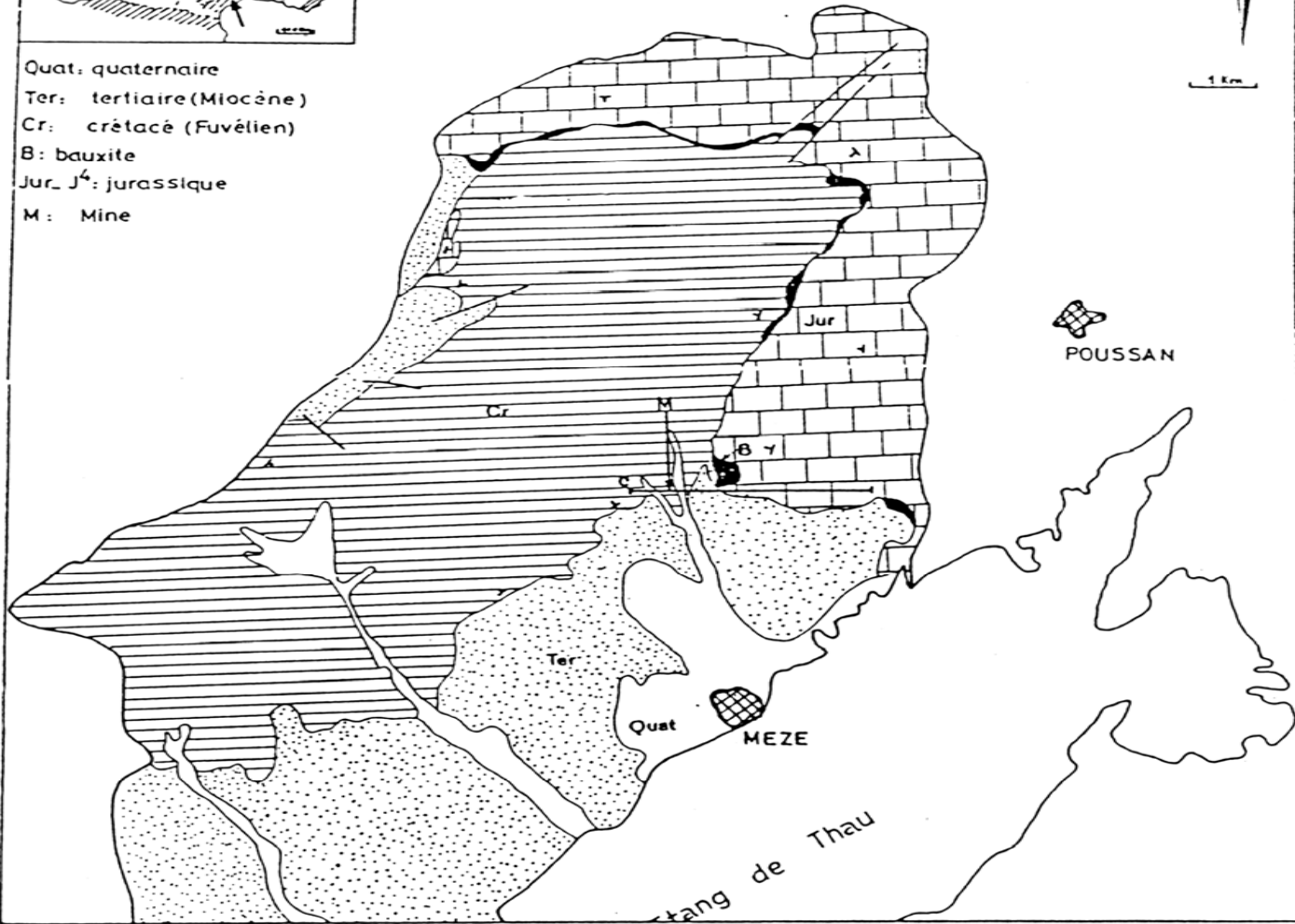


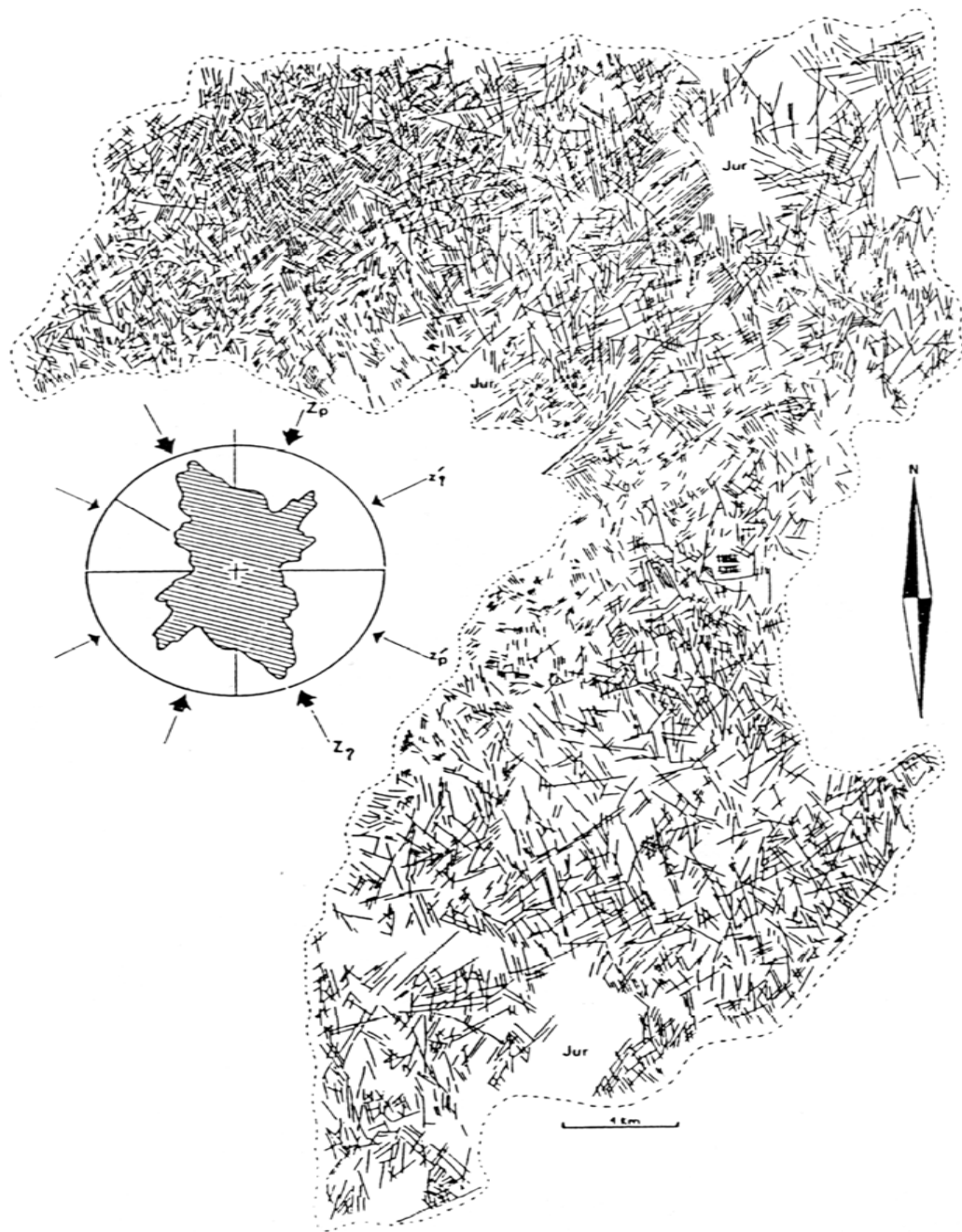
**FIGURE 6-2** Vertical aerial view showing joints in the flat-lying Cedar Mesa Sandstone (Permian) in Canyonlands National Park, Utah. The two sets of systematic joints intersect with an angle of  $70^\circ$  and crosscut each other without deflection. A rose diagram of the orientations of the systematic joints is shown. The nonsystematic joints do not crosscut the systematic joints, but abut them at a high angle, approaching  $90^\circ$ . The area of the photograph is about 500 m by 700 m. (Photograph by George E. McGill.)

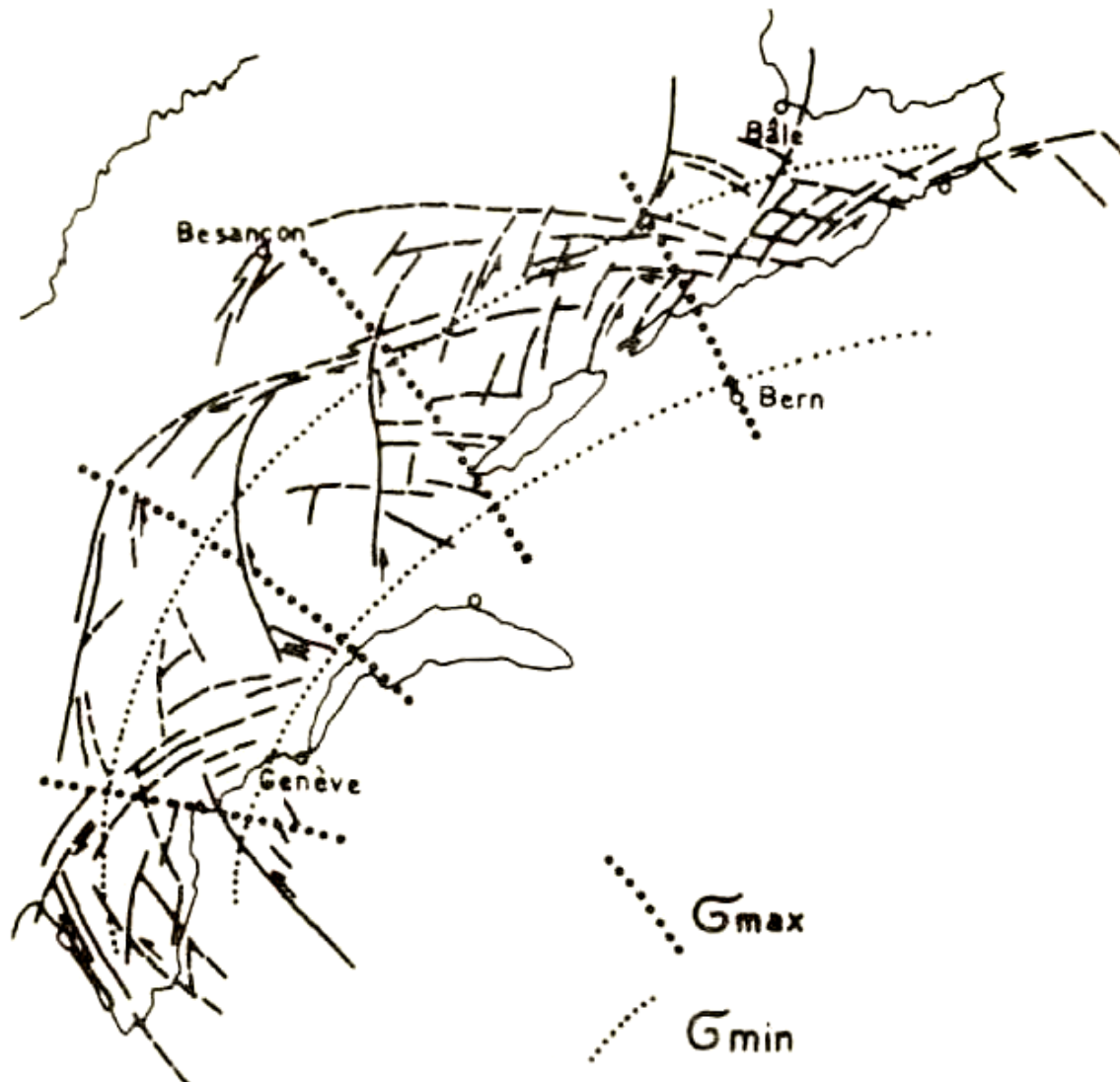


1 Km

Quat: quaternaire  
 Ter: tertiaire (Miocène)  
 Cr: crétacé (Fuvélien)  
 B: bauxite  
 Jur. J<sup>4</sup>: jurassique  
 M: Mine





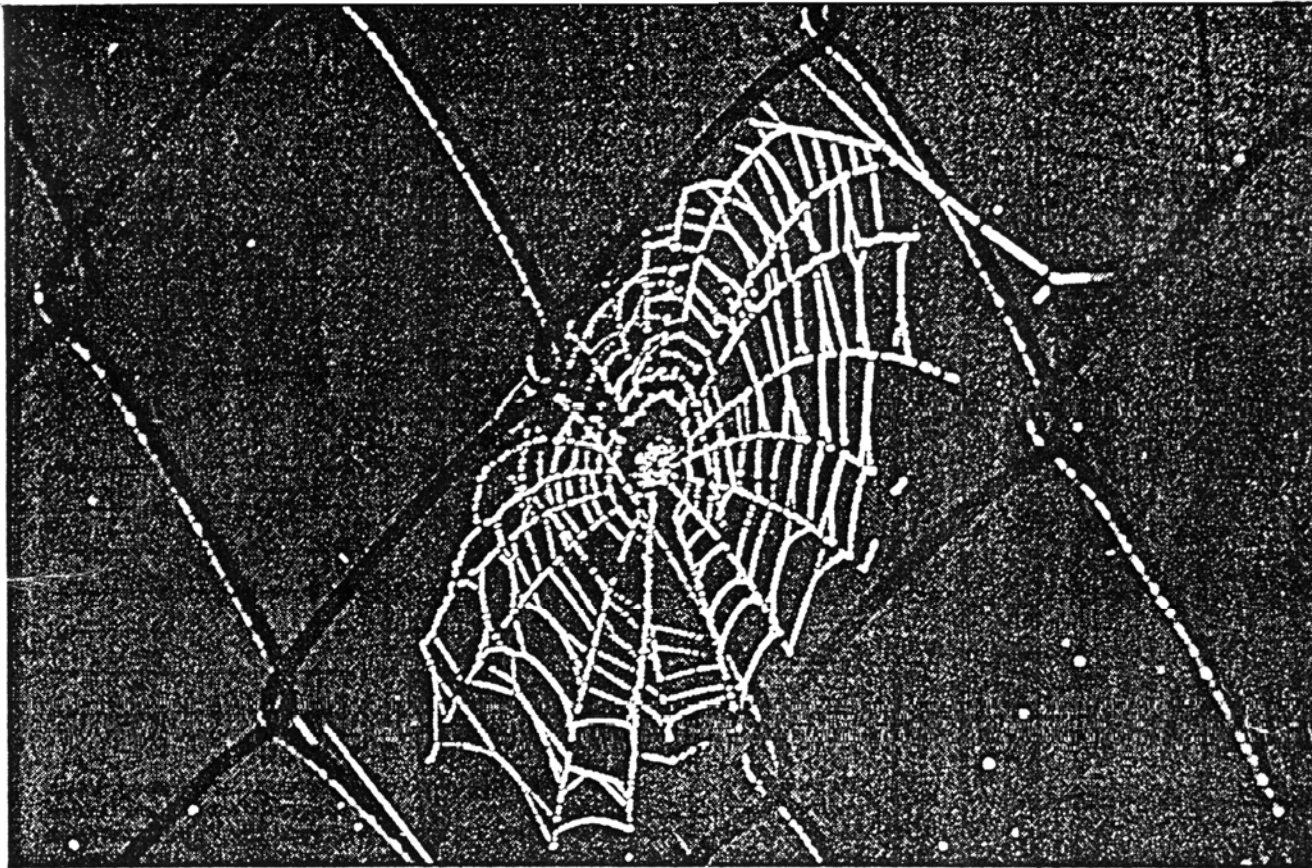


Trajectoires hypothétiques des contraintes principales dans le Jura d'après les grands cisaillements dextres et senestres. Plan de décrochements : d'après N. PAVONI, 1961.

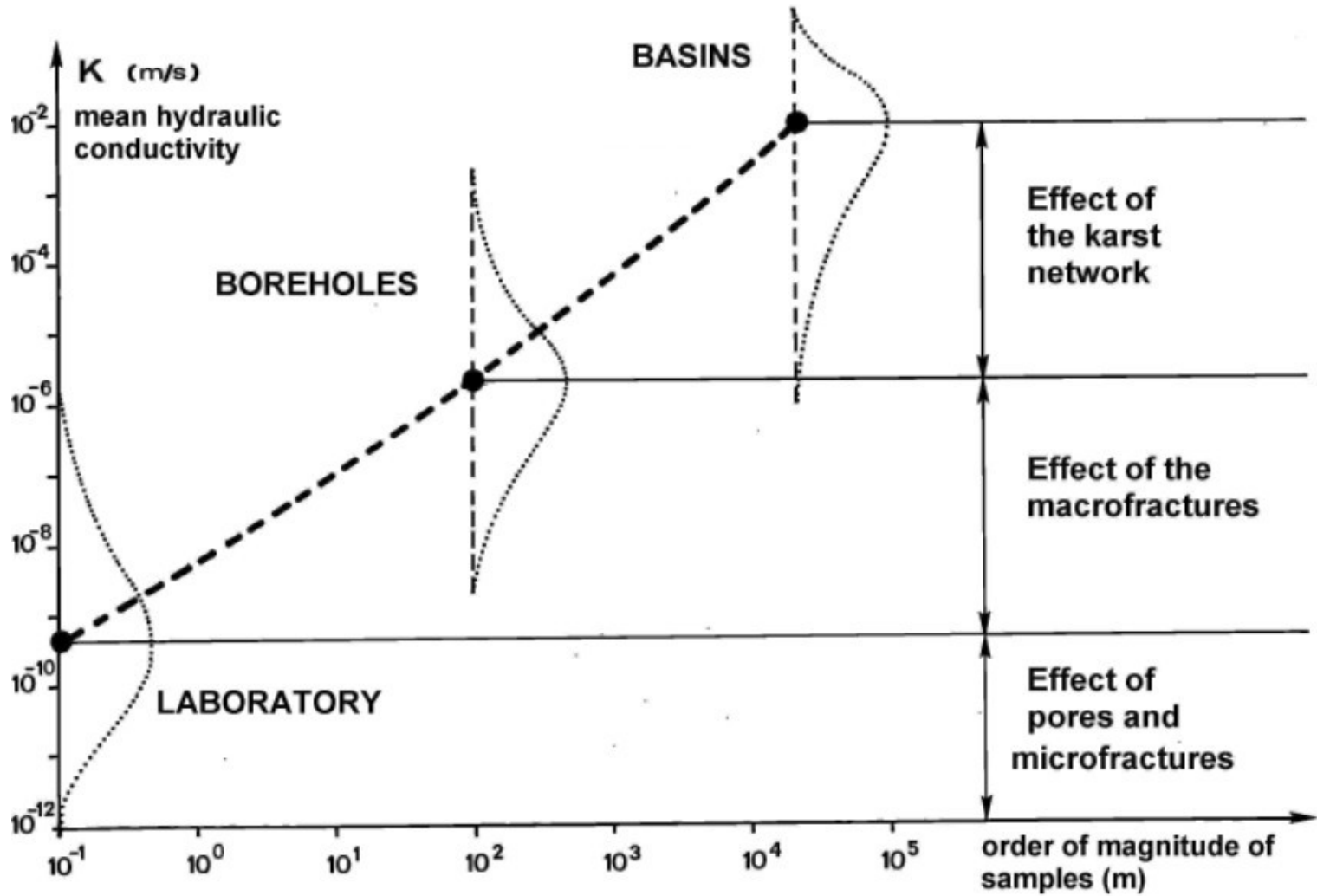
Nested network of discontinuities of different magnitude

*Récréation*

## Petites et grosses mailles

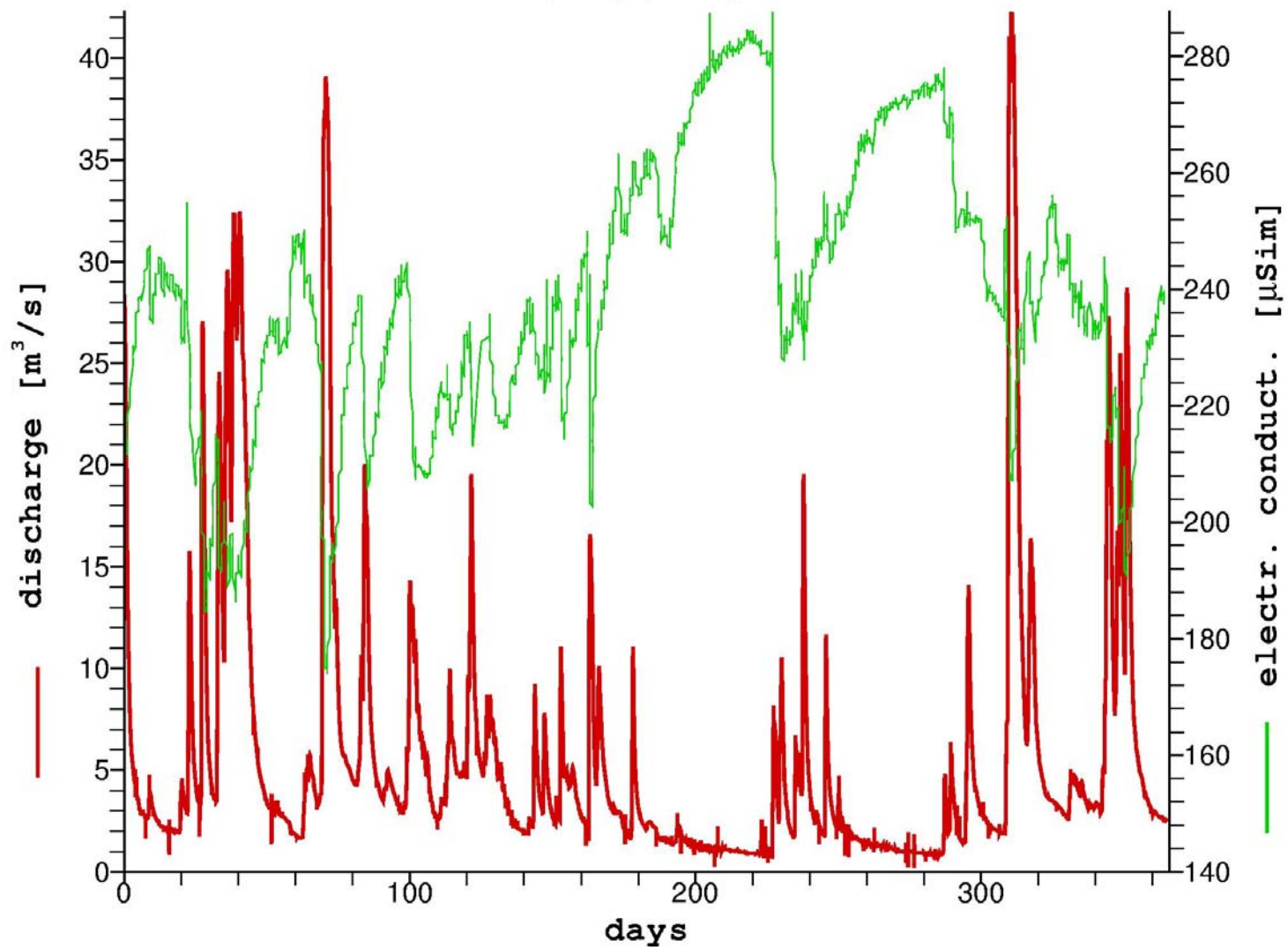


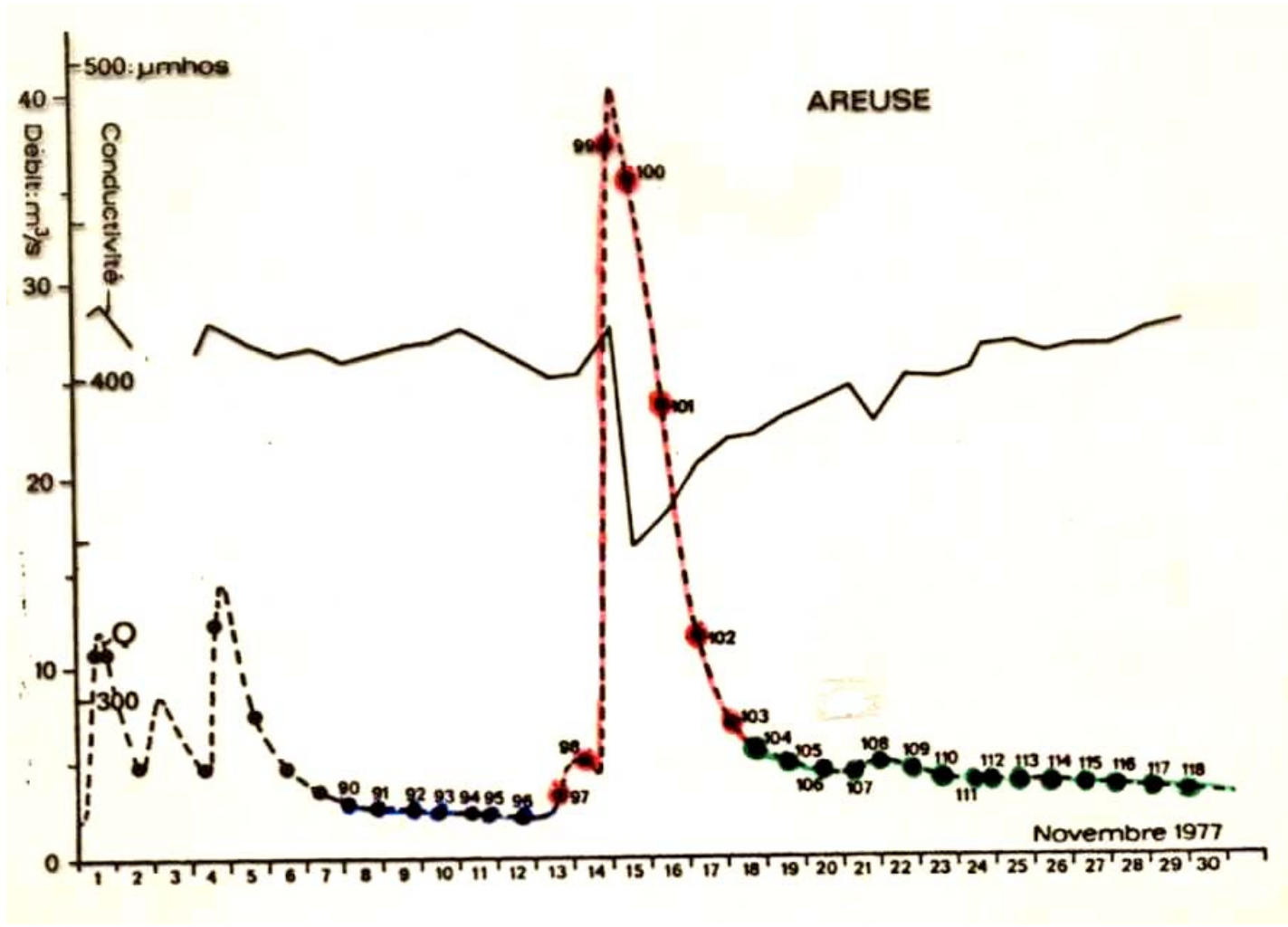
# Scale effect on the hydraulic conductivity

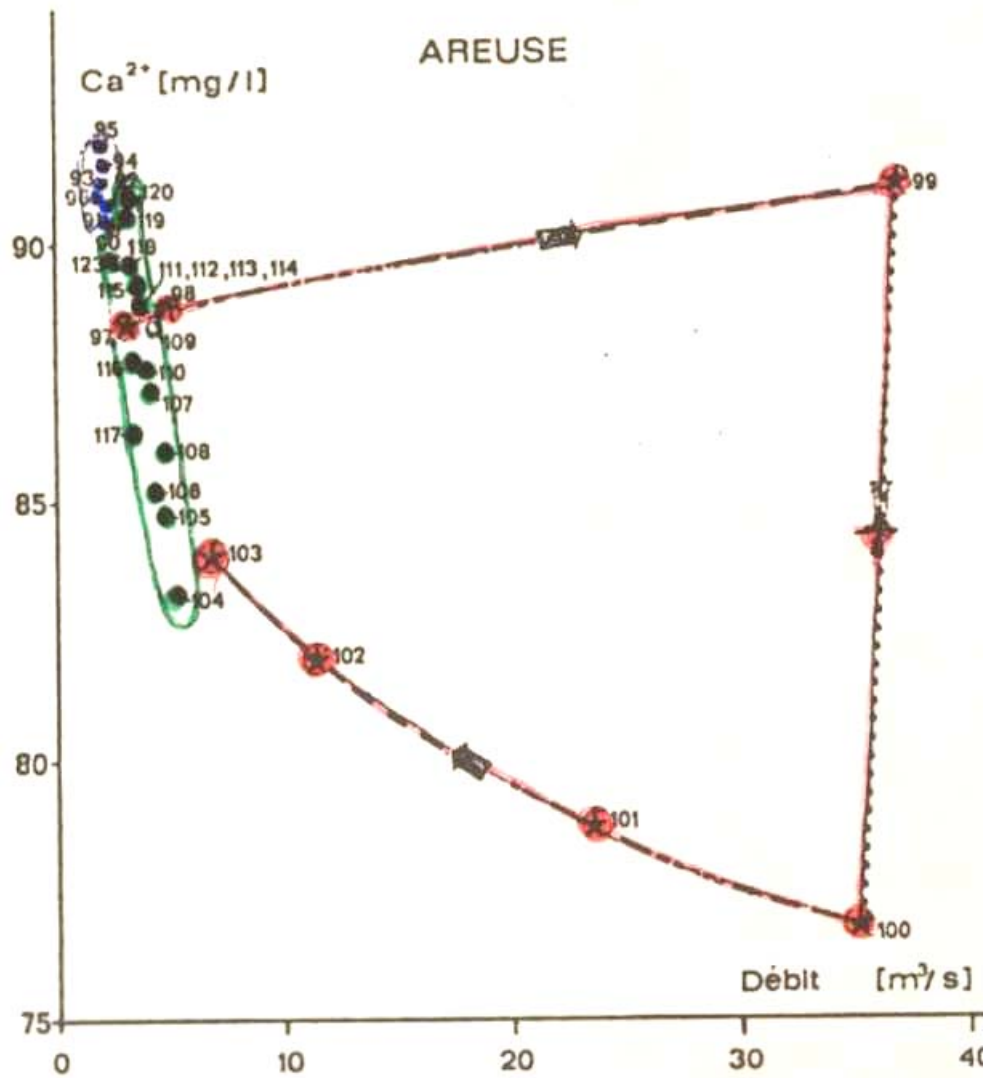


(after Kiraly 1973)

### AREUSE spring (1979)

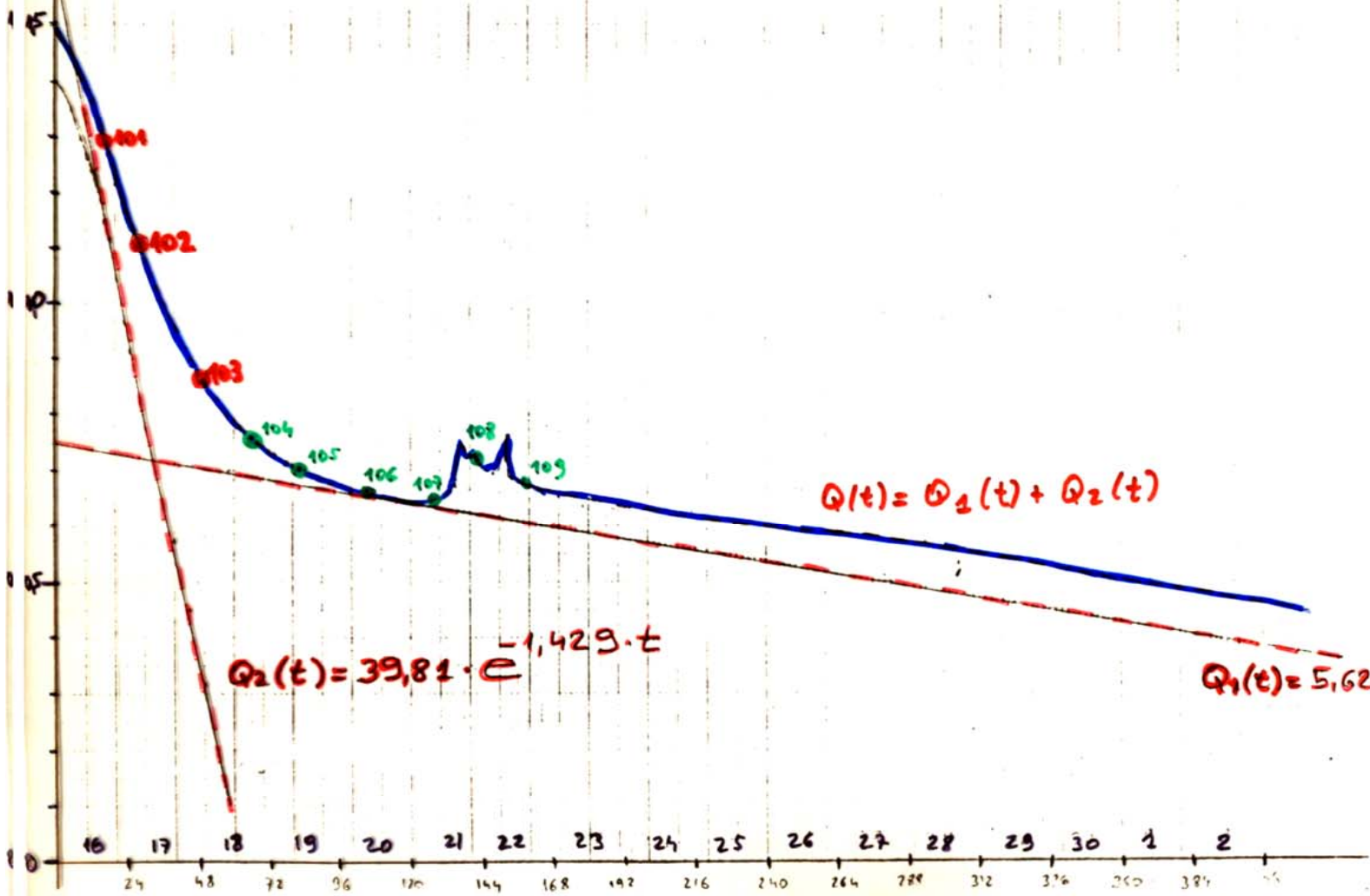






log Q

AREUSE - NOVEMBRE 1977



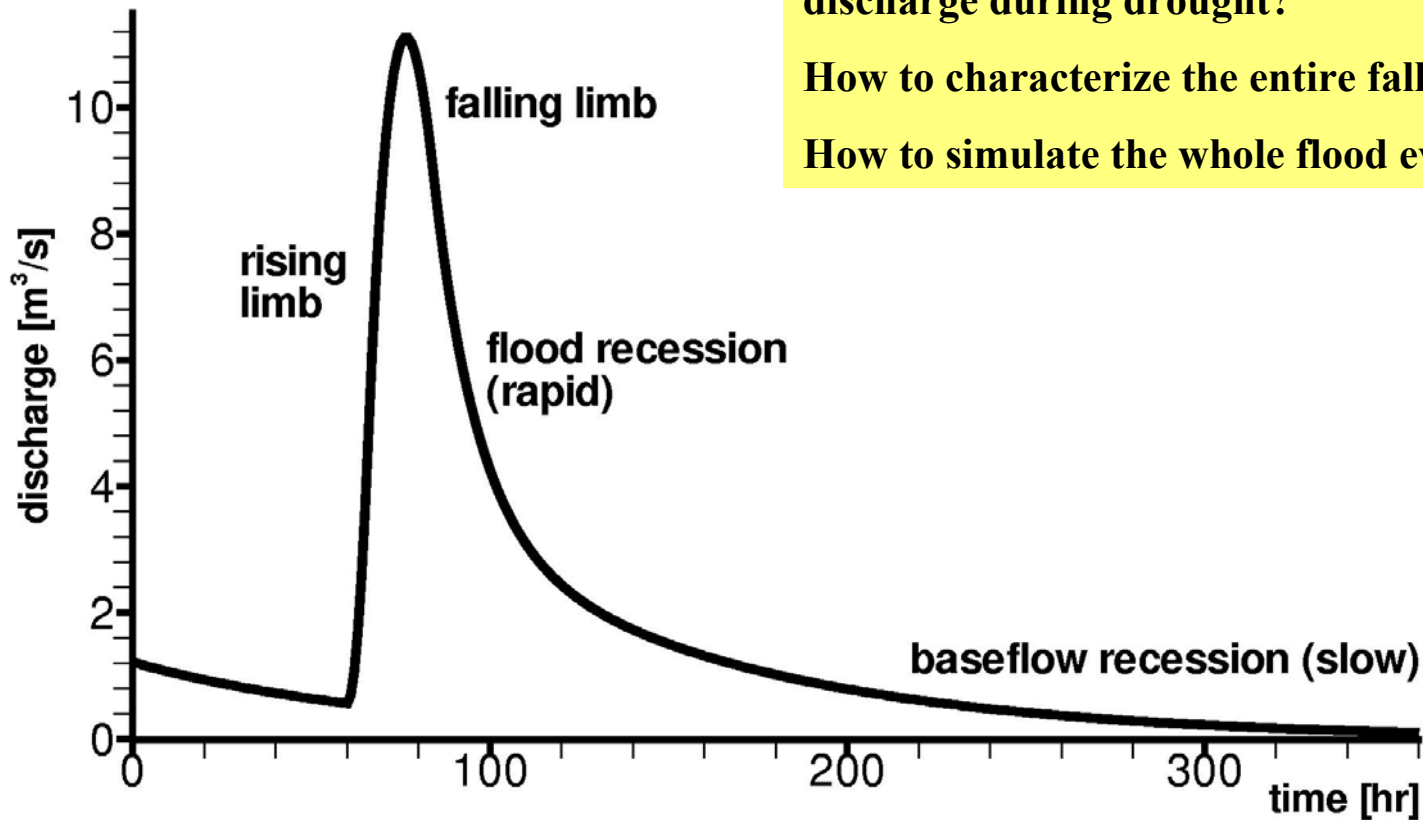
$$Q_2(t) = 39,81 \cdot e^{-1,429 \cdot t}$$

$$Q(t) = Q_1(t) + Q_2(t)$$

$$Q_1(t) = 5,623 \cdot e^{-0,0506 \cdot t}$$

→ t

## Analysis of a single flood event

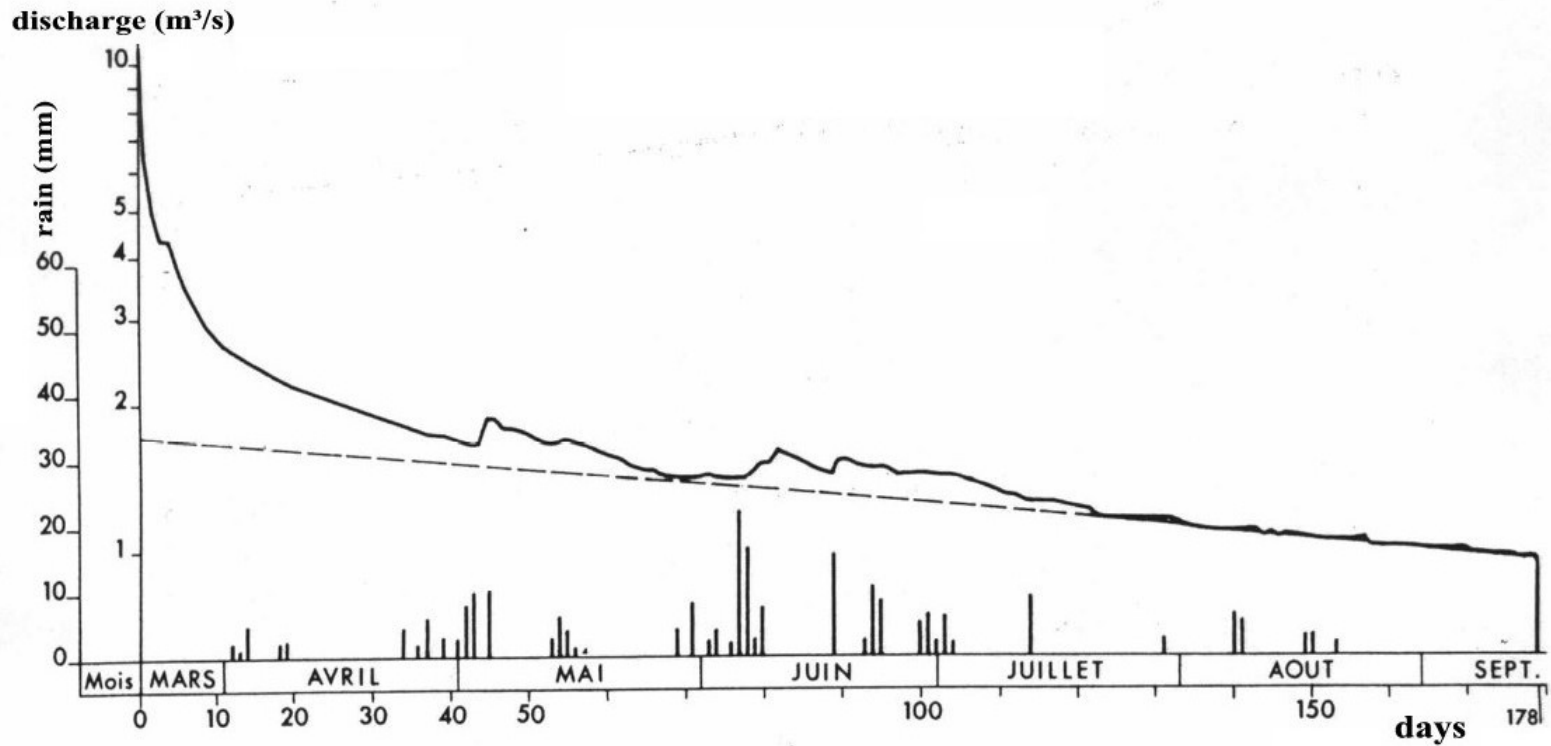


How to characterize the depletion (the baseflow recession) curve? How to forecast the spring discharge during drought?

How to characterize the entire falling limb?

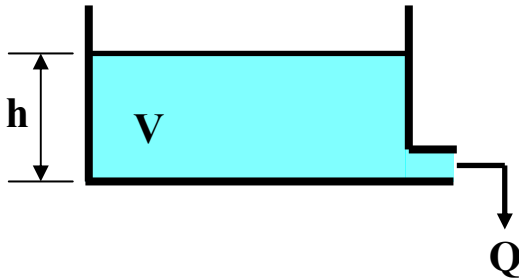
How to simulate the whole flood event?

# Basics for the "global" models (1)



## Basics for the “global” models (2)

Emptying of a reservoir:



If  $n=1$ , the recession of  $Q$  is exponential:

$$\frac{dV}{V} = -\alpha dt \quad \text{and the integral gives}$$

$$V(t) = V_0 e^{-\alpha t}$$

$$Q(t) = Q_0 e^{-\alpha t}$$

The hydrograph  $Q(t)$  and  $\alpha$  allow to estimate the volume  $V$  by  $V(t)=Q(t) / \alpha$ . Caution if  $Q$  is given in  $[m^3/s]$  and  $\alpha$  is given in  $[1/day]$ : 1 day = 86400 seconds.

### Hypotheses

volume  $V$  is proportional to  $h$  and discharge  $Q$  is proportional to a power of  $h$  ( $\rightarrow V$ )

$$Q = - \frac{dV}{dt} \quad Q = K V^n$$

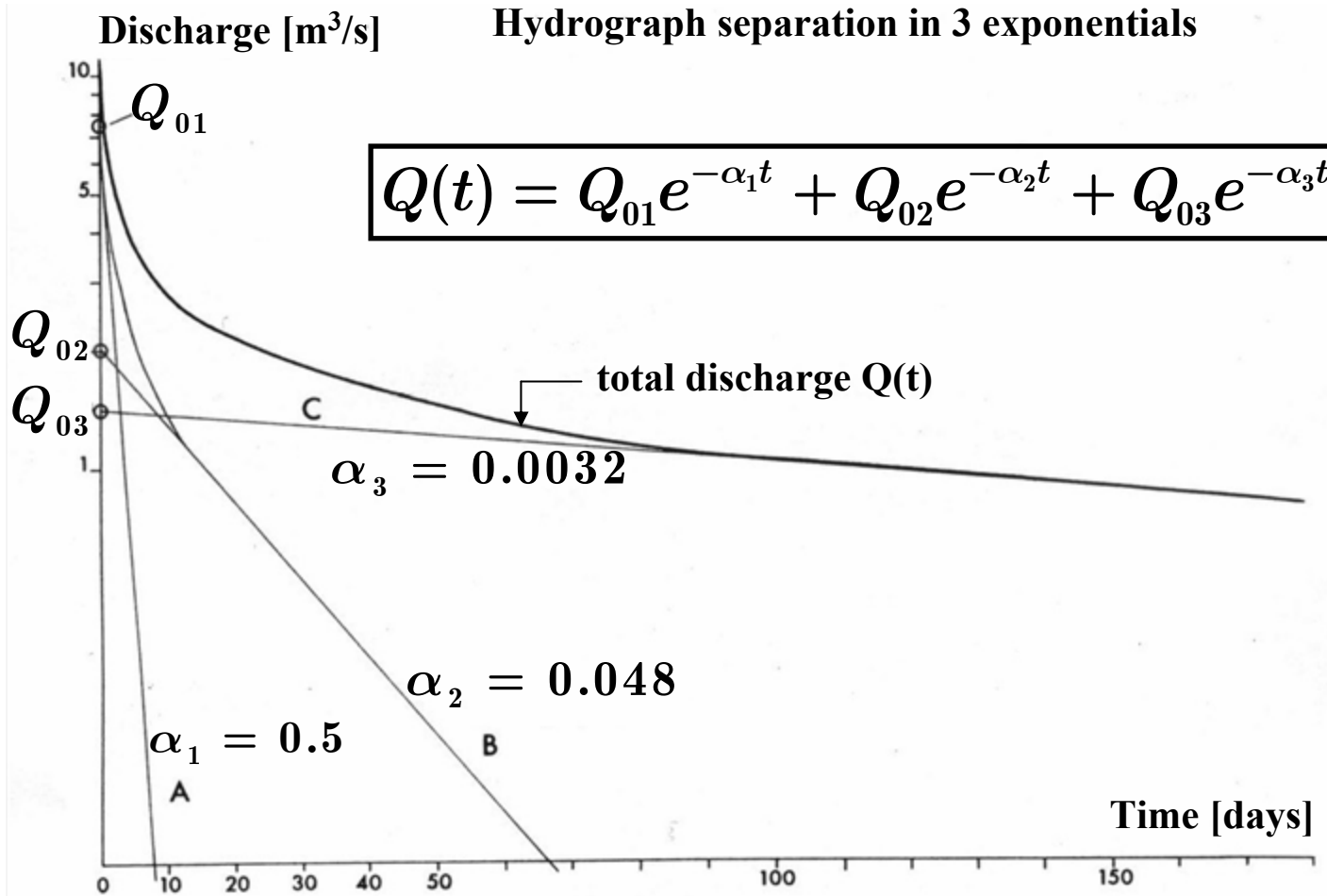
$$\alpha = Q / V \quad \text{and we have}$$

$$\frac{dV}{dt} + K V^n = 0 \quad \text{for emptying}$$

In a diagram  $\ln Q$  versus  $t$  the exponential part of the recession hydrograph appears as a straight line. If we know two points  $(Q_1, t_1)$  and  $(Q_2, t_2)$  on the exponential part, we can determine  $\alpha$  by:

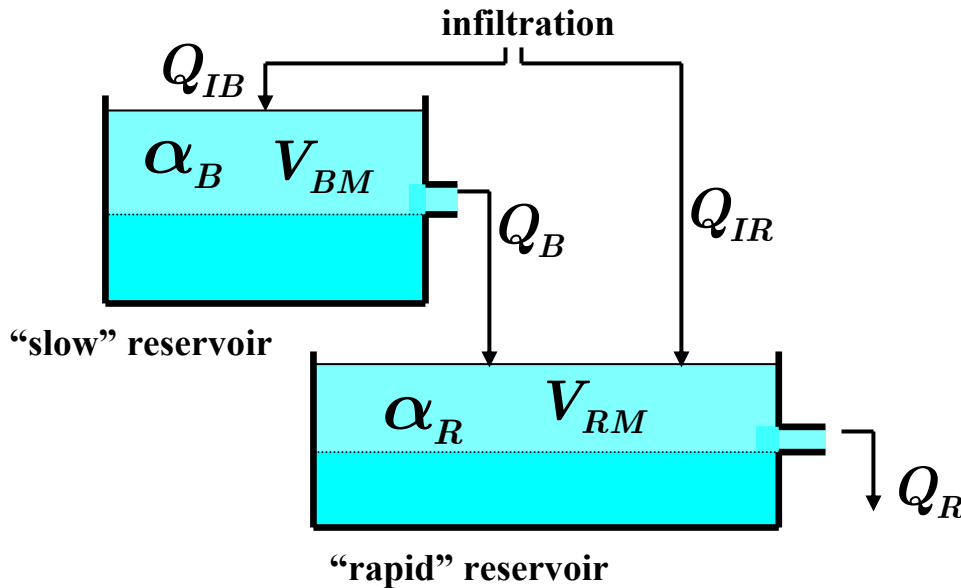
$$\alpha = \frac{1}{t_2 - t_1} \ln \frac{Q_1}{Q_2}$$

## Basics for the “global” models (3)



(Forkasiewicz and Paloc, 1967)

## Basics for the “global” models (4)



### Double reservoir model

$Q_R$  = spring discharge

$Q_B$  = baseflow component

$\alpha_R$  = recession coefficient for the rapid reservoir

$\alpha_B$  = recession coefficient for the slow reservoir

$Q_{IB}$  = diffuse infiltration into the slow reservoir

$Q_{IR}$  = direct infiltration into the rapid reservoir

$V_{BM}$  = “mobile” volume of the slow reservoir

$V_{RM}$  = “mobile” volume of the rapid reservoir

$$\frac{dV_{BM}}{dt} = Q_{IB} - \alpha_B V_{BM}$$

$$\frac{dV_{RM}}{dt} = Q_{IR} + \alpha_B V_{BM} - \alpha_R V_{RM}$$

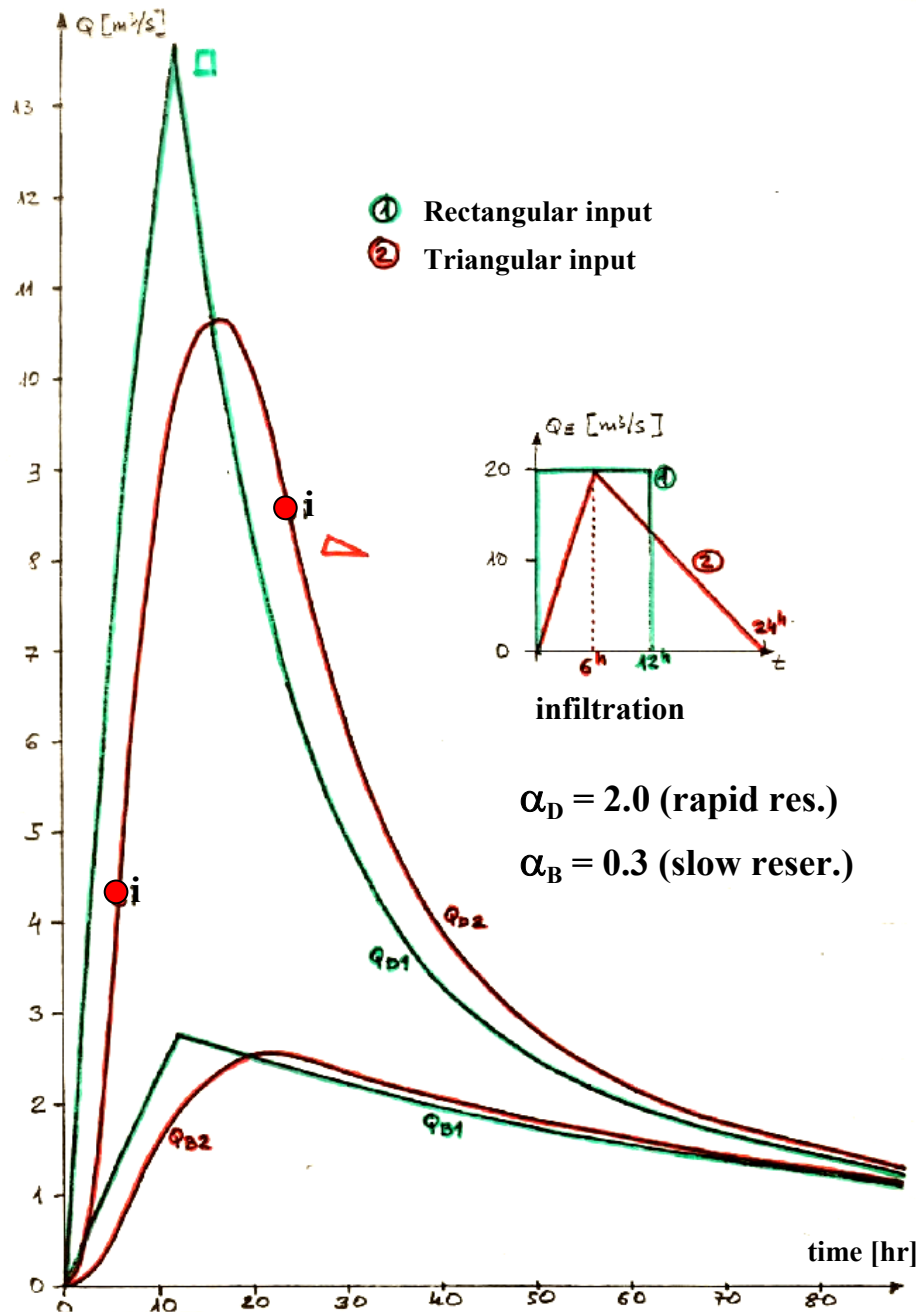
## Basics for the “global” models (5)

Spring hydrographs obtained by the double-reservoir model: effect of the form of input functions on the hydrographs

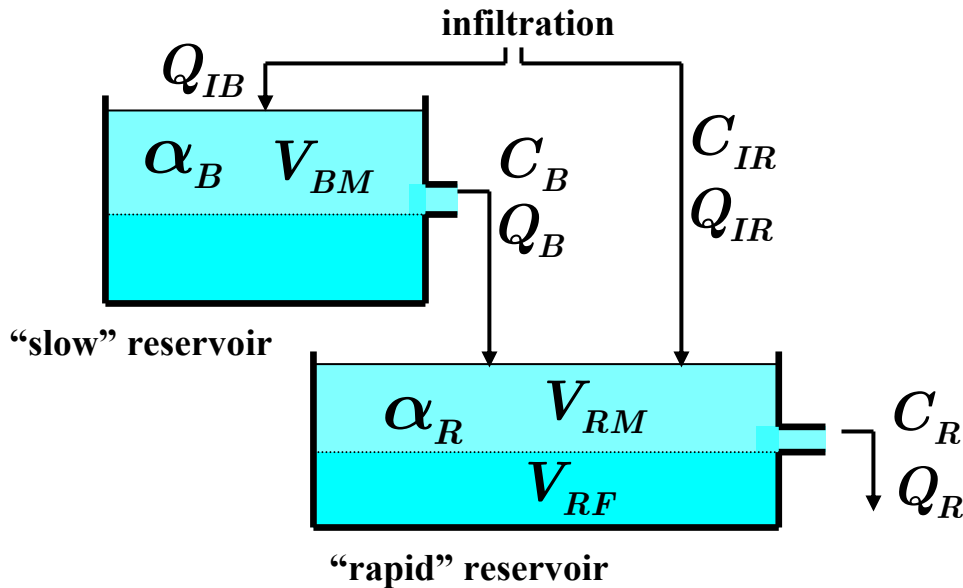
If you can avoid, do not use rectangular input functions

Observe the 2 inflexion points “i” on the curve  $Q_{D2}$  obtained by the triangular input function. The first inflexion point is at 6 hr (infiltration has its maximum value) and the second is at 24 hr (the infiltration is ceased).

Observing the inflexion points on real spring hydrographs would perhaps allow to make a guess on the real input function.



## Basics for the “global” models (6): dilution effect at the spring



$$\frac{dV_{BM}}{dt} = Q_{IB} - \alpha_B V_{BM}$$

$$\frac{dV_{RM}}{dt} = Q_{IR} + \alpha_B V_{BM} - \alpha_R V_{RM}$$

$$\frac{dC_R}{dt} = Q_B \frac{(C_B - C_R)}{(V_{RM} + V_{RF})} + Q_{IR} \frac{(C_{IR} - C_R)}{(V_{RM} + V_{RF})}$$

$Q_R$  : spring discharge

$Q_B$  : baseflow component

$\alpha_R$  : recession coefficient for the rapid reservoir

$\alpha_B$  : recession coefficient for the slow reservoir

$Q_{IB}$  : diffuse infiltration into the slow reservoir

$Q_{IR}$  : direct infiltration into the rapid reservoir

$V_{BM}$  : “mobile” volume of the slow reservoir

$V_{RM}$  : “mobile” volume of the rapid reservoir

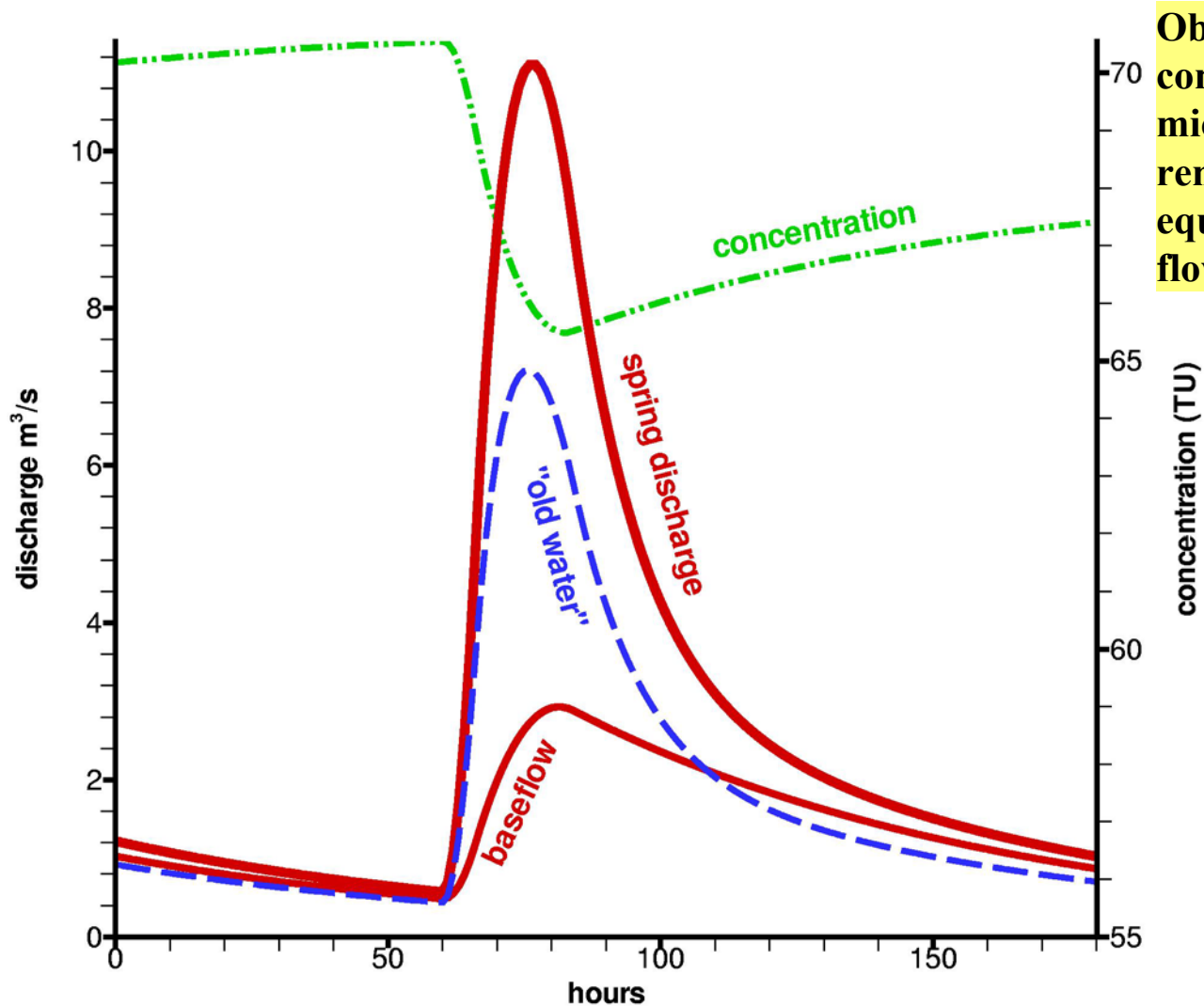
$V_{RF}$  : “fixed” volume of the rapid reservoir

$C_B$  : concentration in baseflow

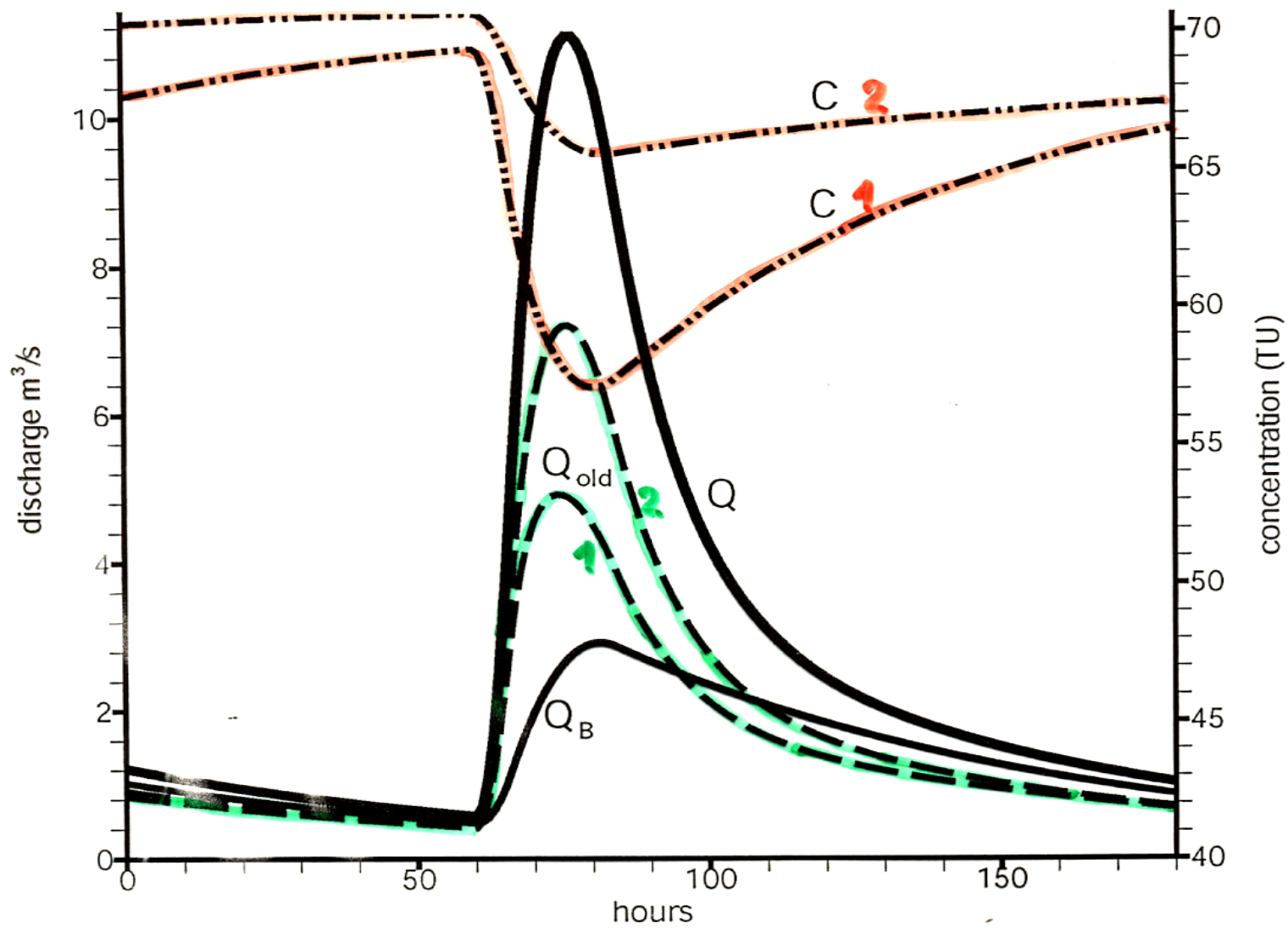
$C_R$  : concentration in spring

$C_{IR}$  : concentration in direct input

## Basics for the “global” models (7): dilution effect at the spring



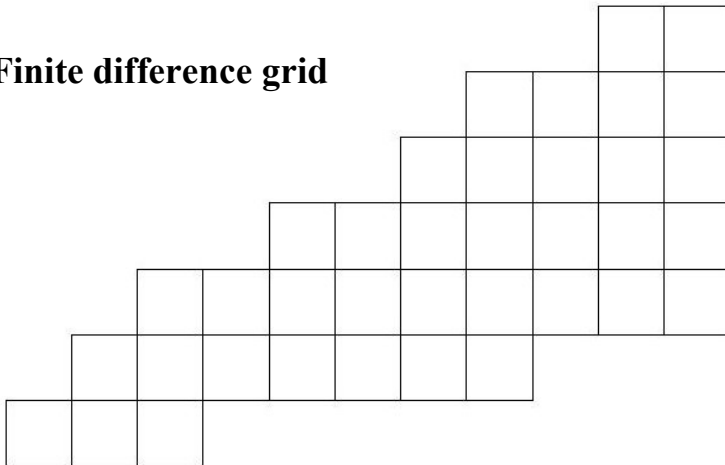
Observe that “old water” component and hydrodynamic baseflow are two different concepts!!! Do not equate “old water” to “baseflow”!!



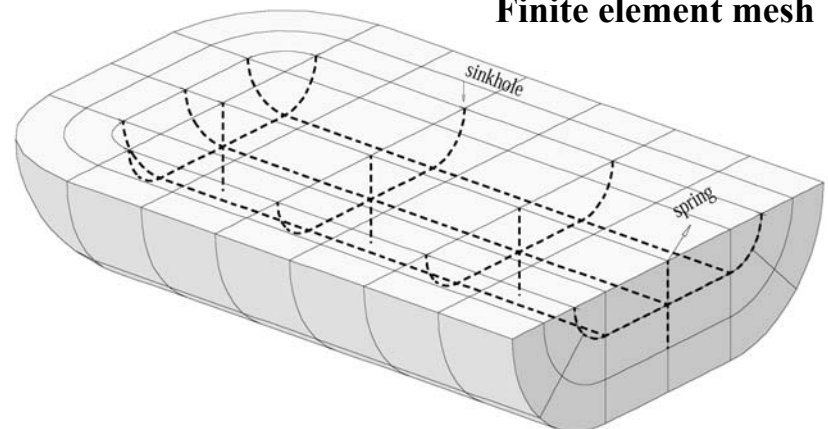
# DISTRIBUTIVE MODELS

In the distributive models the flow problem is solved in a (generally great) number of “discrete” points (“nodes” or nodal points) which allow to interpolate the results over the whole region under consideration. The two most common techniques are represented by the **Finite Difference** models and by the **Finite Element** models. In both cases the exact, but unknown solution of the governing partial differential equation will be approximated by a simpler function of known type in the finite difference cells or over the finite elements (for example, constant head value in the cells and linear, quadratic or cubic function over the finite elements) which allow to obtain a (generally linear) equation for each node of the model. The system of simultaneous linear equations is then solved by iterative or direct numerical methods. **Data necessary for the distributive models and how to obtain them?**

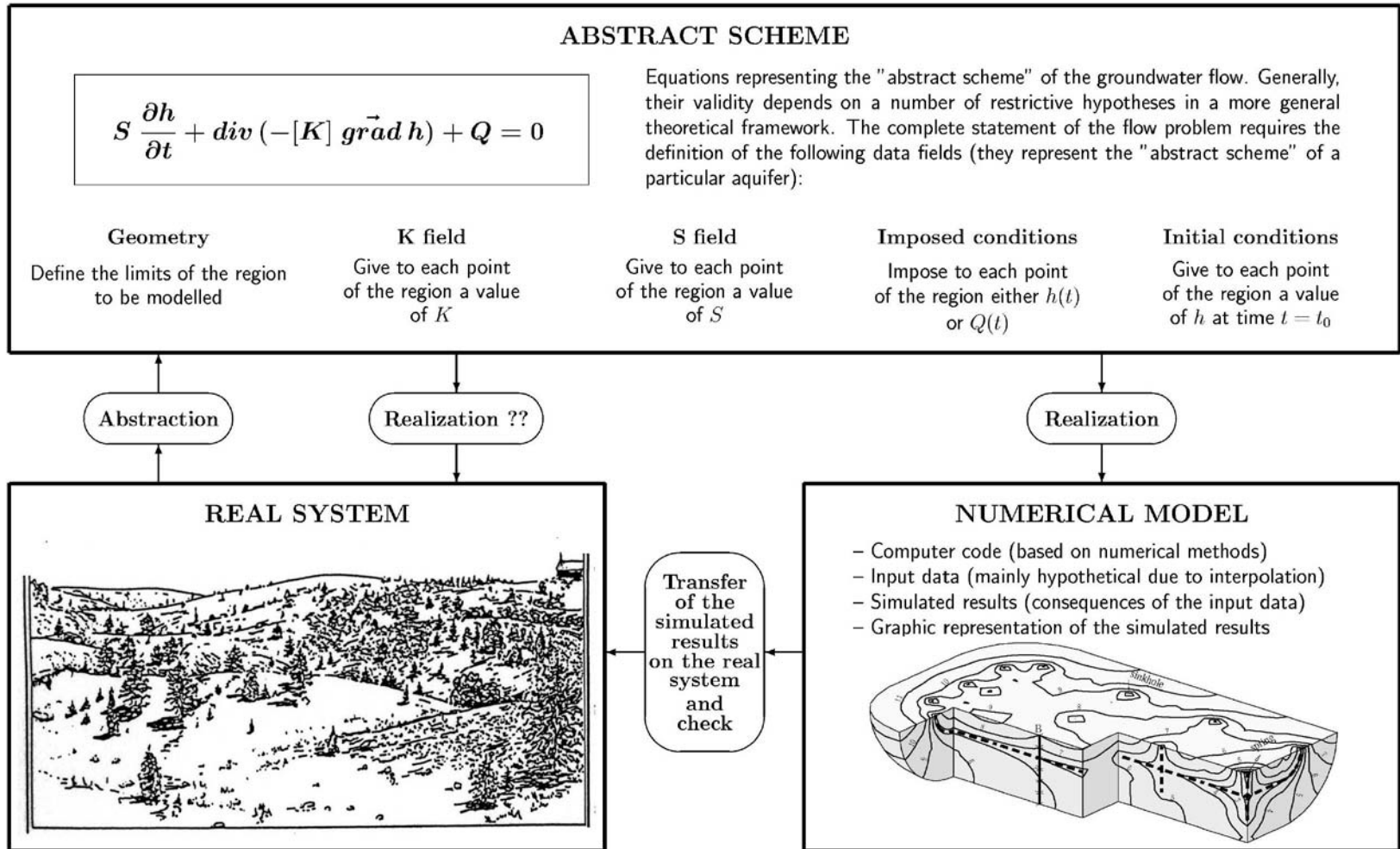
Finite difference grid

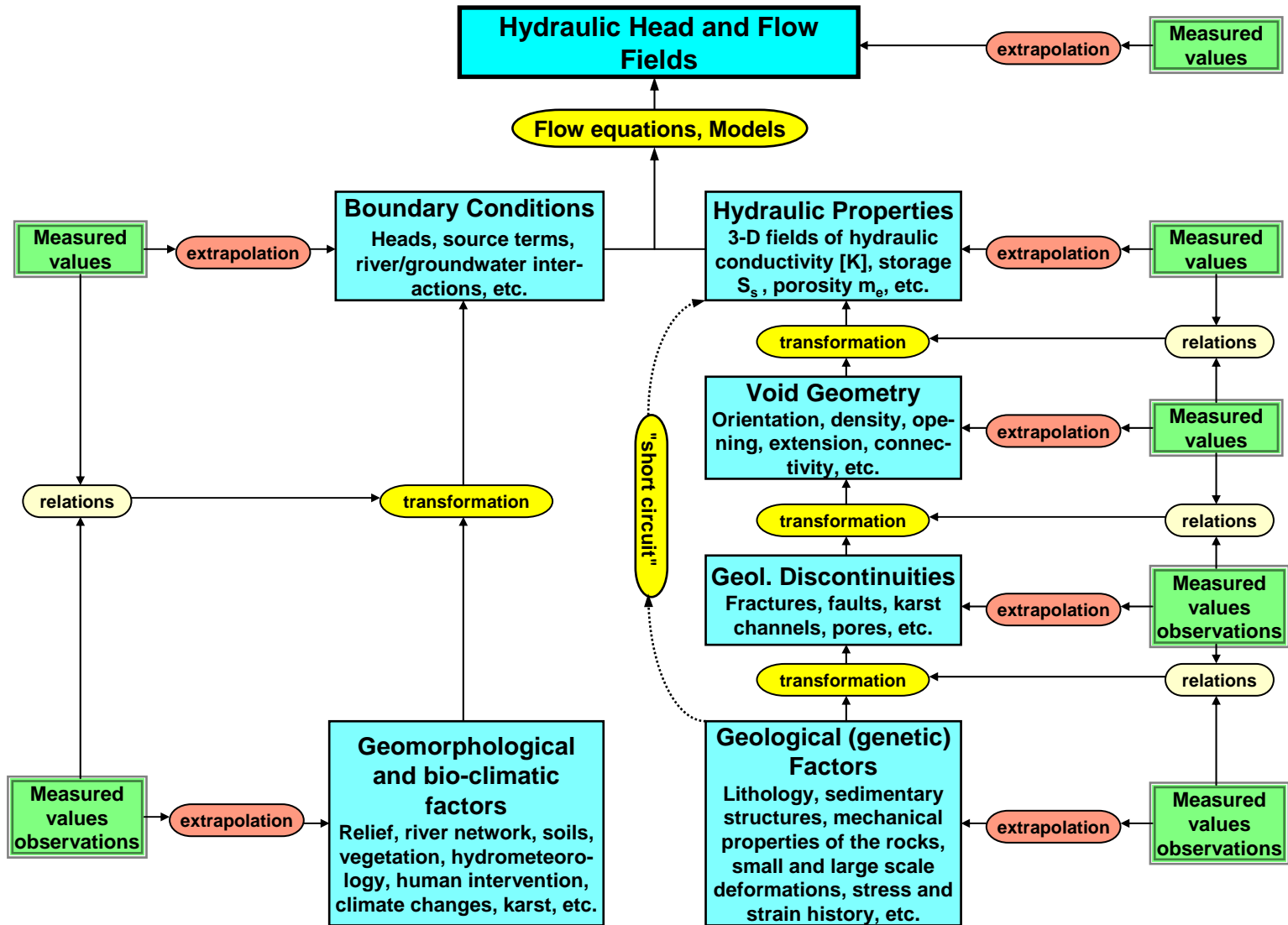


Finite element mesh



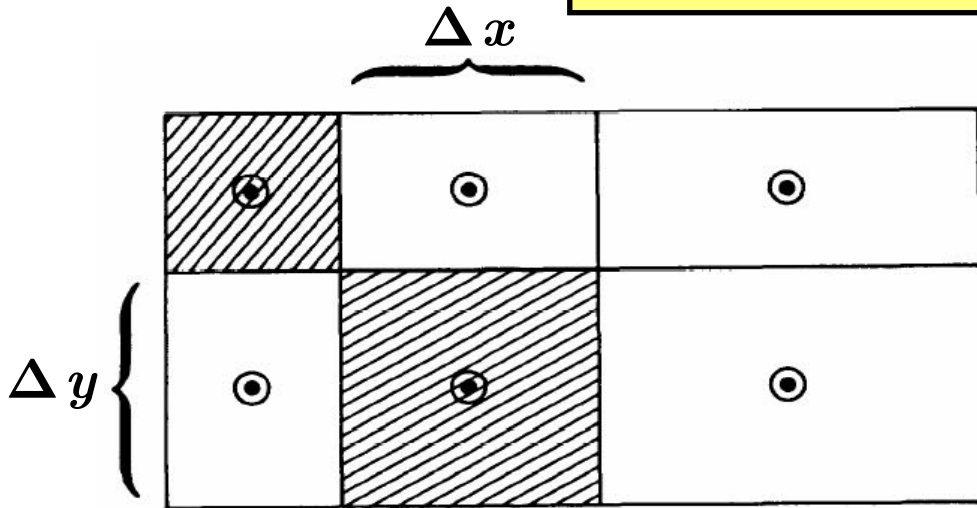
## Representation of the principal problems in modelling groundwater flow





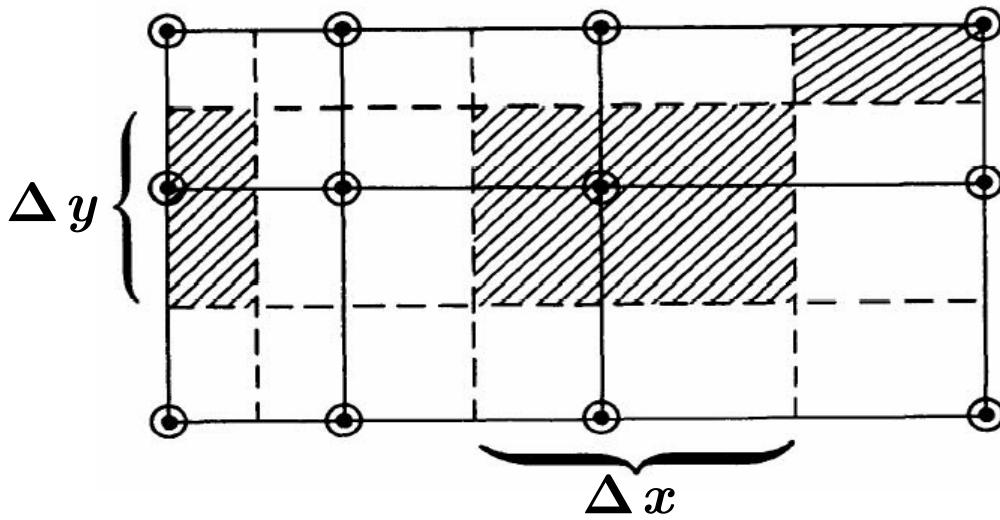
Problems related to the indirect reconstruction of the hydraulic parameter fields and boundary conditions (interpolation or extrapolation of the measured values or observations is unavoidable!!)

# Finite difference models







Block-centered Grid System

Point-centered Grid System



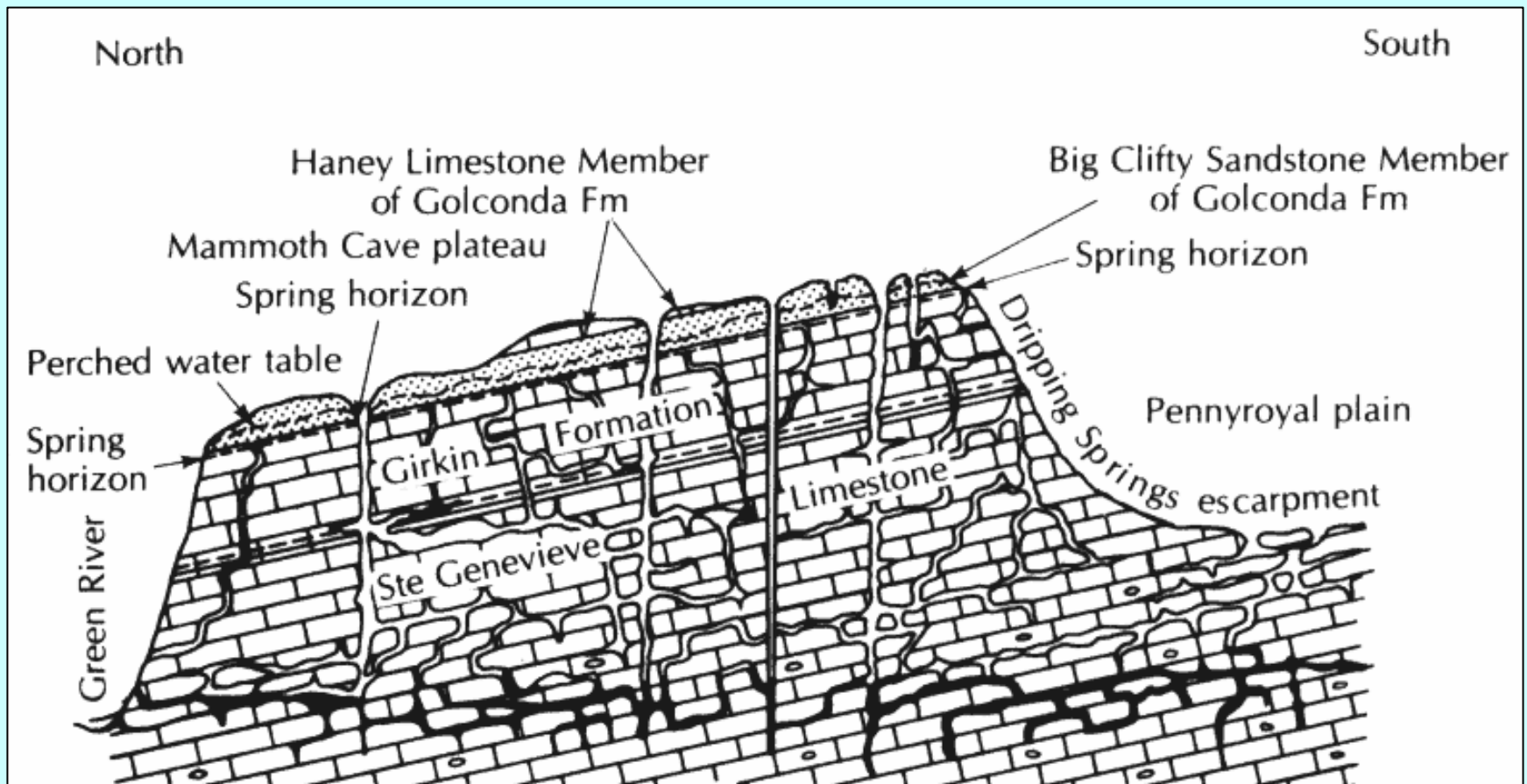
**Block-centered and point-centered grid systems for Finite Difference models**

**Note that in each cell the hydraulic head is considered as being constant!! If possible, do not use Finite Difference models to simulate karst aquifers: Finite Element models are better for solving karst problems.**

- Explanation
-  Nodes
  -  Grid Lines
  -  Cell Boundaries for Point Centered Formulation
  -  Cells Associated With Selected Nodes

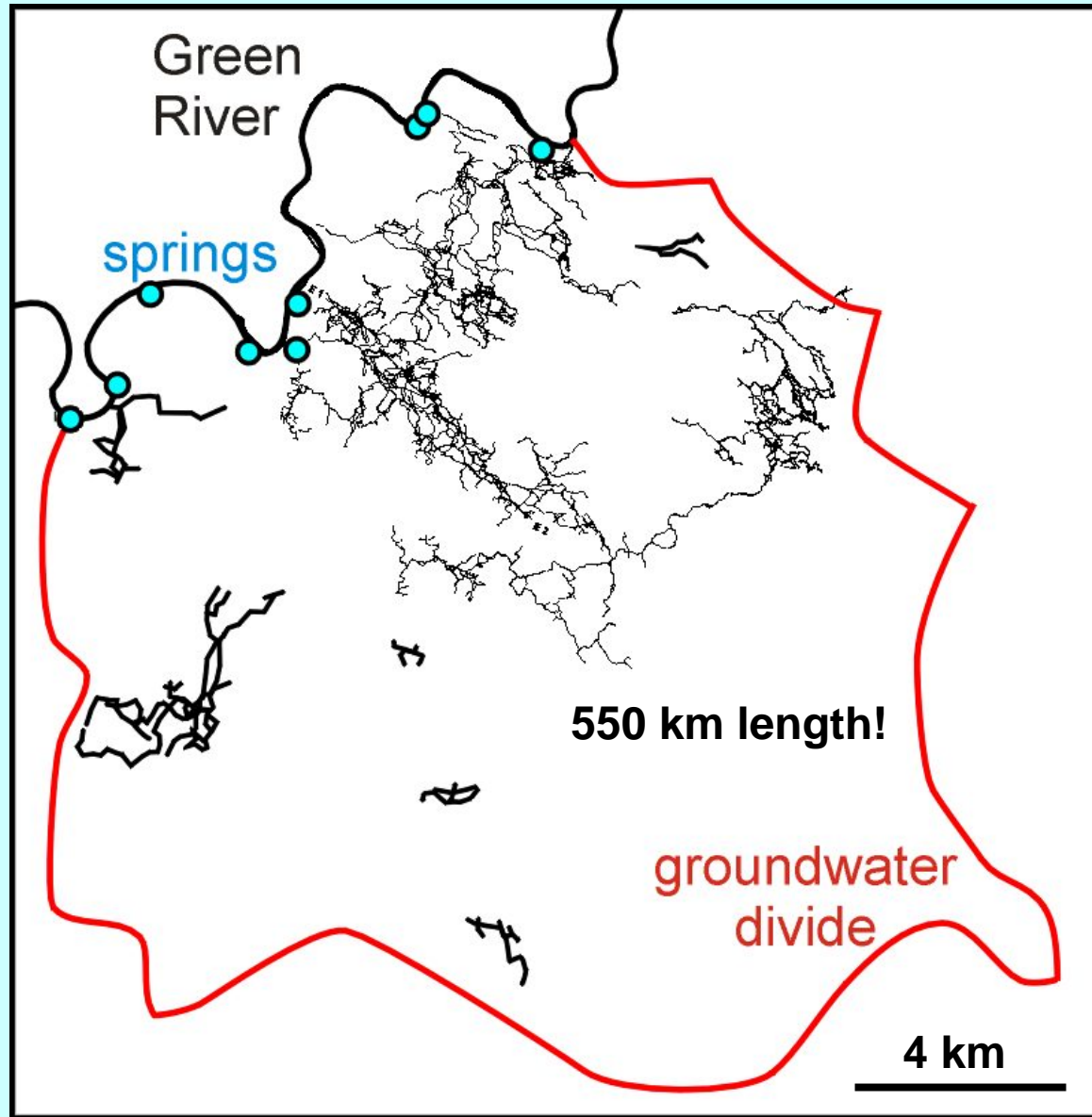
# Extended example: Numerical simulation of the aquifer at Mammoth Cave (MODFLOW)

(Steven Worthington, unpublished data)



hydrogeological cross section through the aquifer

# Map of the Mammoth Cave area



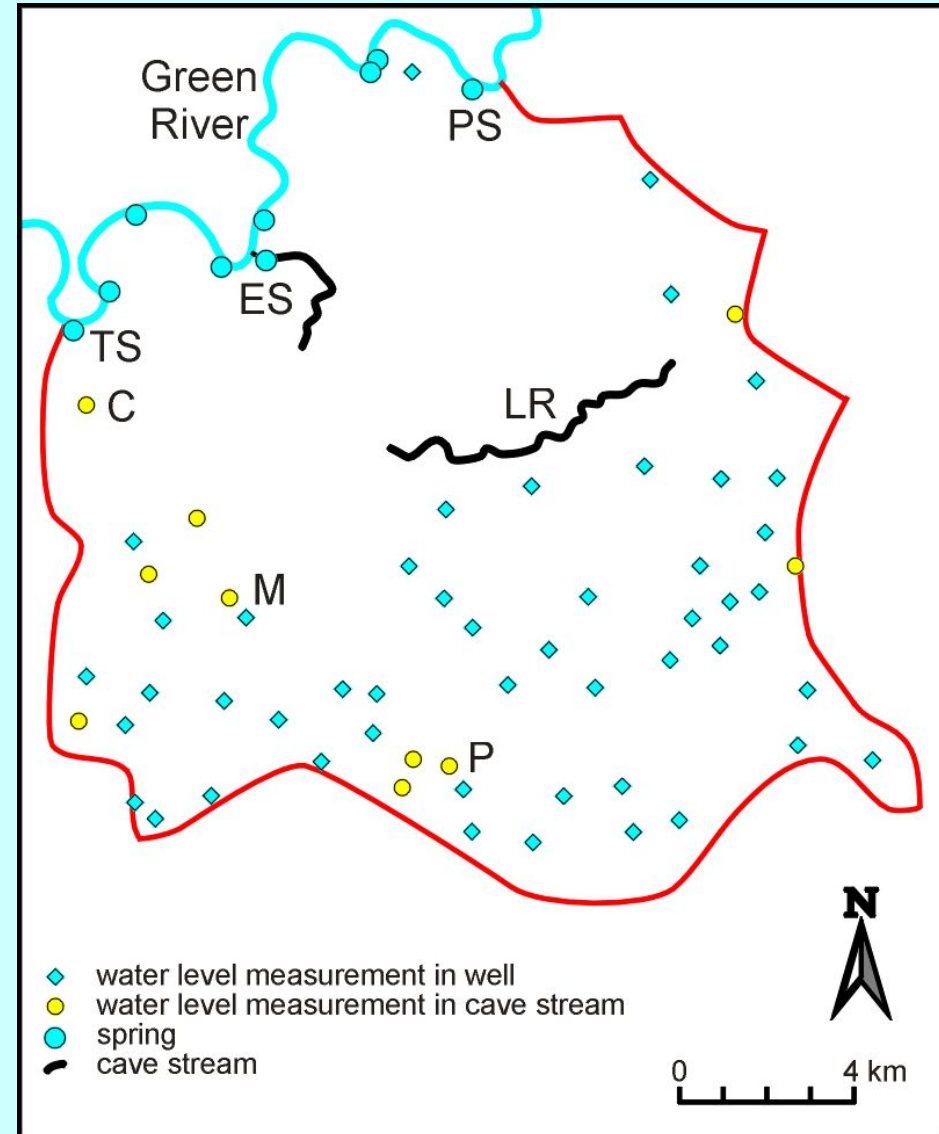
(Steven Worthington)

# Model 1: homogeneous Equivalent Porous Medium (EPM)

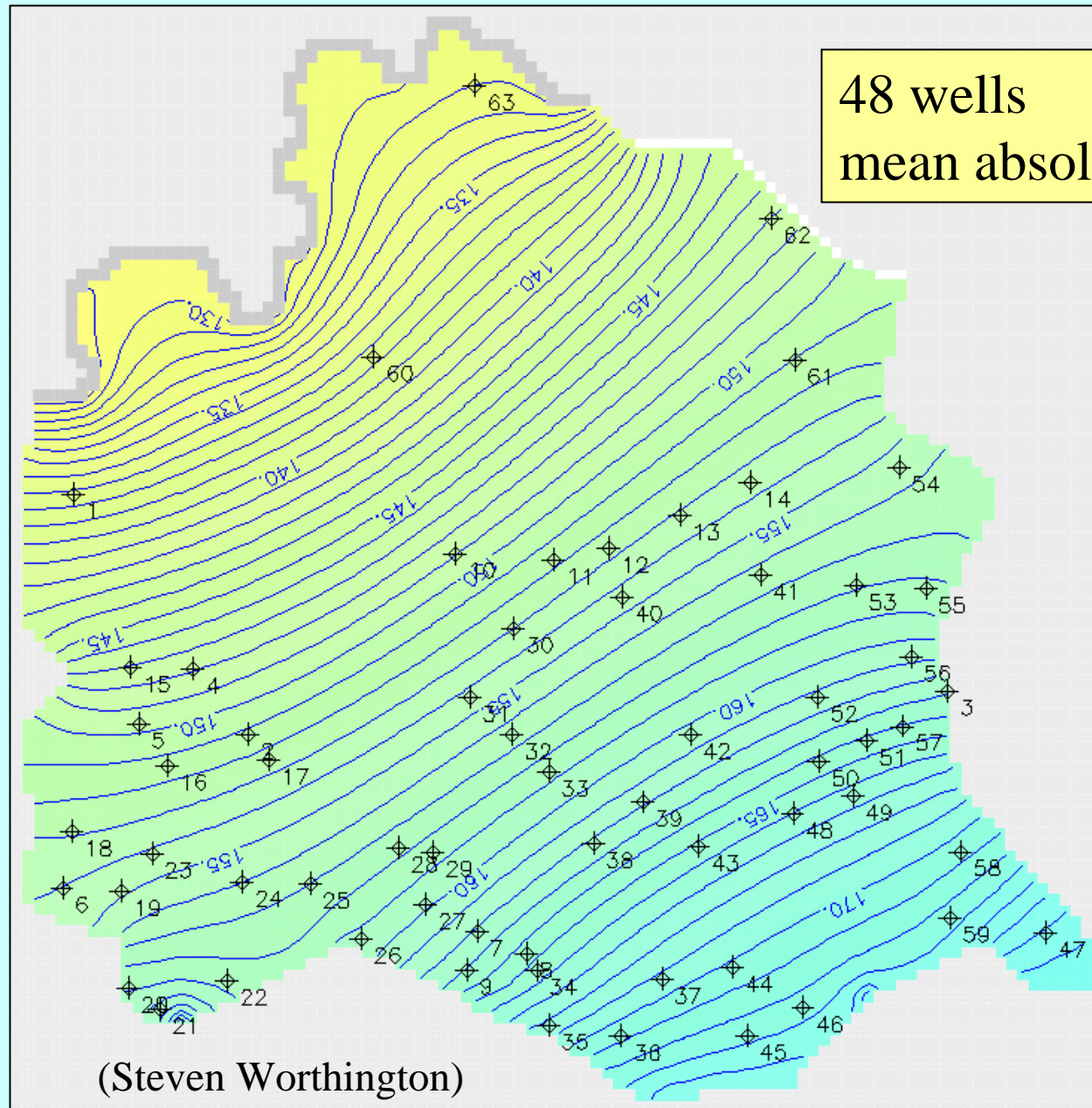
## Data for calibration

- Heads in wells
- Hydraulic conductivity from well tests

Matrix	$2 \times 10^{-11}$ m/s
Slug tests (geo. mean)	$6 \times 10^{-6}$ m/s
Slug test (arith. mean)	$3 \times 10^{-5}$ m/s
Pumping tests	$3 \times 10^{-4}$ m/s
MODFLOW (EPM)	$1 \times 10^{-3}$ m/s



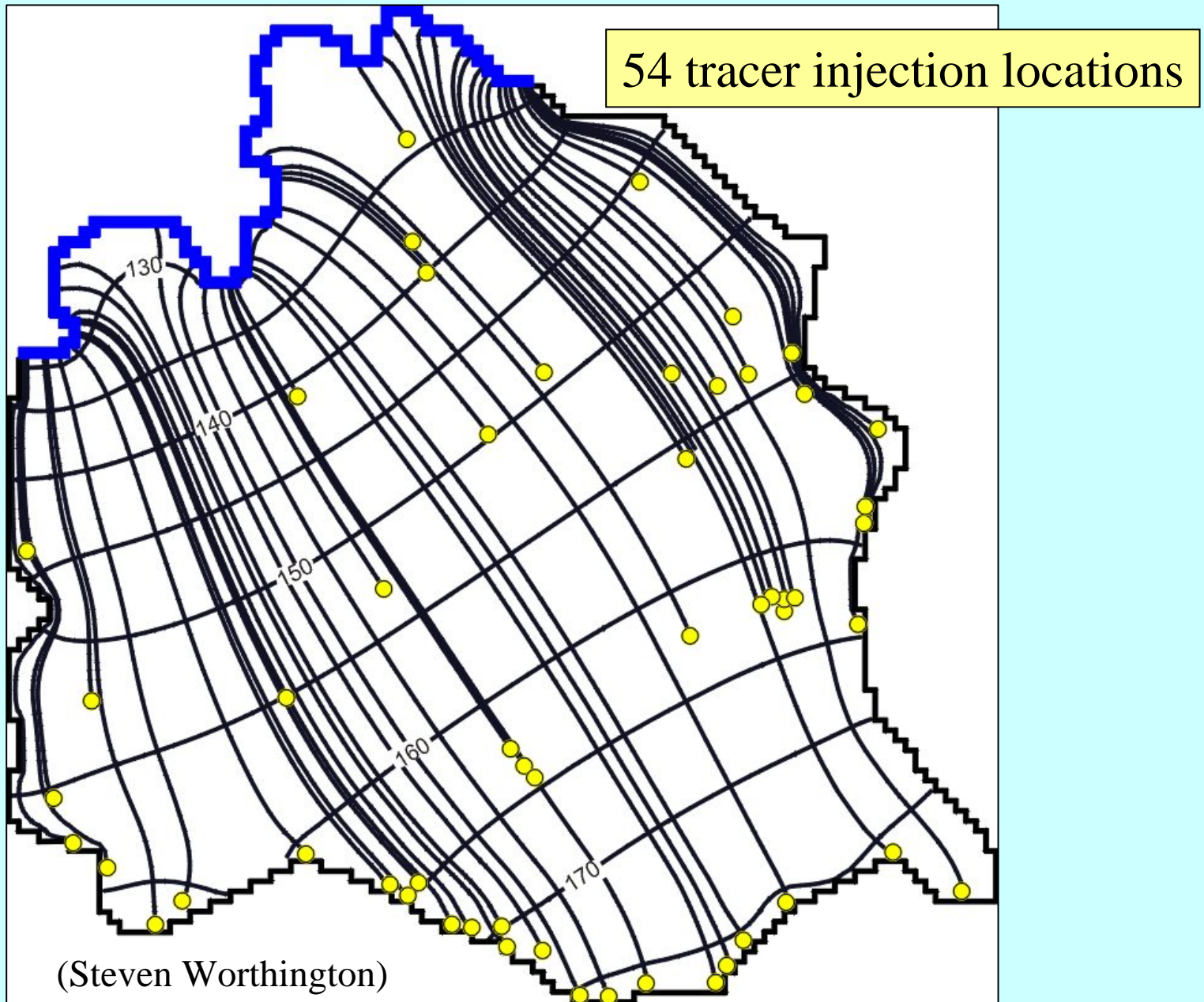
# Results: groundwater contour lines



48 wells  
mean absolute error = 12 m

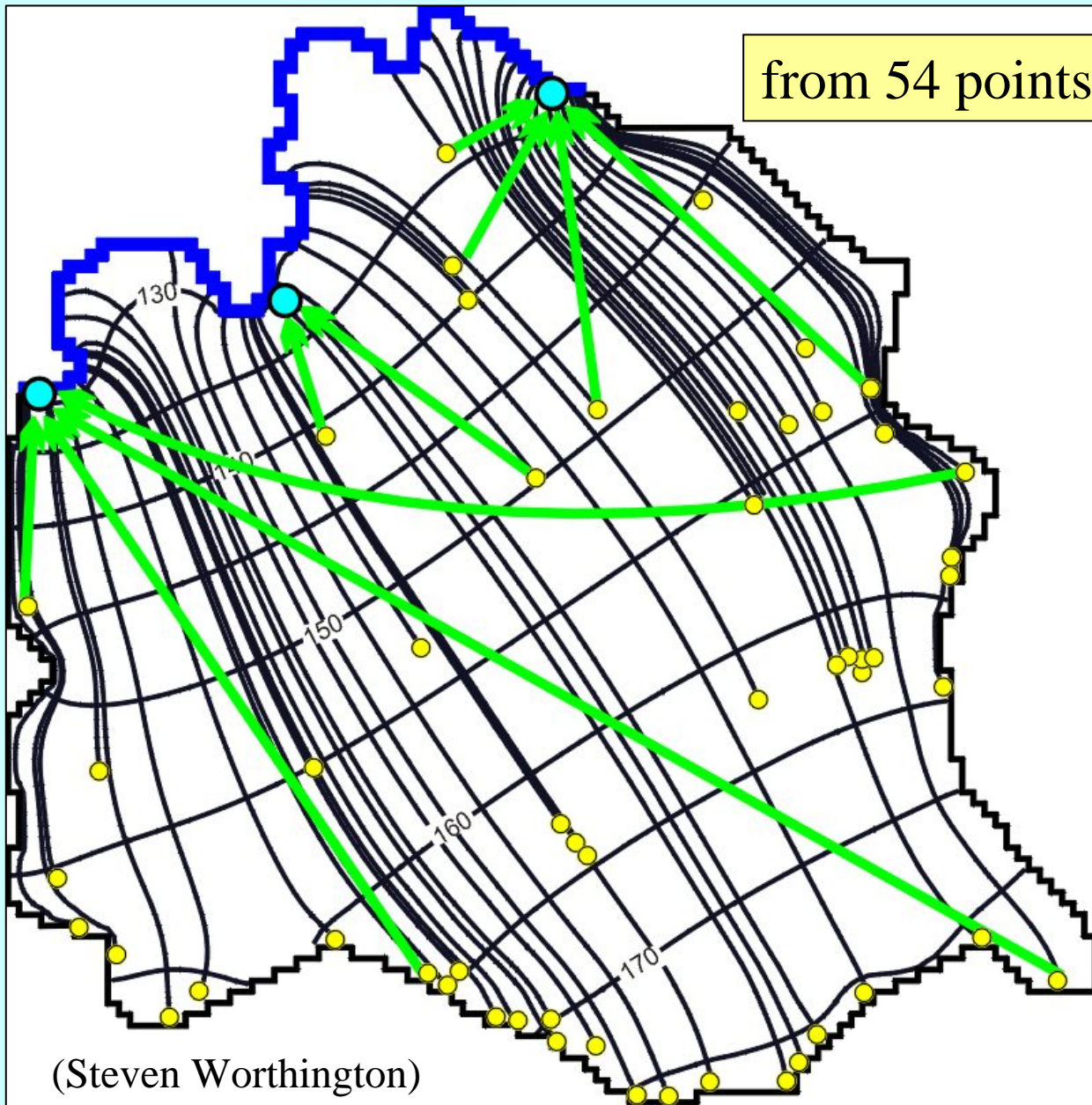
(Steven Worthington)

# Results: Simulated tracer paths



# Actual tracer paths

from 54 points to 3 springs

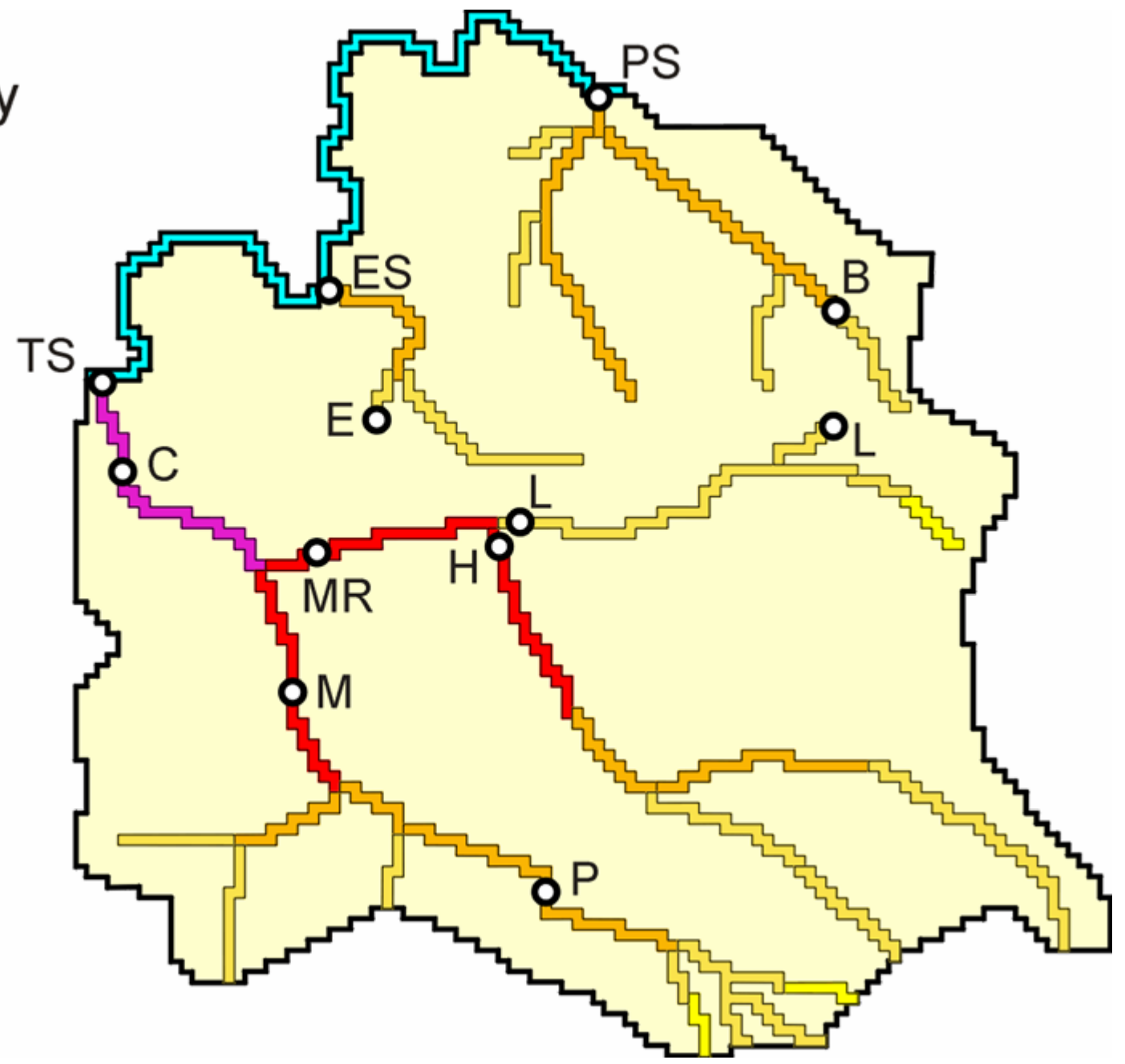
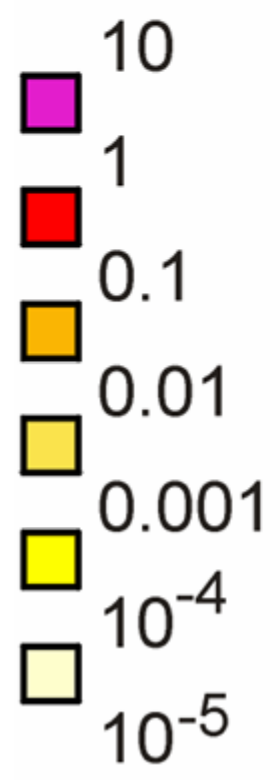


## **Model 2: EPM with ‘conduit cells’**

- Aquifer has integrated conduit network
- Can be simulated with high conductivity cells
- Useful data for calibration
  - 1) Heads in wells
  - 2) Hydraulic conductivity from well tests
  - 3) Heads and discharge in conduits
  - 4) Tracer tests

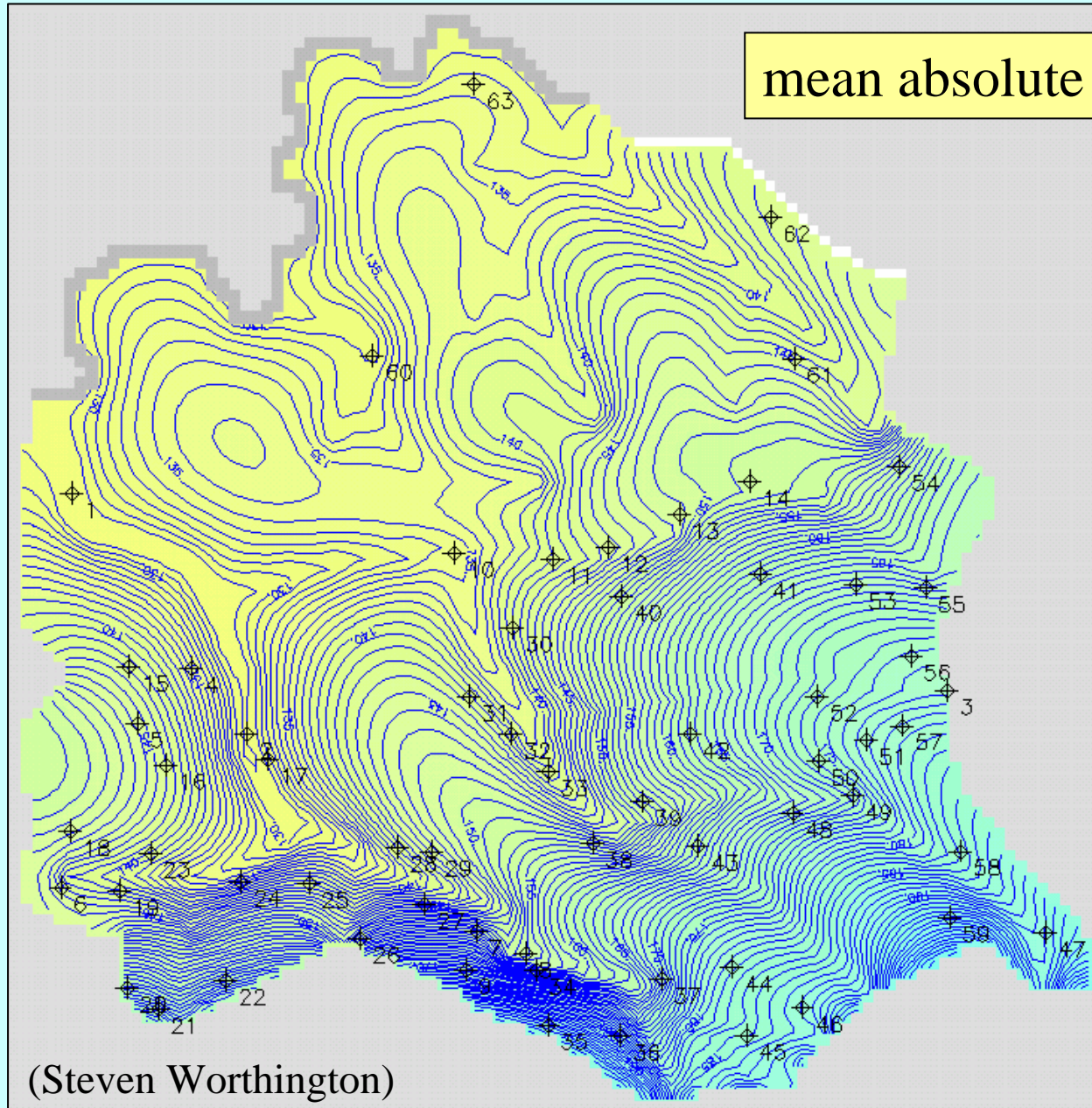
# Hydraulic conductivity distribution

$K$  m/s

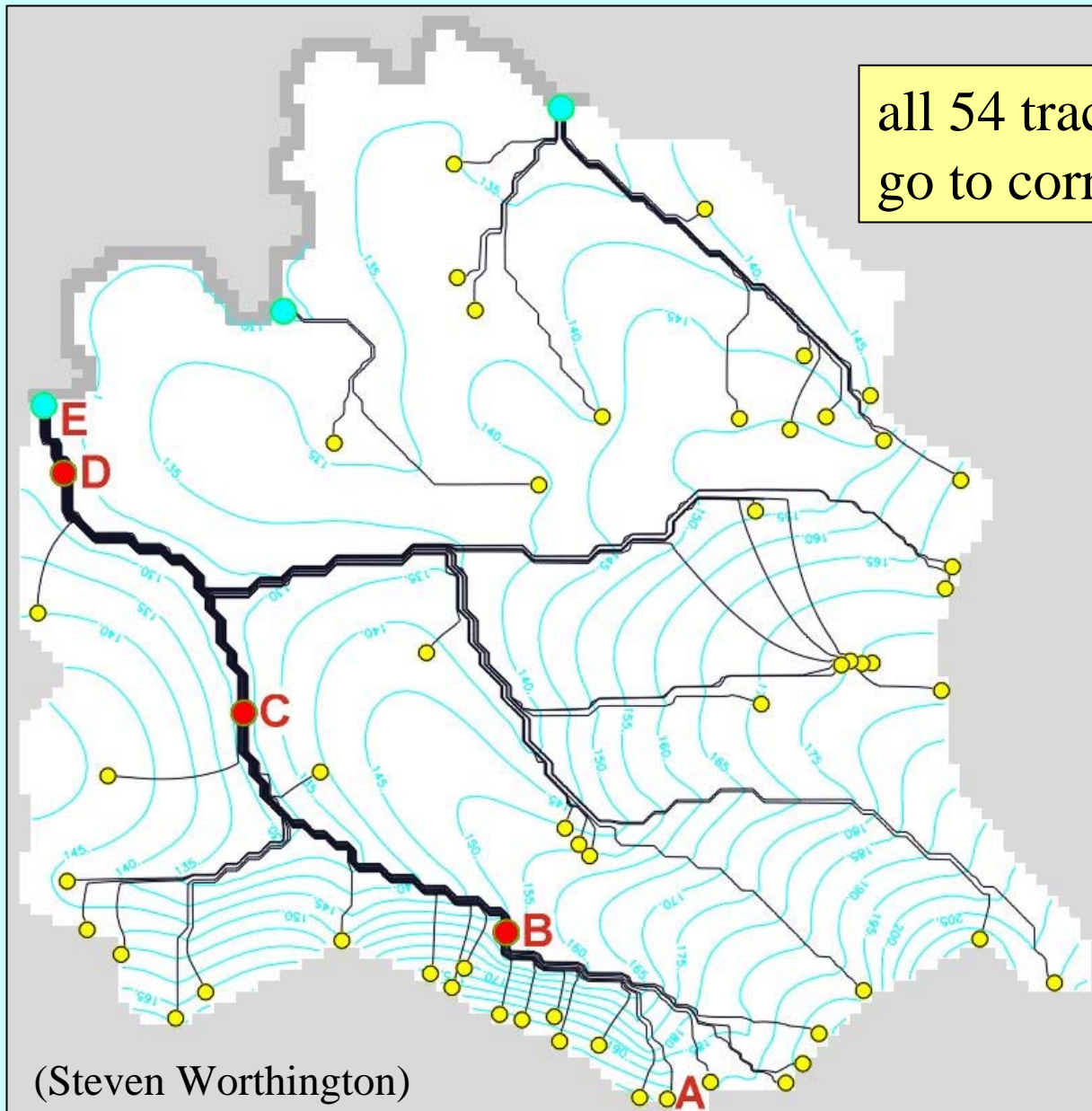


(Steven Worthington)

# Results: groundwater contour lines



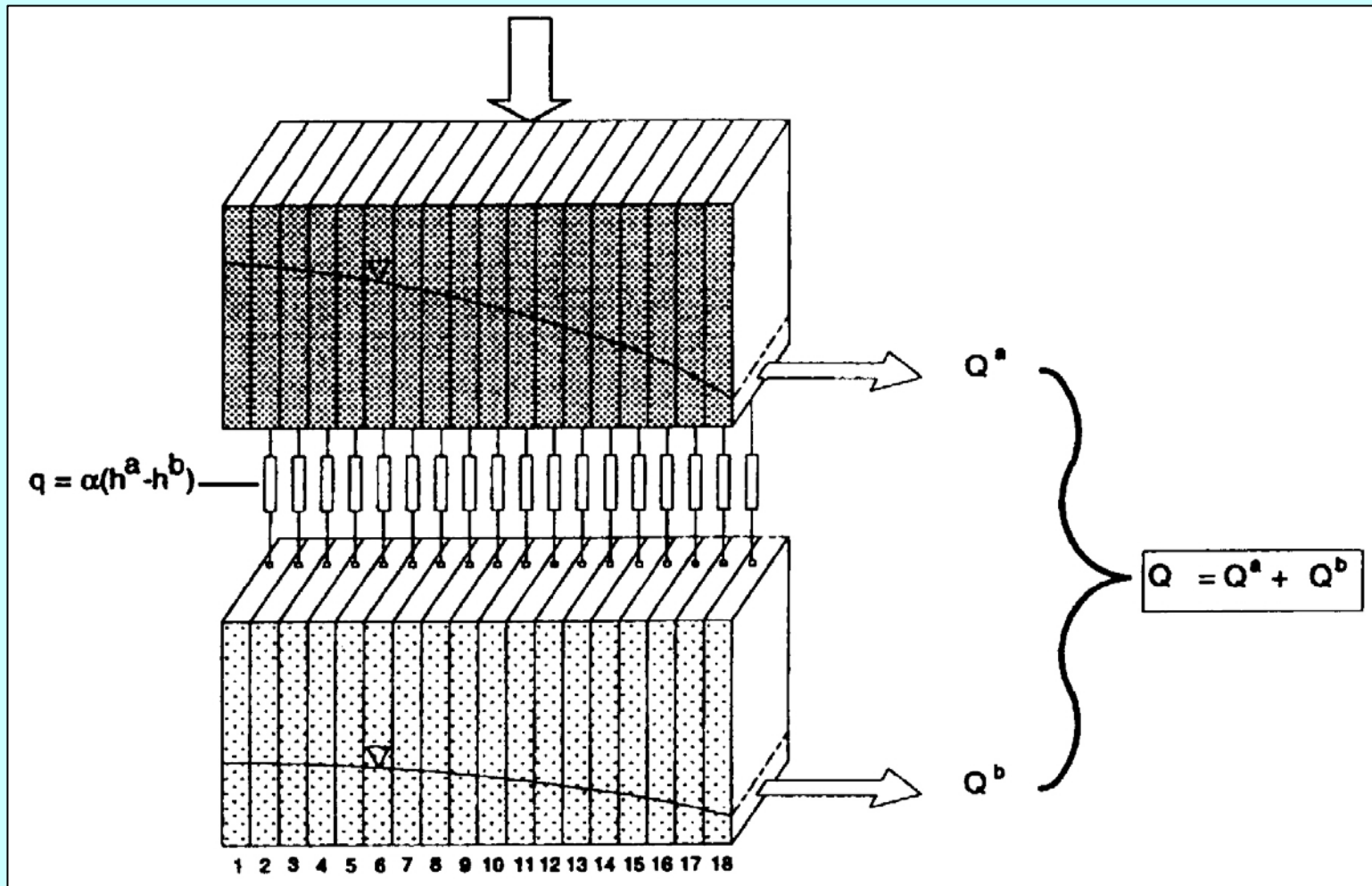
# Results: Simulated tracer paths



all 54 tracer paths  
go to correct spring

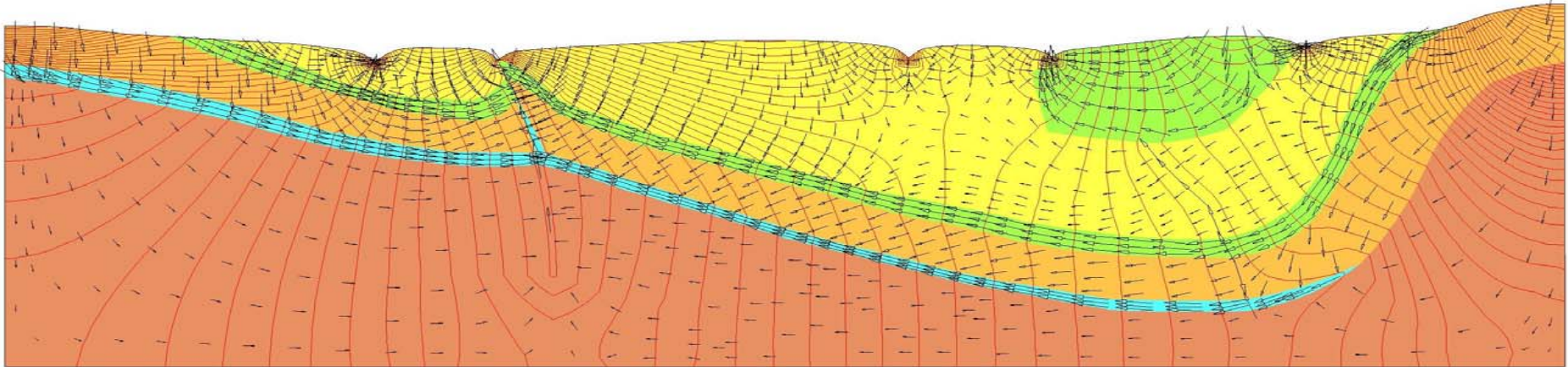
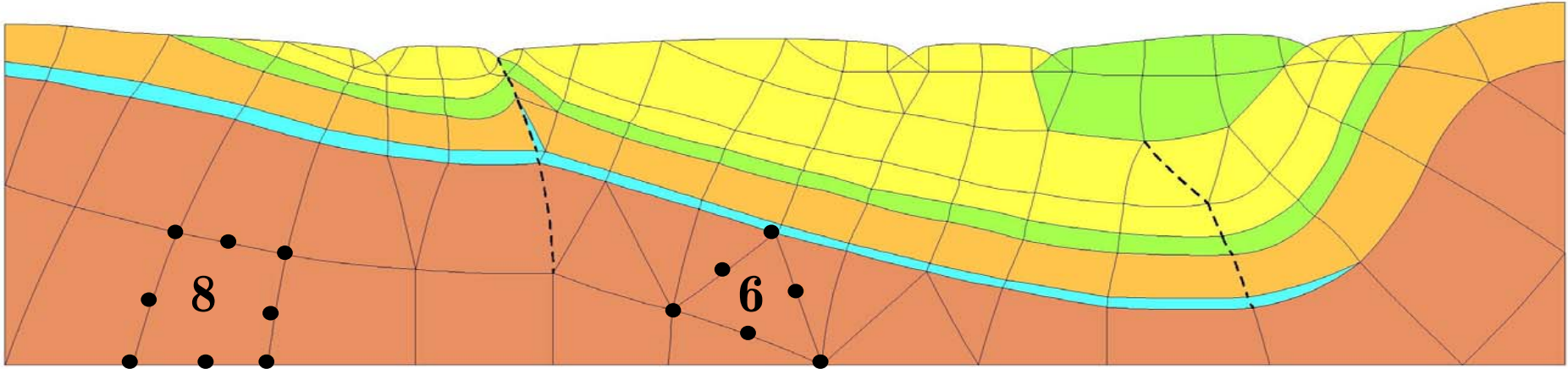
(Steven Worthington)

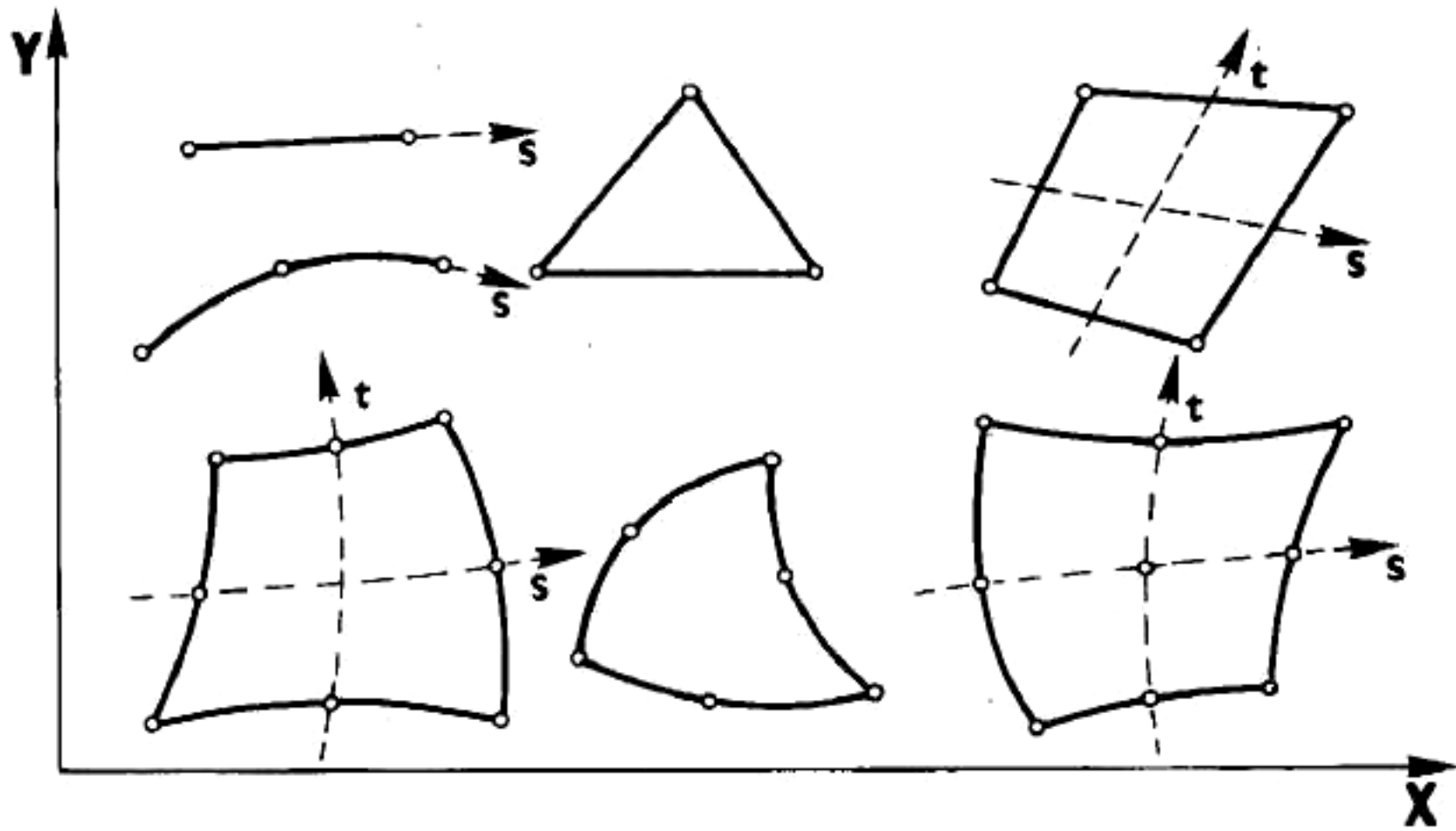
# Double Continuum Approach (DC)

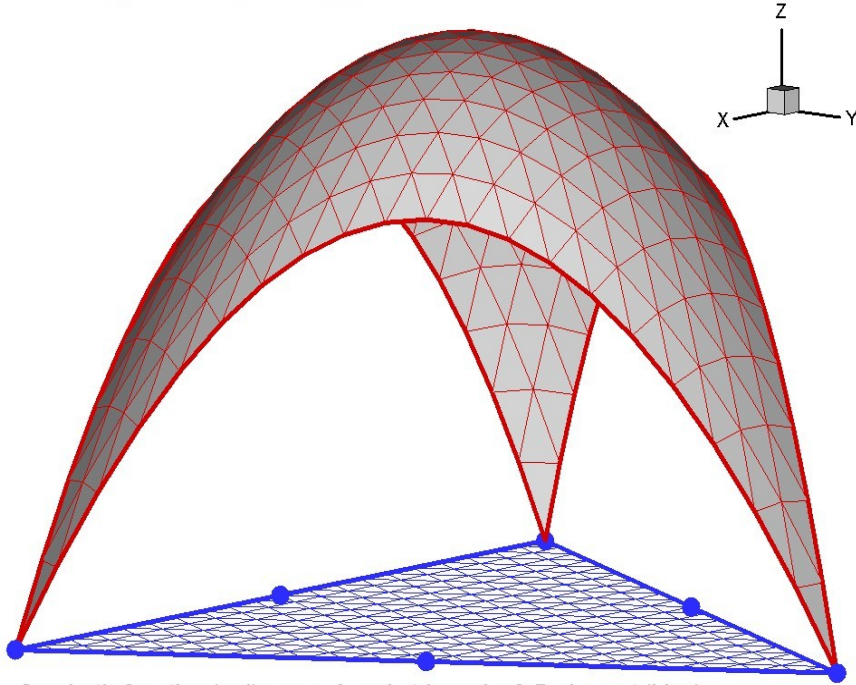


# EXAMPLE OF FINITE ELEMENT MODEL

**6: six-node quadratic triangle    8: eight-node quadratic rectangle**  
**- - - - - : three-node 1-D quadratic elements simulating faults**

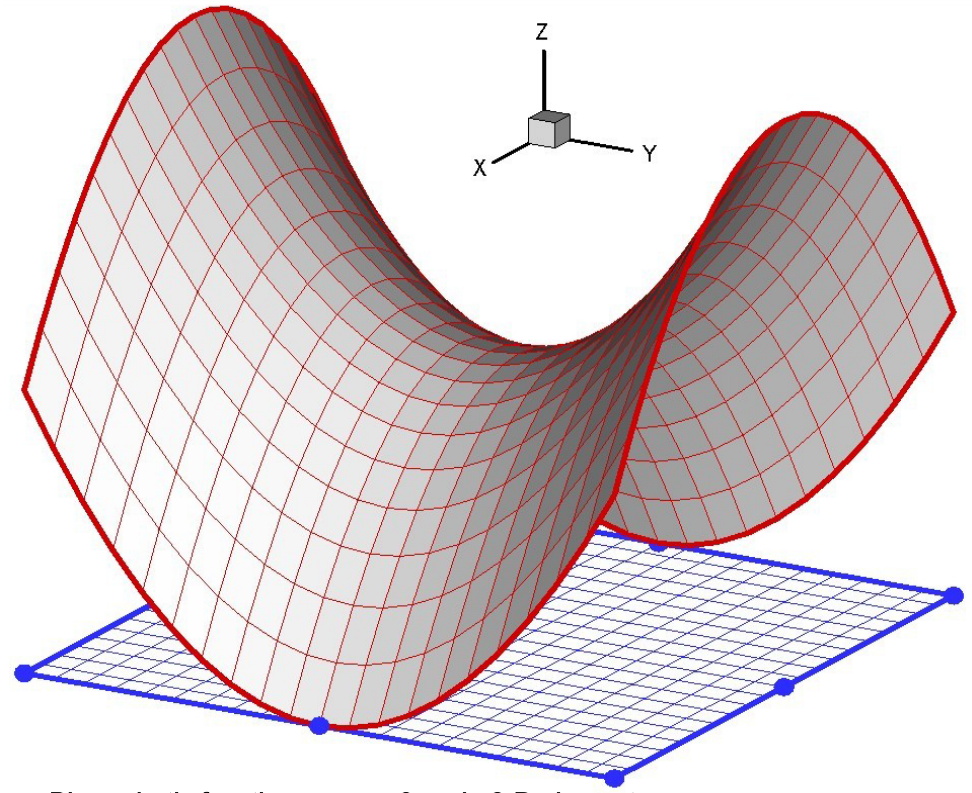






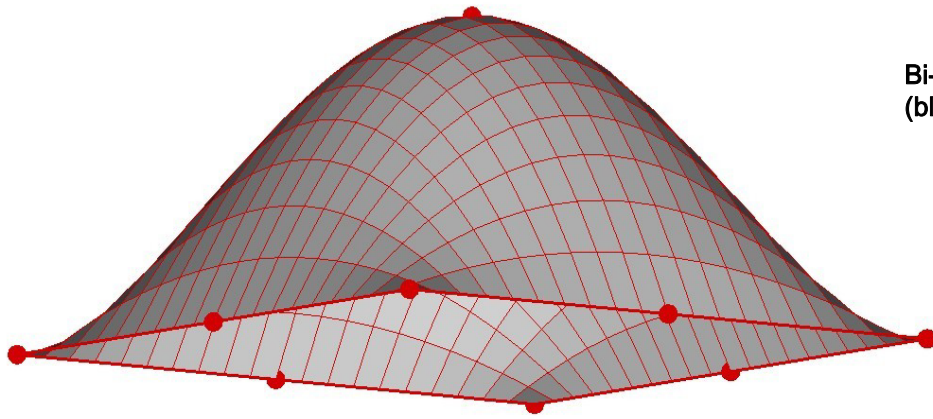
**Quadratic function (red) over a 6-node triangular 2-D element (blue)**

circles: nodal points on the 2-D element  
thin lines: local coordinate lines on the 2-D element



**Bi-quadratic function over an 8-node 2-D element**

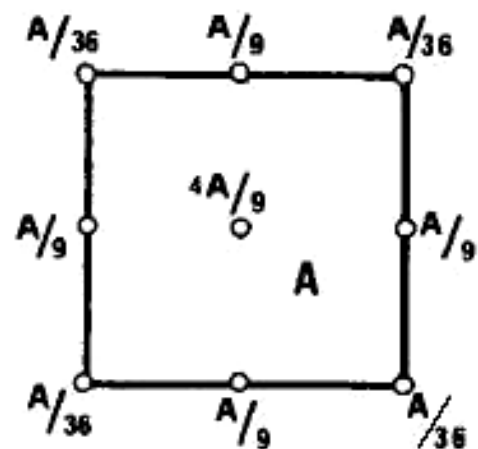
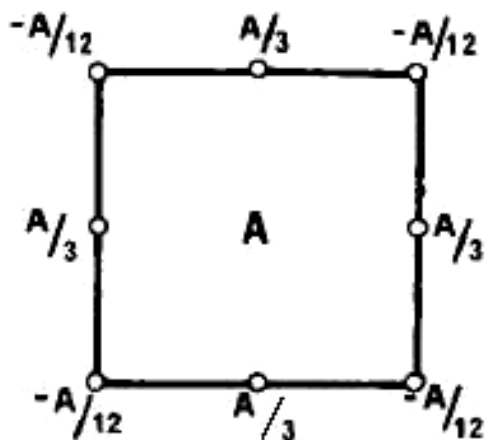
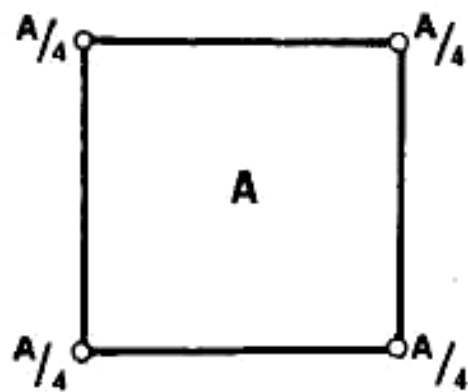
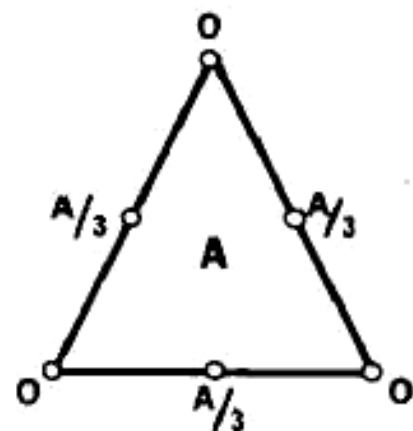
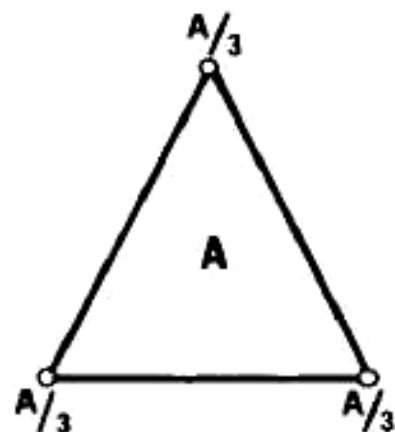
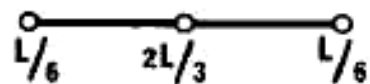
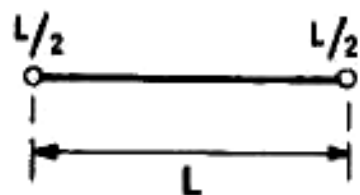
(blue) circles: nodal points on the 2-D element

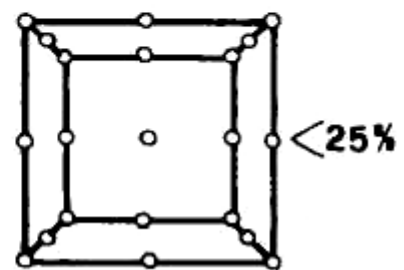
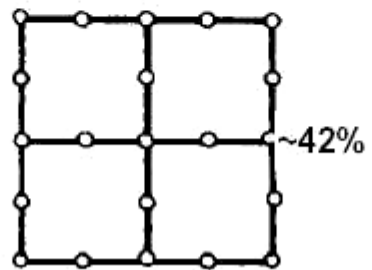
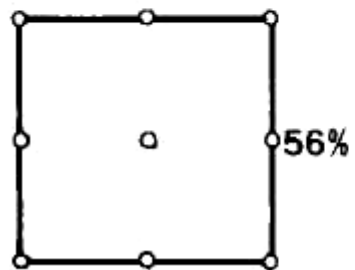
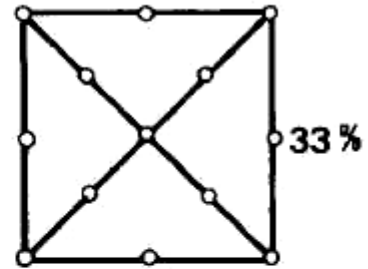
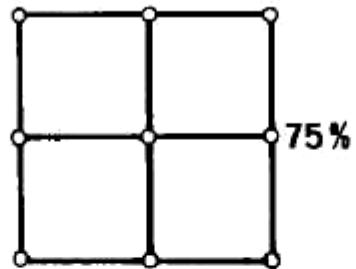
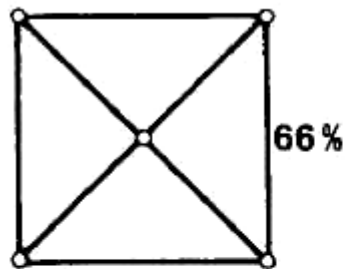


**Bi-quadratic function over a 9-node 2-D element**

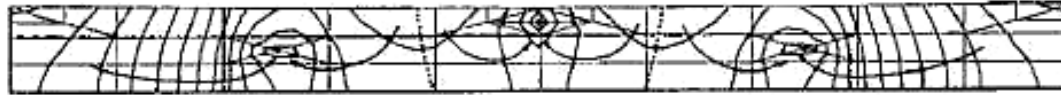
circles: nodal points of the 2-D element  
thin lines: local coordinate lines on the 2-D element

**Examples of quadratic functions over 2-D quadratic finite elements.**





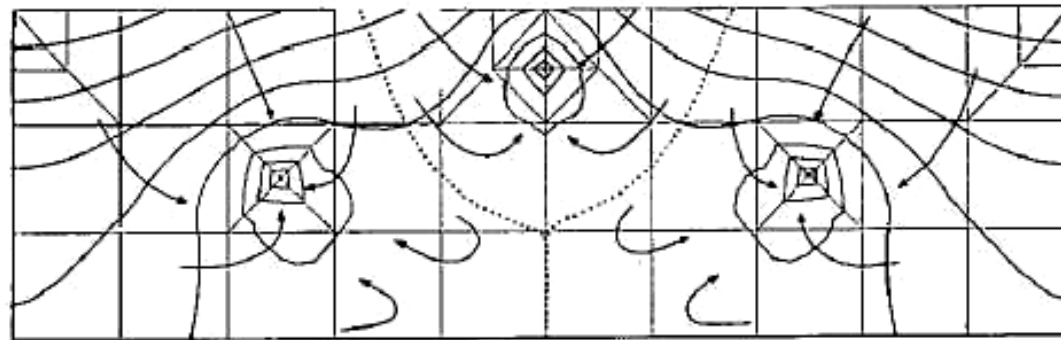
**a**

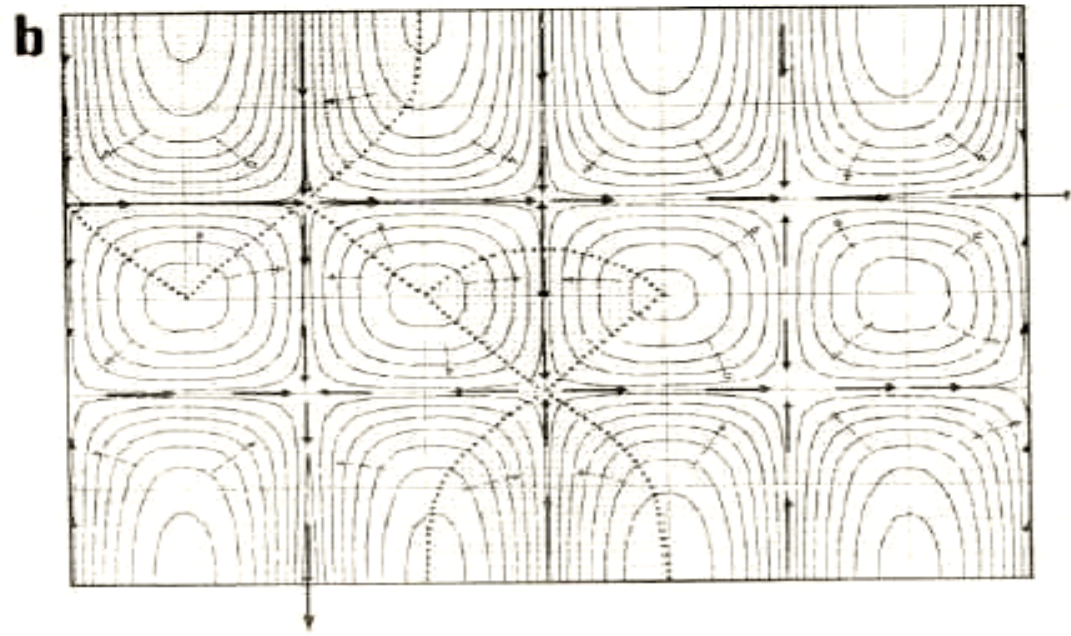
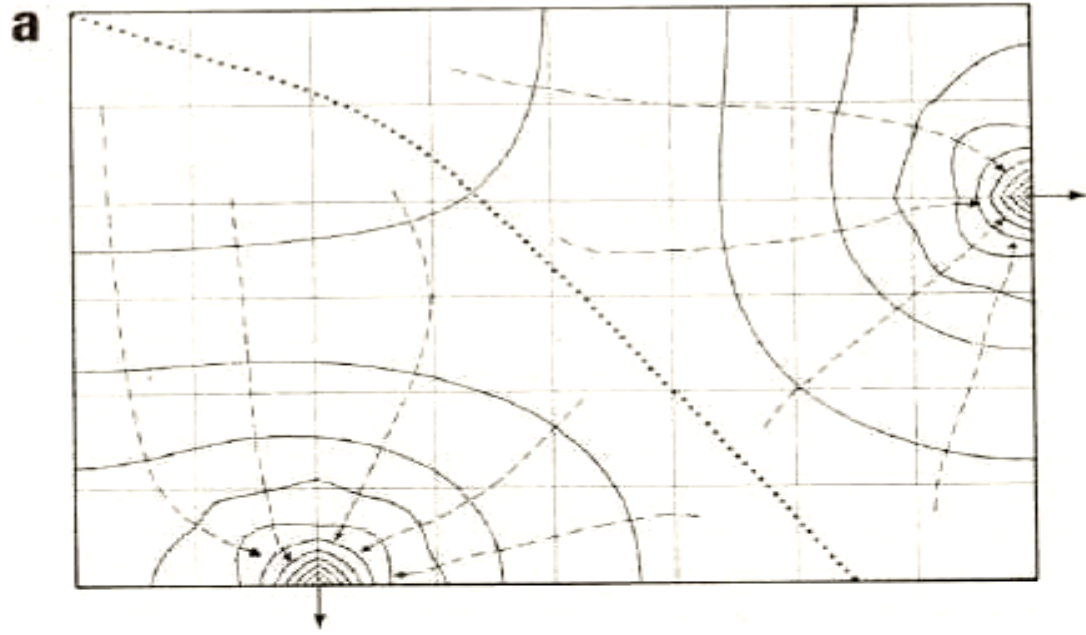


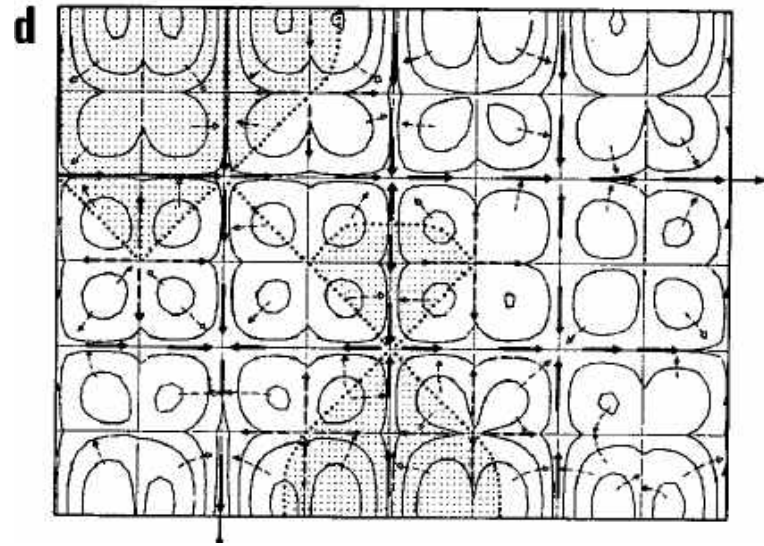
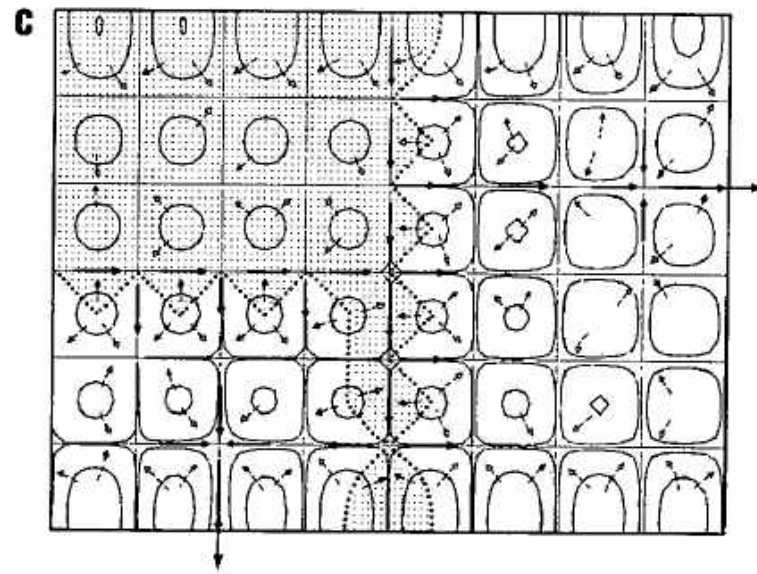
**b**



**c**







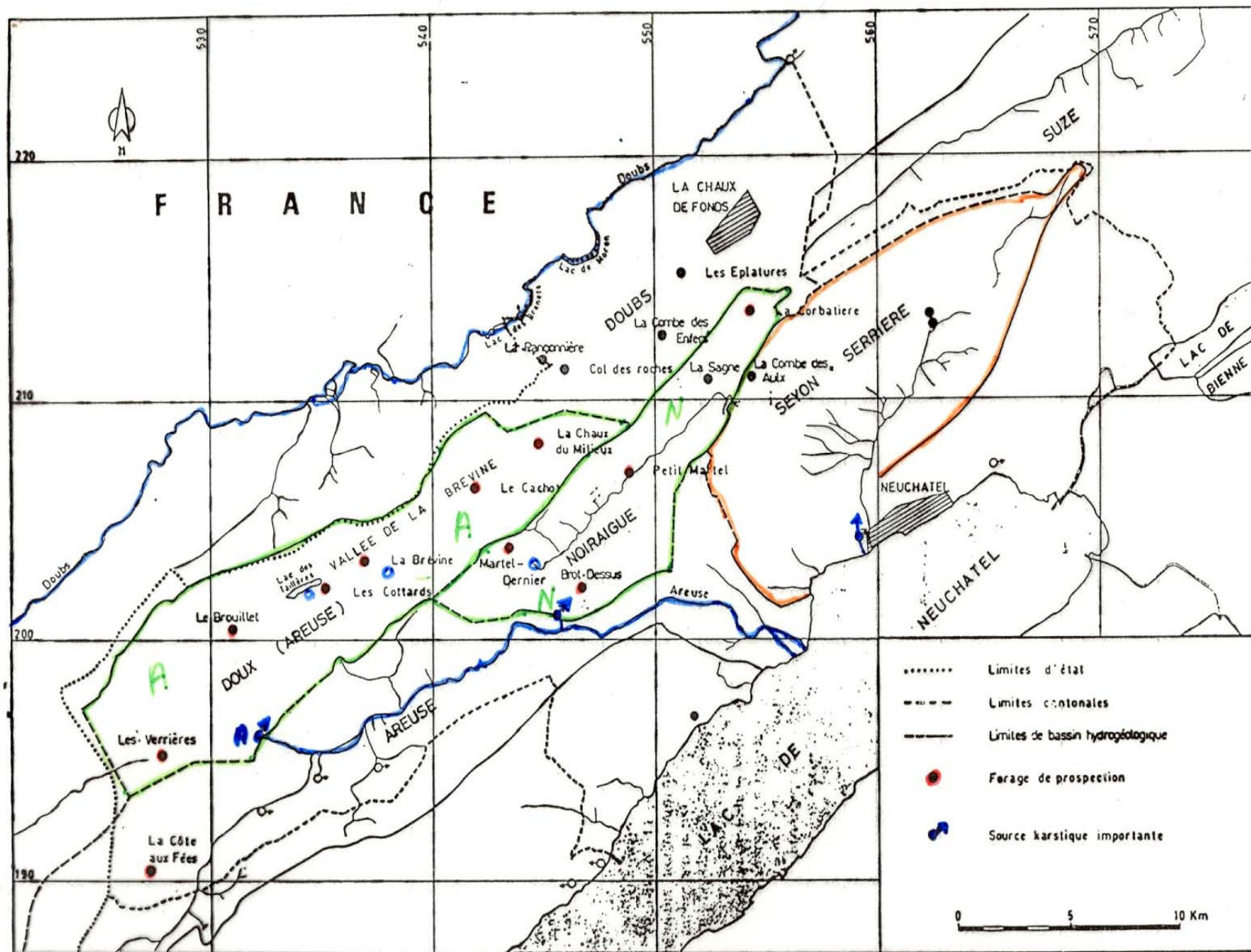
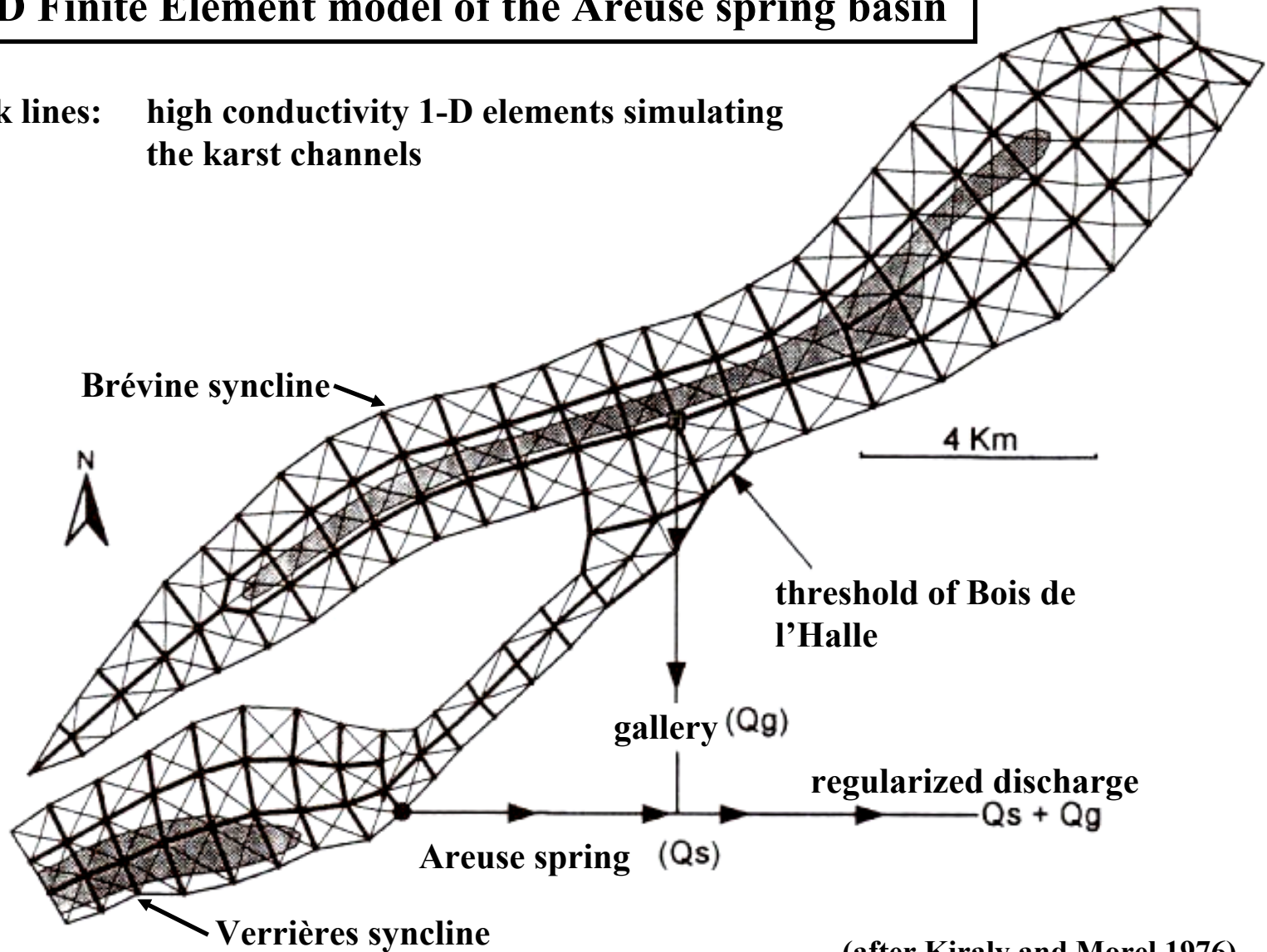


Fig. 1. Bassins hydrogéologiques importants, emplacement des forages profonds dans le canton de Neuchâtel et principales sources karstiques.

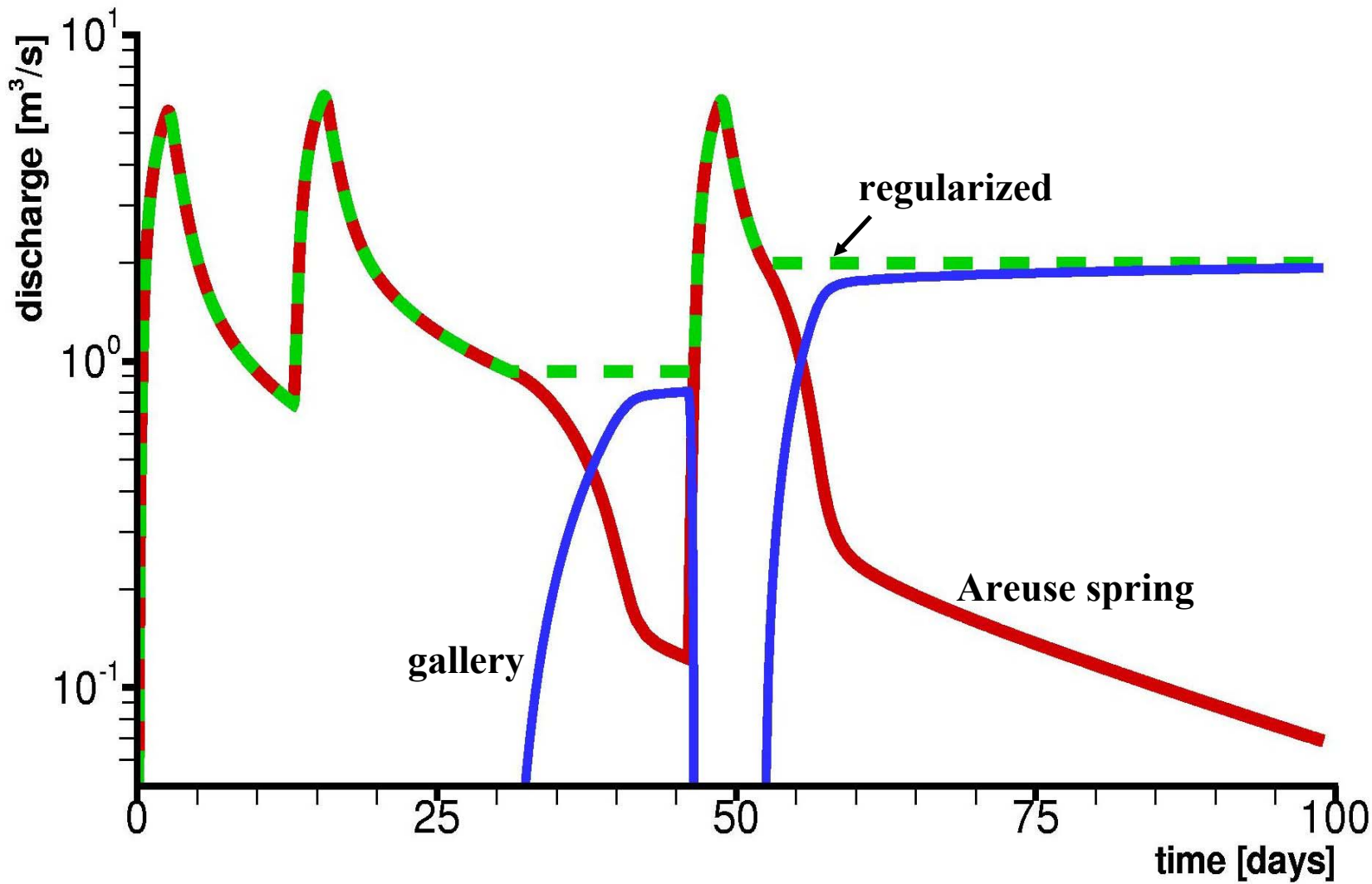
## 2-D Finite Element model of the Areuse spring basin

thick lines: high conductivity 1-D elements simulating the karst channels

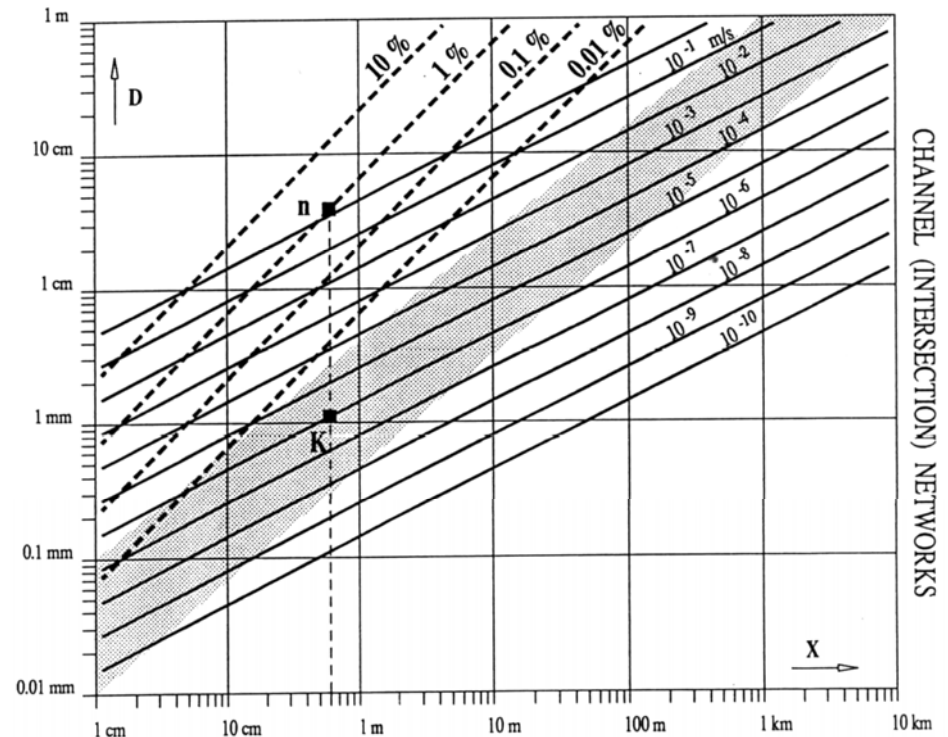
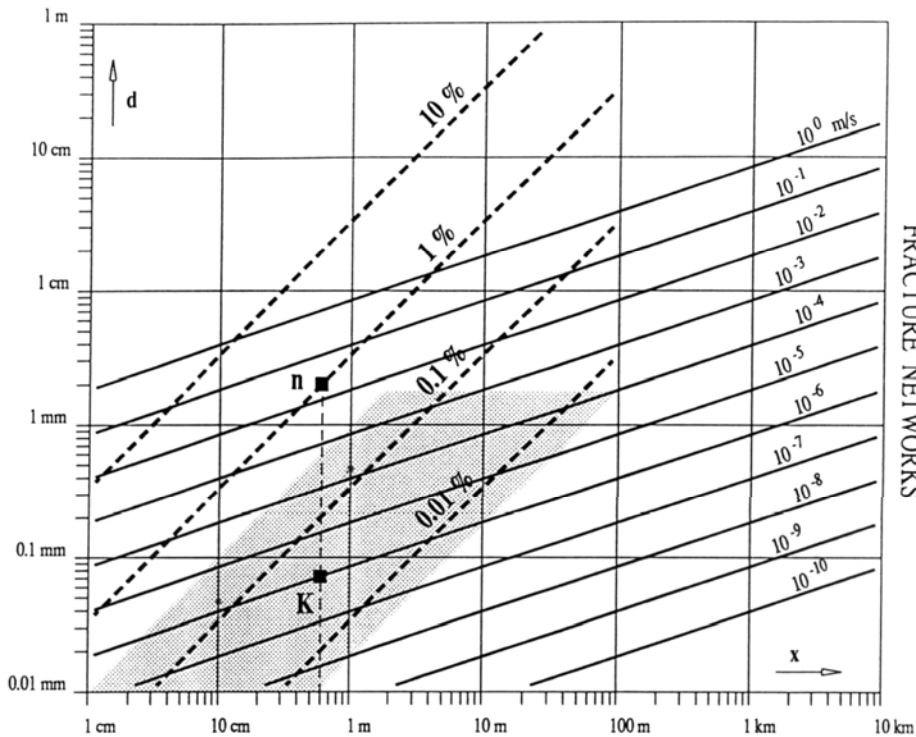


(after Kiraly and Morel 1976)

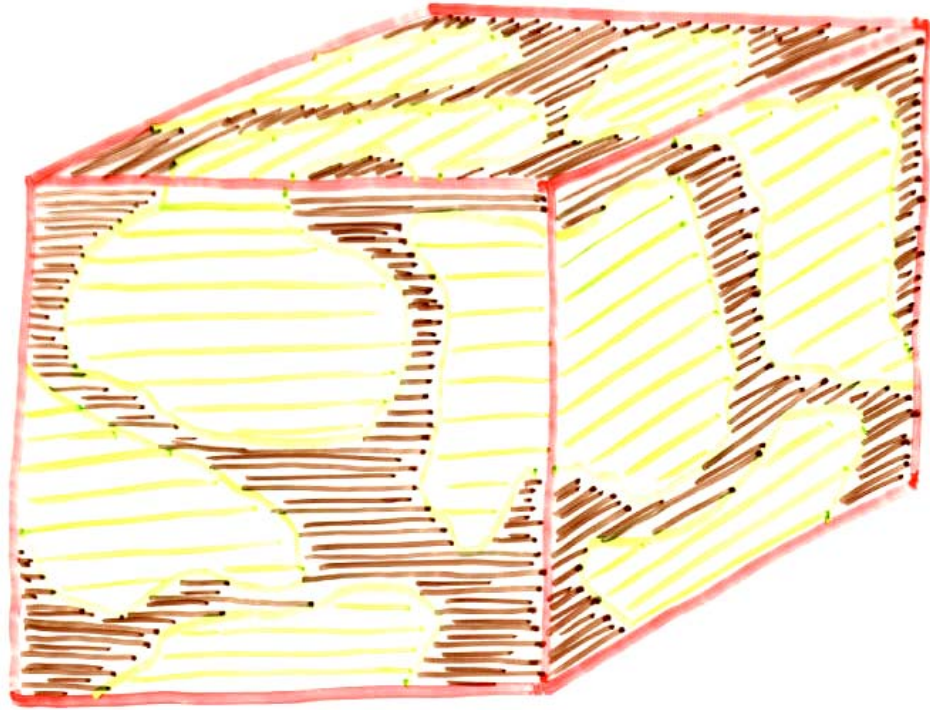
**Example of regularization of the Areuse river**



**Hydraulic conductivity and efficient porosity values for various networks of fractures (left) and intersections of fractures or karst channels (right)**



(after Kiraly 1975, modified)

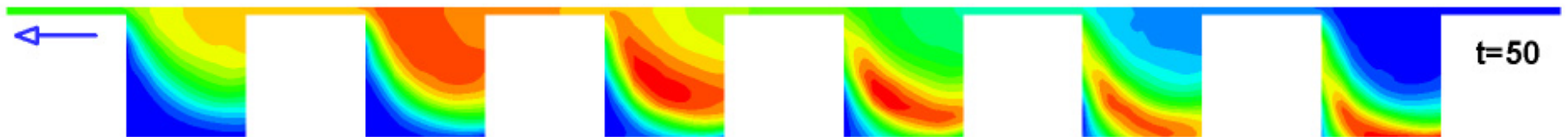
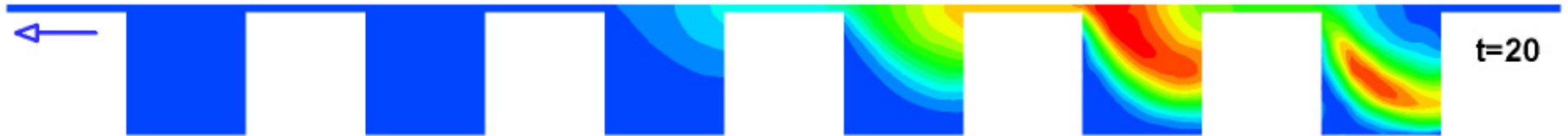
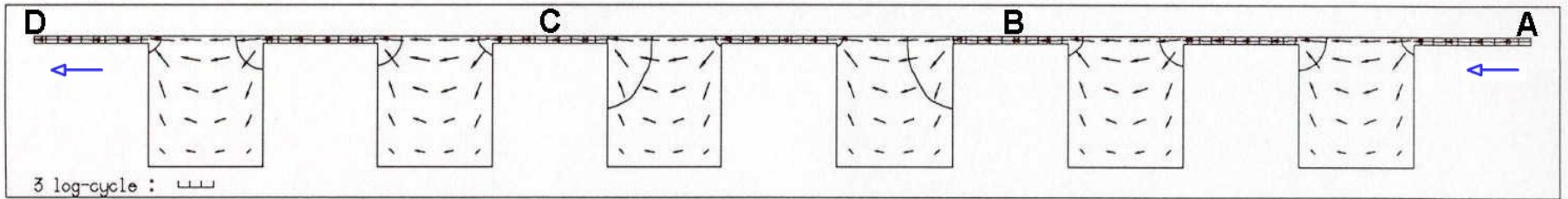


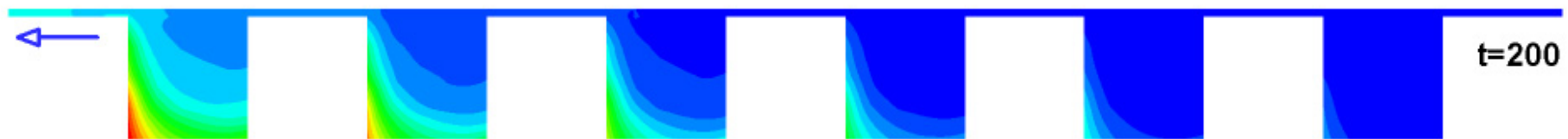
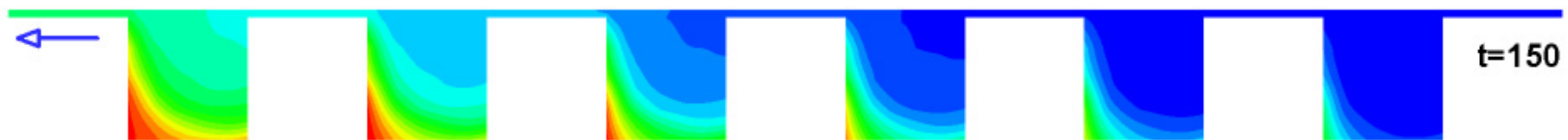
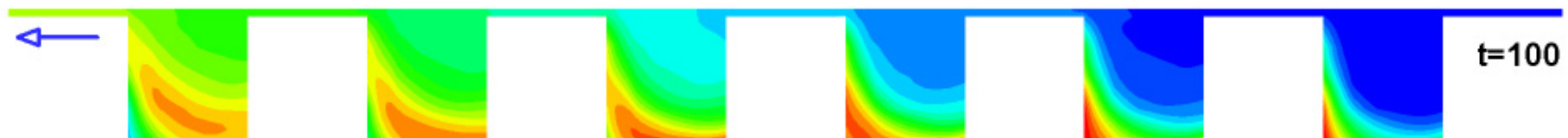
$K$  is controlled by the intersections —

$\epsilon_e$  is controlled by the openings  
in the fracture planes

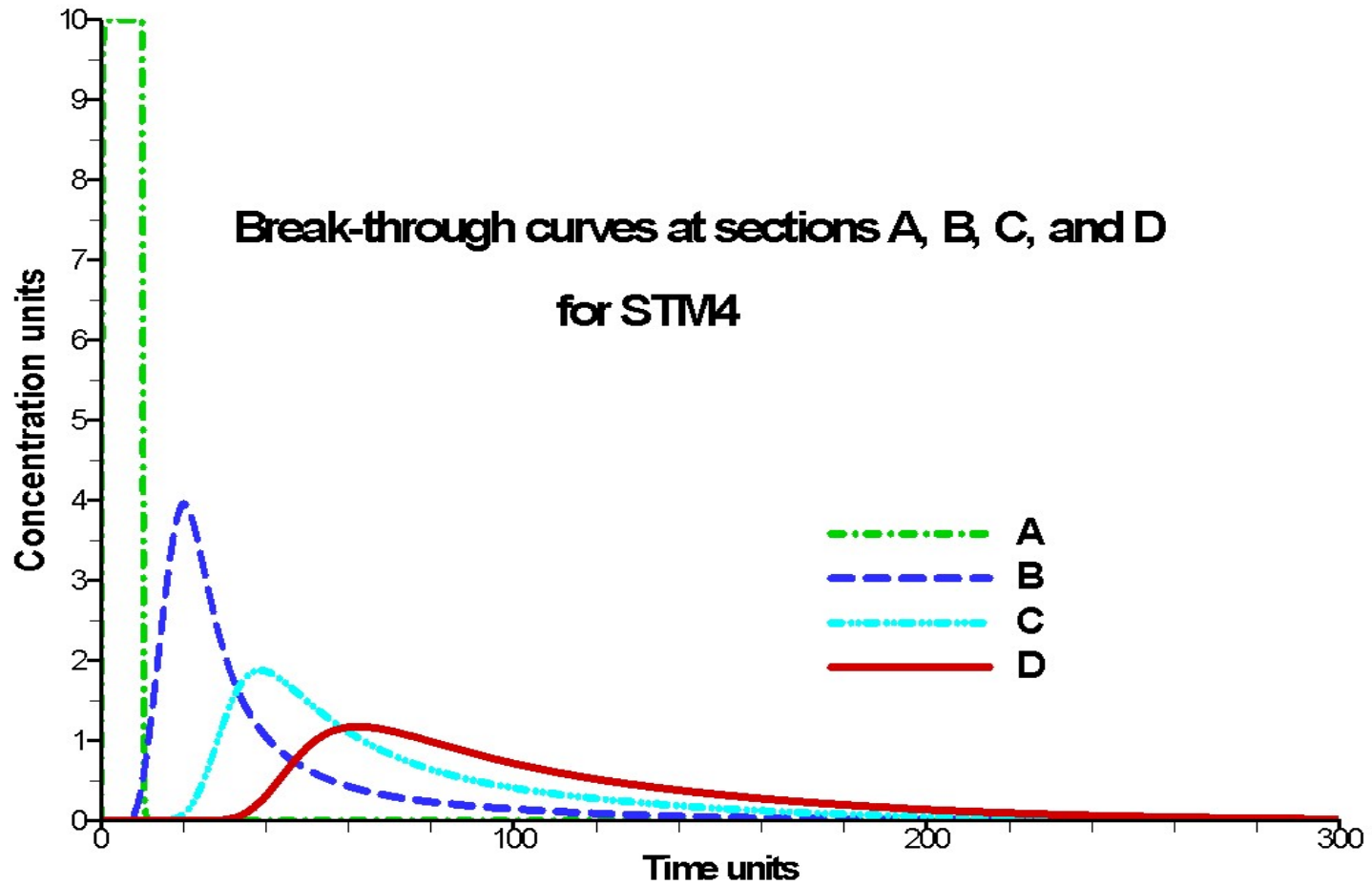
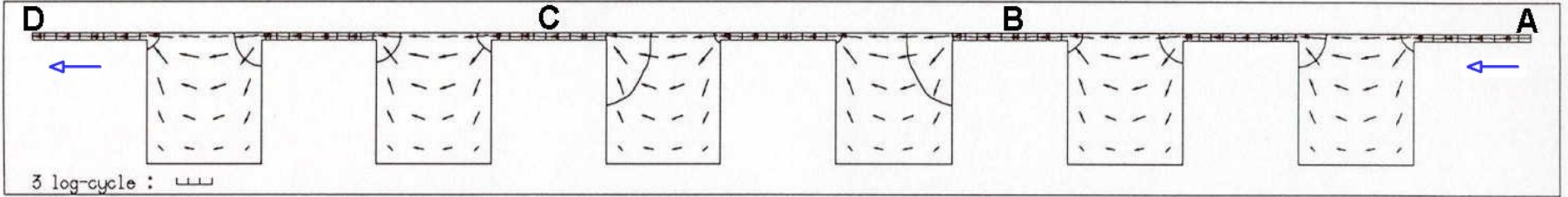


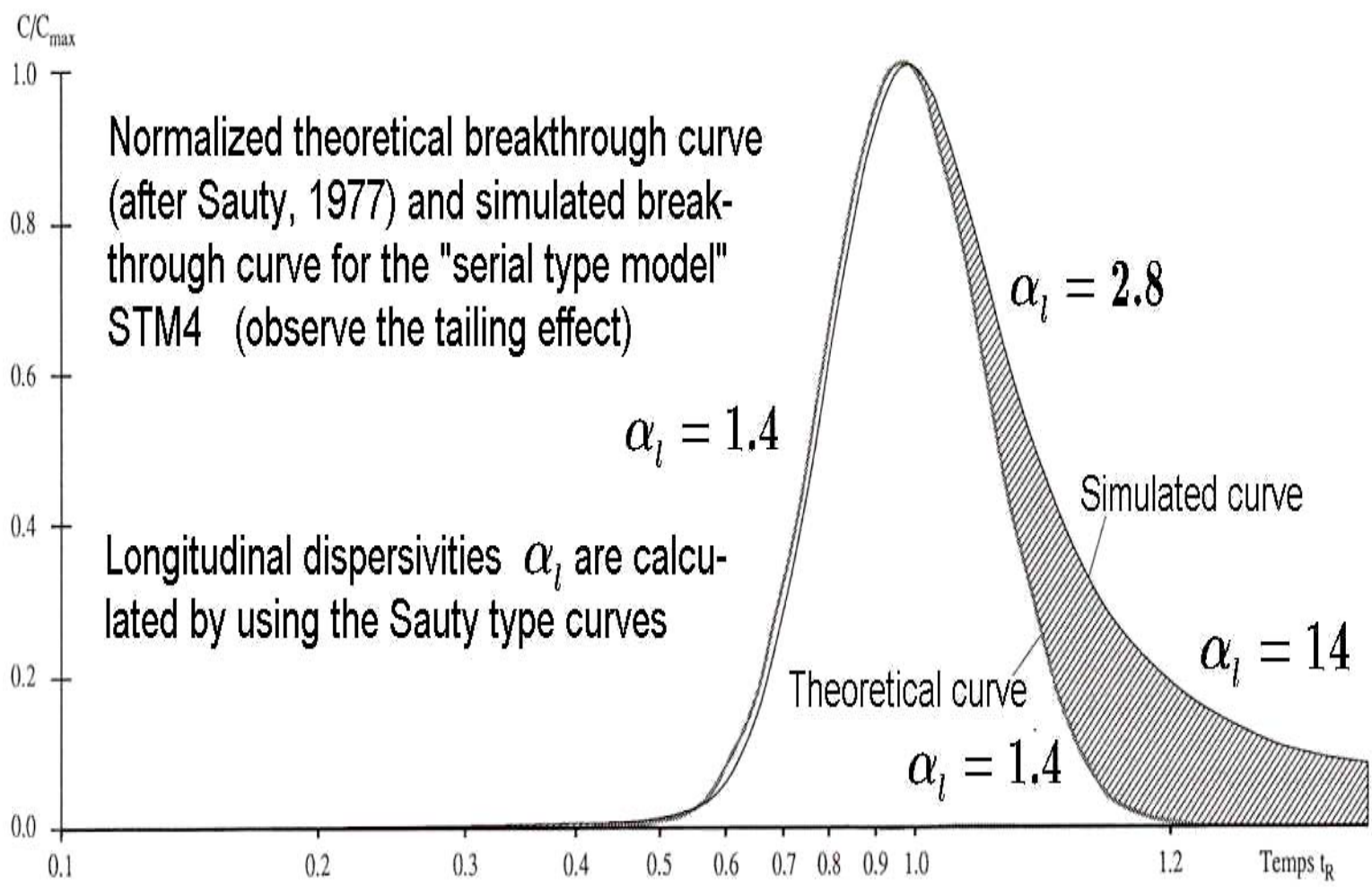
STM4 - "SERIAL TYPE MODEL" (FLOW PATTERNS)



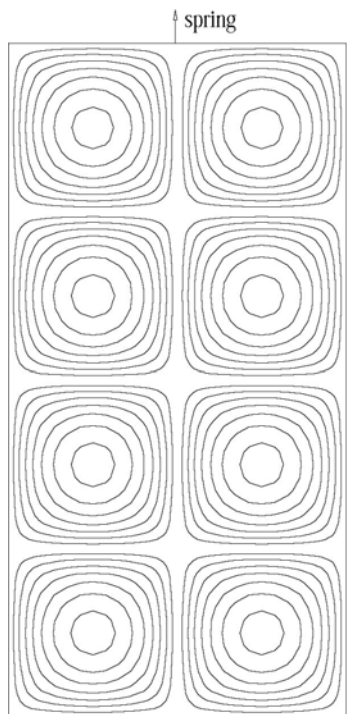


STM4 - "SERIAL TYPE MODEL" (FLOW PATTERNS)

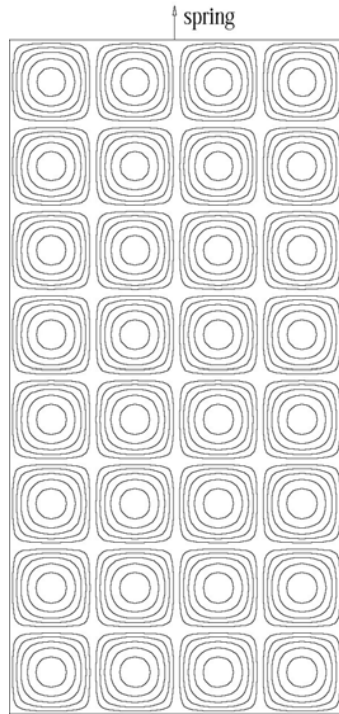




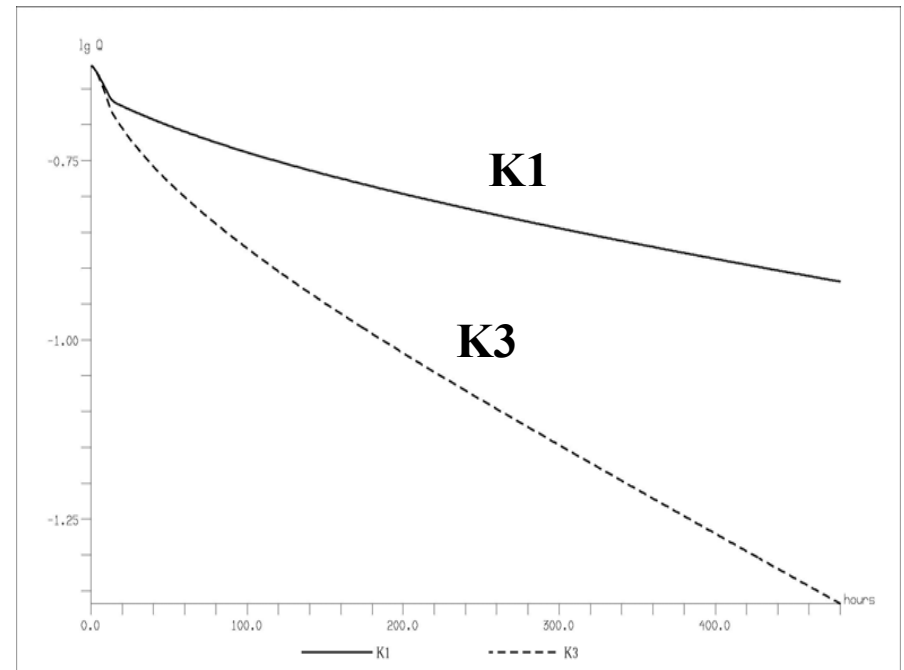
# Effect of the density of the high conductivity drainage network on the recession curve of karst springs.

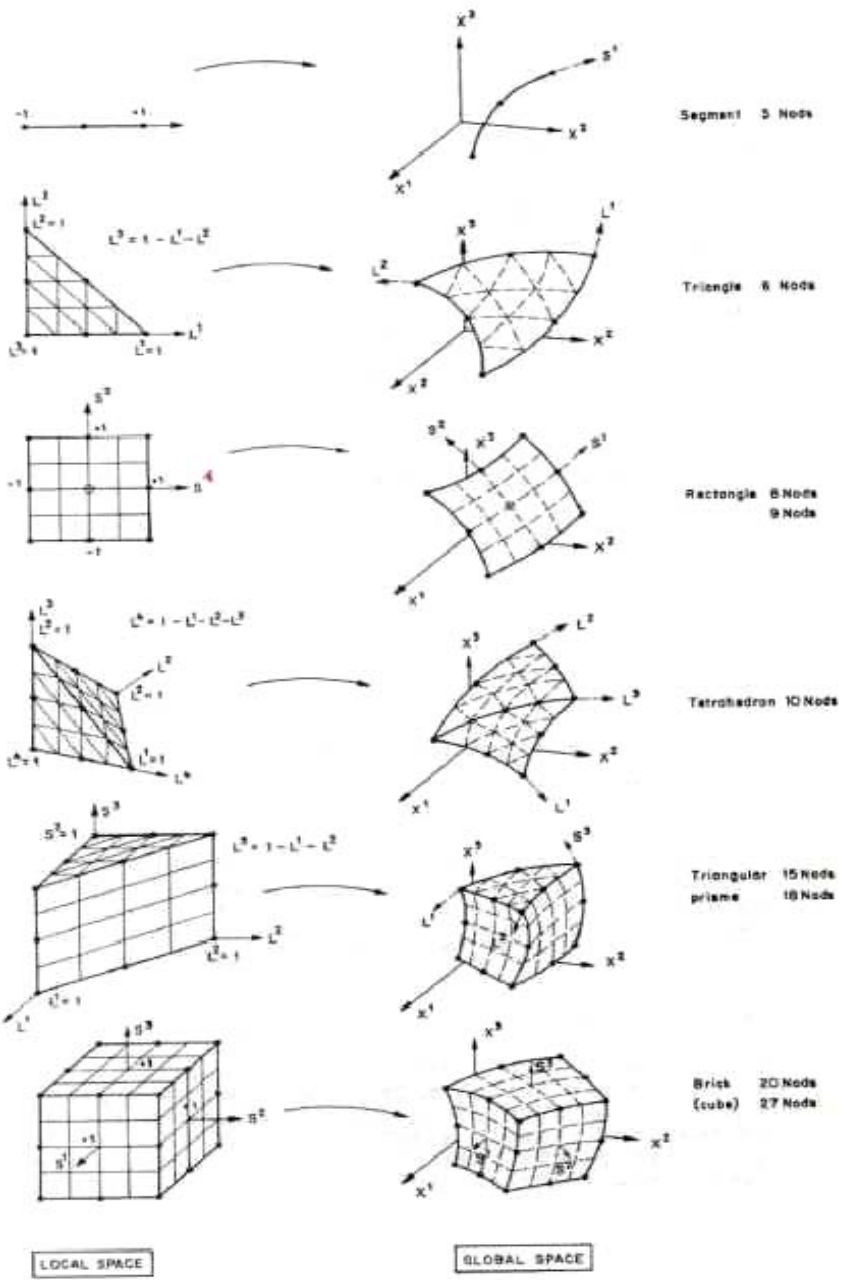


K1 (Karst net spacing: 1.0 km)



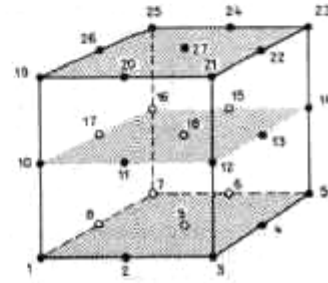
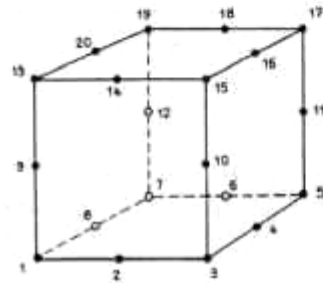
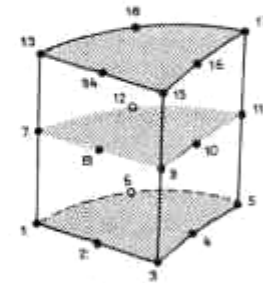
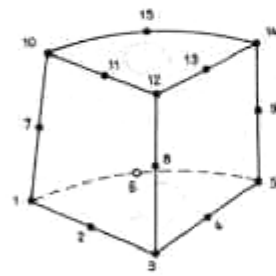
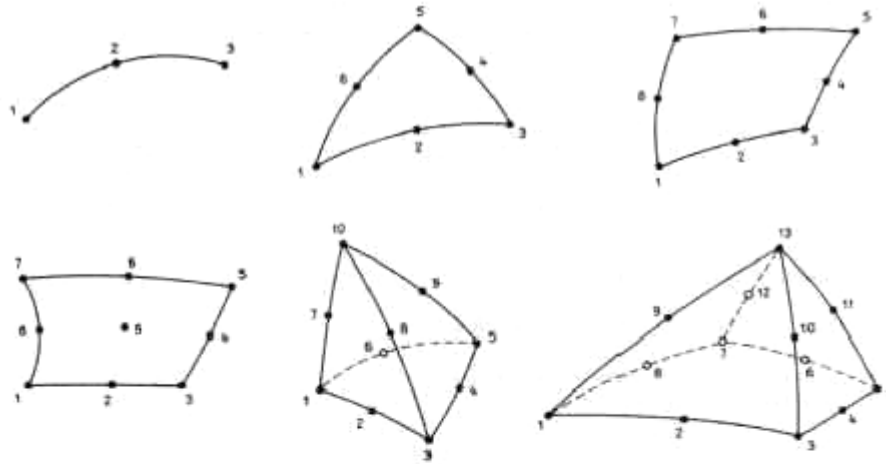
K3 (Karst net spacing: 0.5 km)

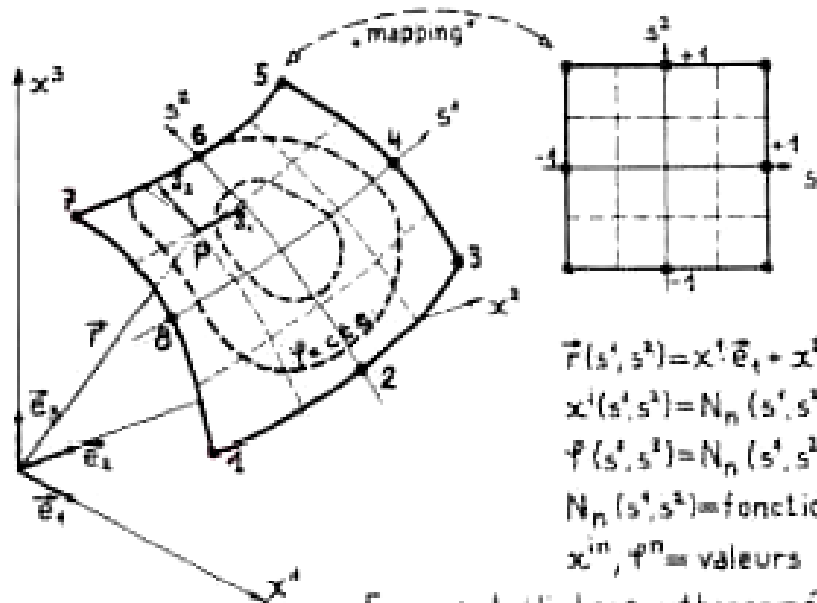




LOCAL SPACE

GLOBAL SPACE





$$\vec{r}(s^1, s^2) = x^1 \vec{e}_1 + x^2 \vec{e}_2 + x^3 \vec{e}_3$$

$$x^i(s^1, s^2) = N_n(s^1, s^2) \cdot x^{in} \quad n=1,8; \quad i=1,3$$

$$f(s^1, s^2) = N_n(s^1, s^2) \cdot f^n \quad n=1,8$$

$N_n(s^1, s^2)$  = fonctions d'interpolation

$x^{in}, f^n$  = valeurs nodales

Espace tridi: base orthonormée  $(\vec{e}_i)$

Espace bidi: base covariante  $(\vec{a}_k)$   $\vec{a}_k = \partial \vec{r} / \partial s^k$

Tenseur métrique contravariant  $g^{ik} = g_{ik}^{-1} = [\vec{a}_i \cdot \vec{a}_k]^{-1}$

$$\text{grad } \Psi = \frac{\partial \vec{r}}{\partial s^k} \cdot g^{ik} \cdot \frac{\partial \Psi}{\partial s^i}$$

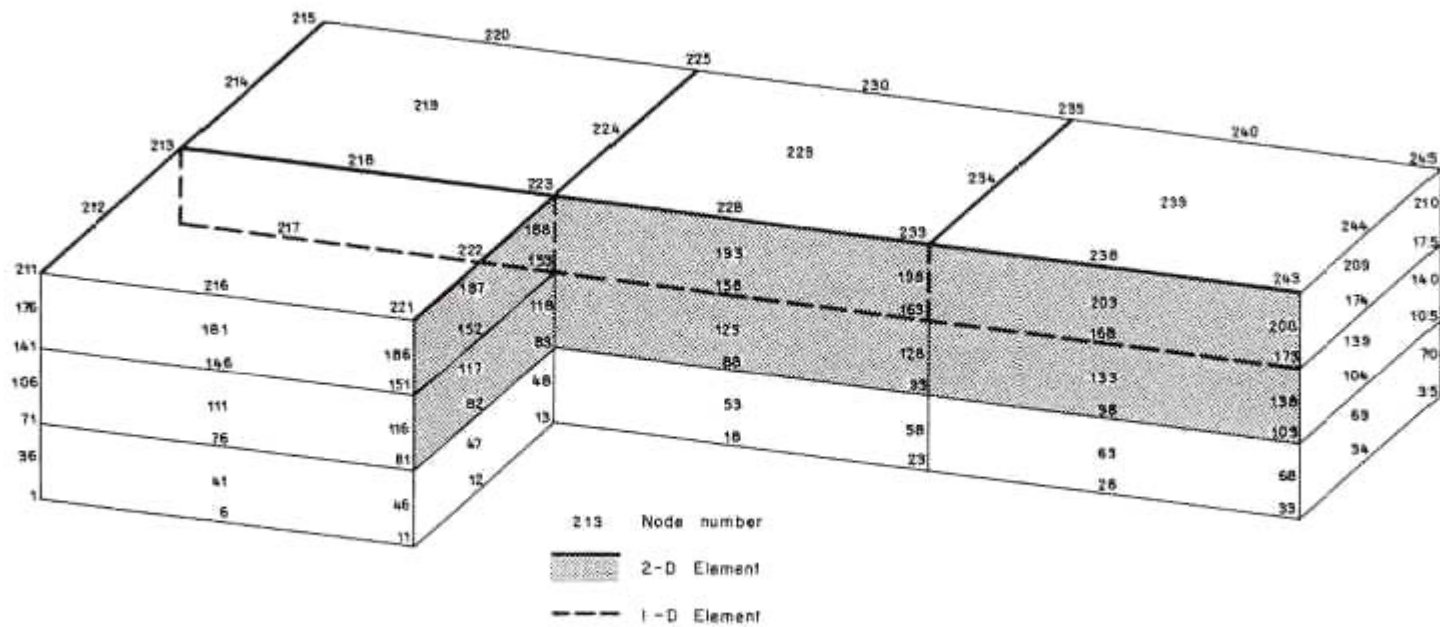
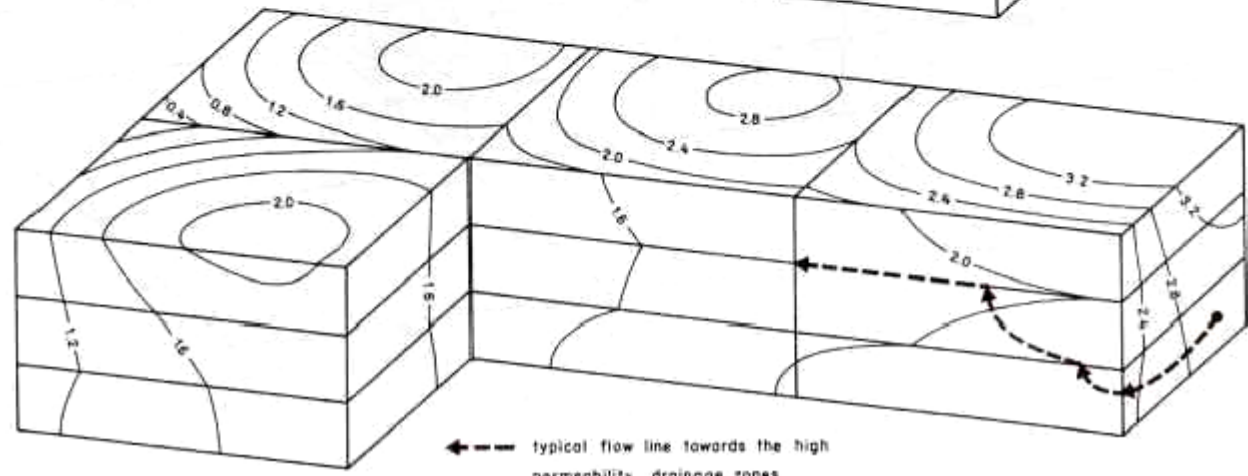
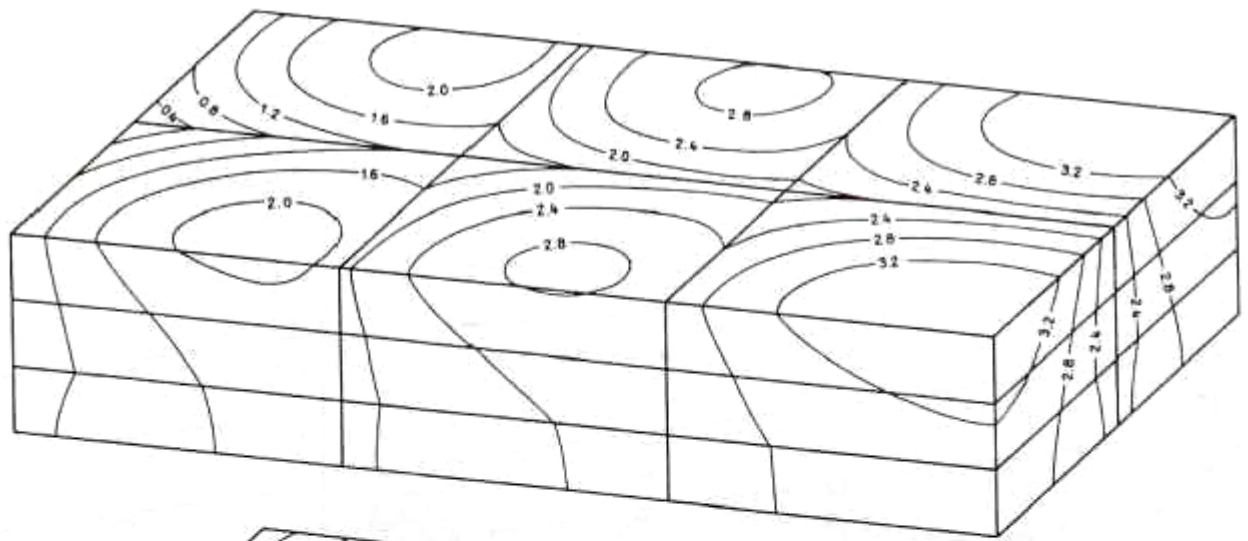
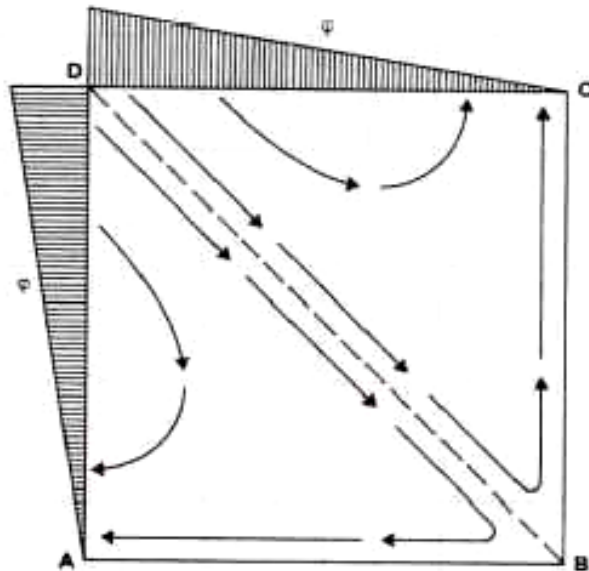


Figure 7-1: Three-Dimensional Fractured Block Model with 1-D, 2-D and 3-D Elements



←--- typical flow line towards the high permeability drainage zones



$$\begin{aligned} \psi_A &= \psi_C = 0 \quad [\text{m}] \\ \psi_D &= 2 \quad [\text{m}] \\ K &= 1 \quad [\text{m/s}] \\ q_n &= 0 \quad \text{on AB and BC.} \end{aligned}$$

Figure 7-10: Boundary conditions for large element example

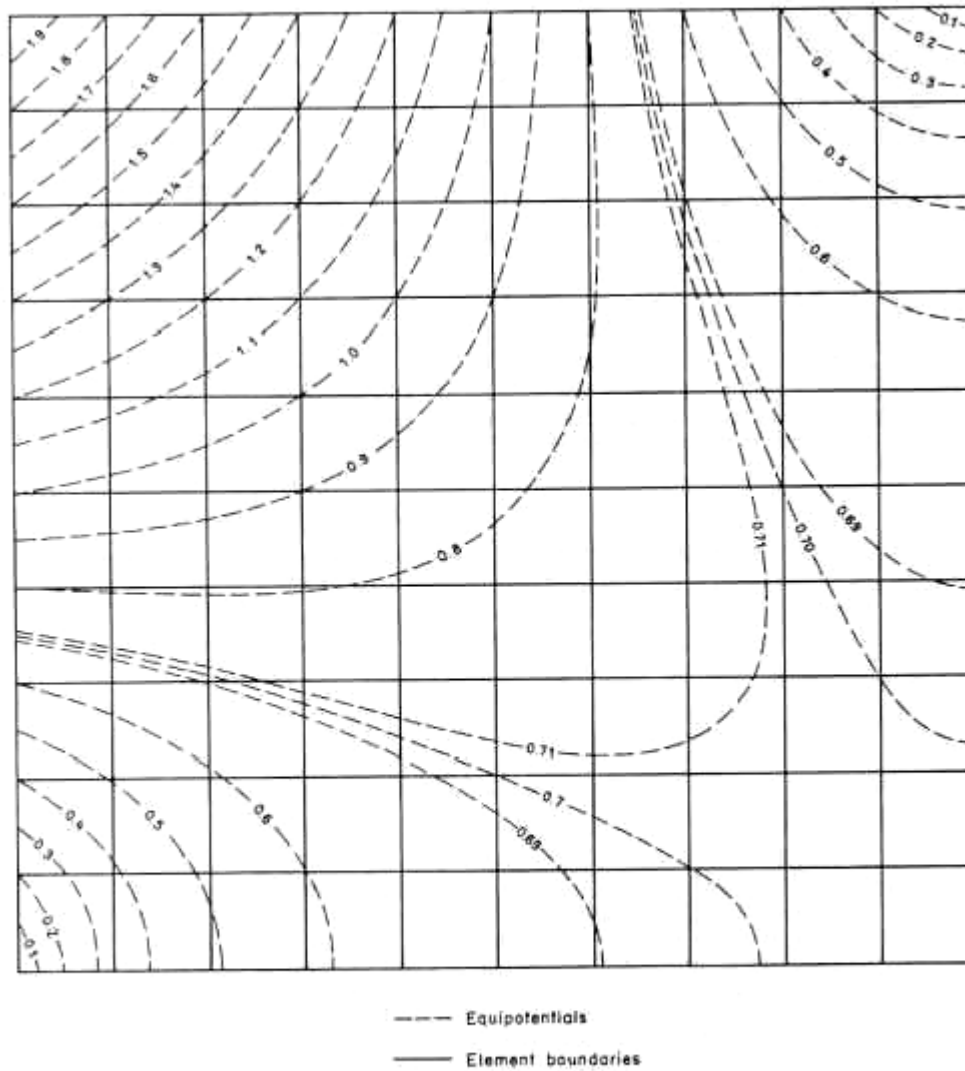


Figure 7-11: Results of large element example  
a) "Exact" solution

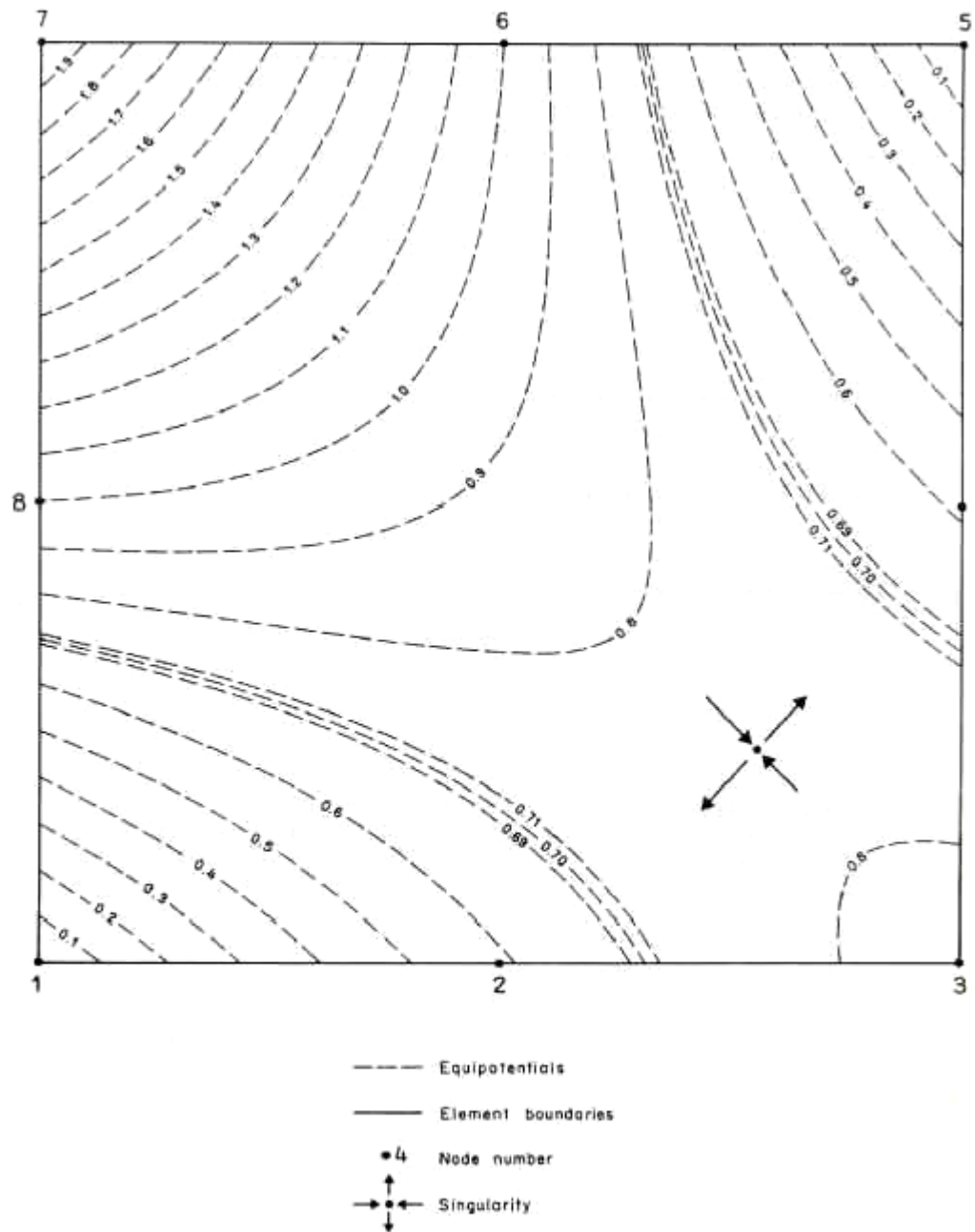
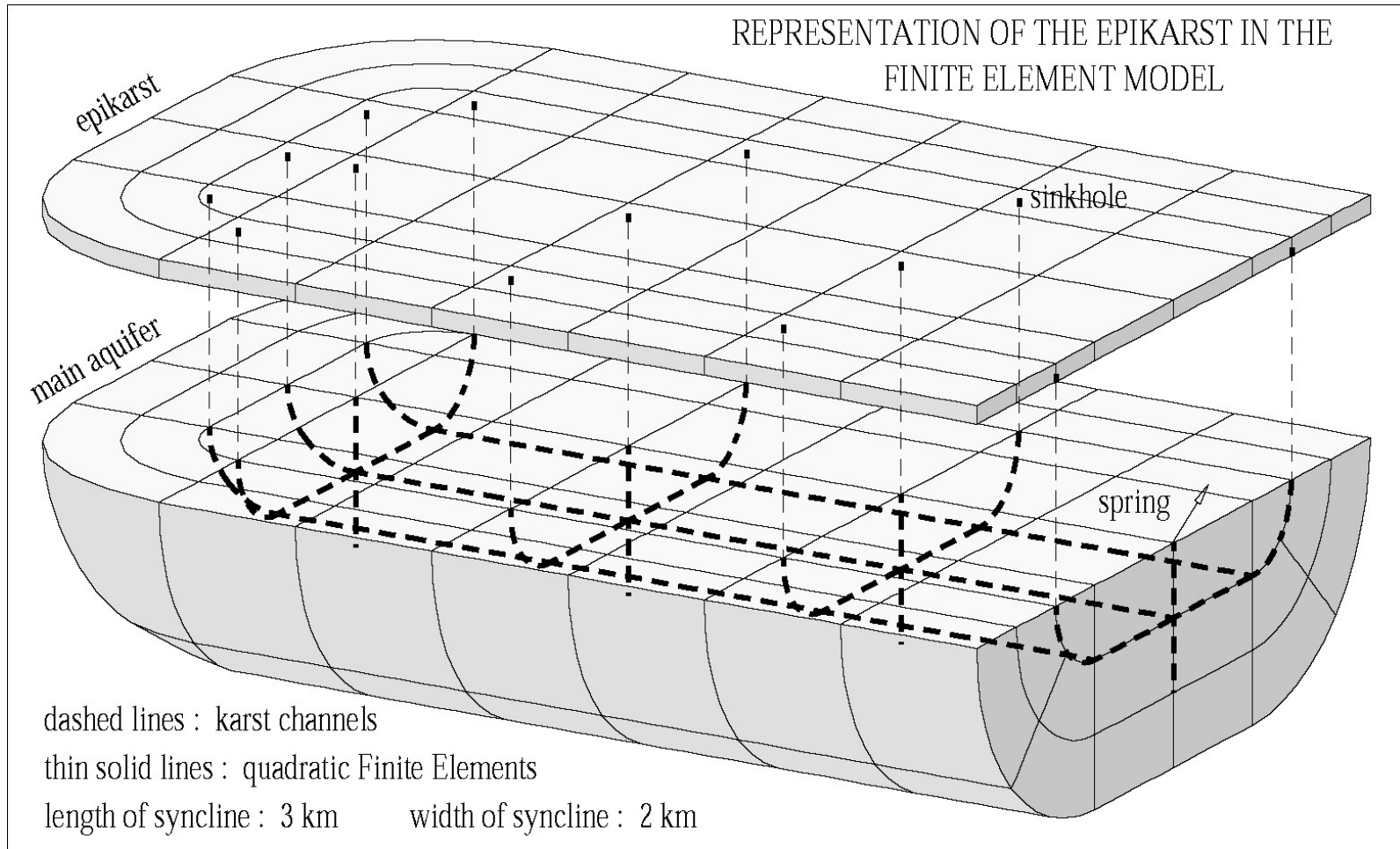
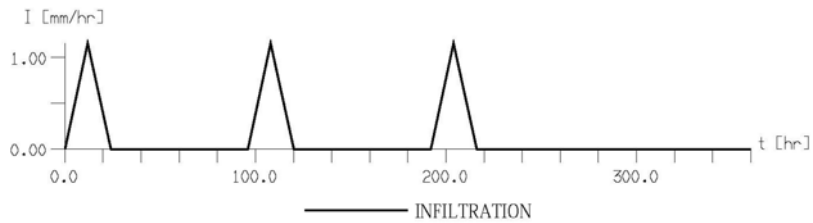


Figure 7-11: Results of large element example  
 b) Single element solution

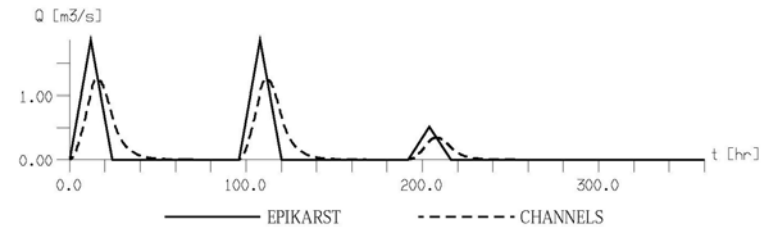
# Representation of the epikarst in the Finite Element model



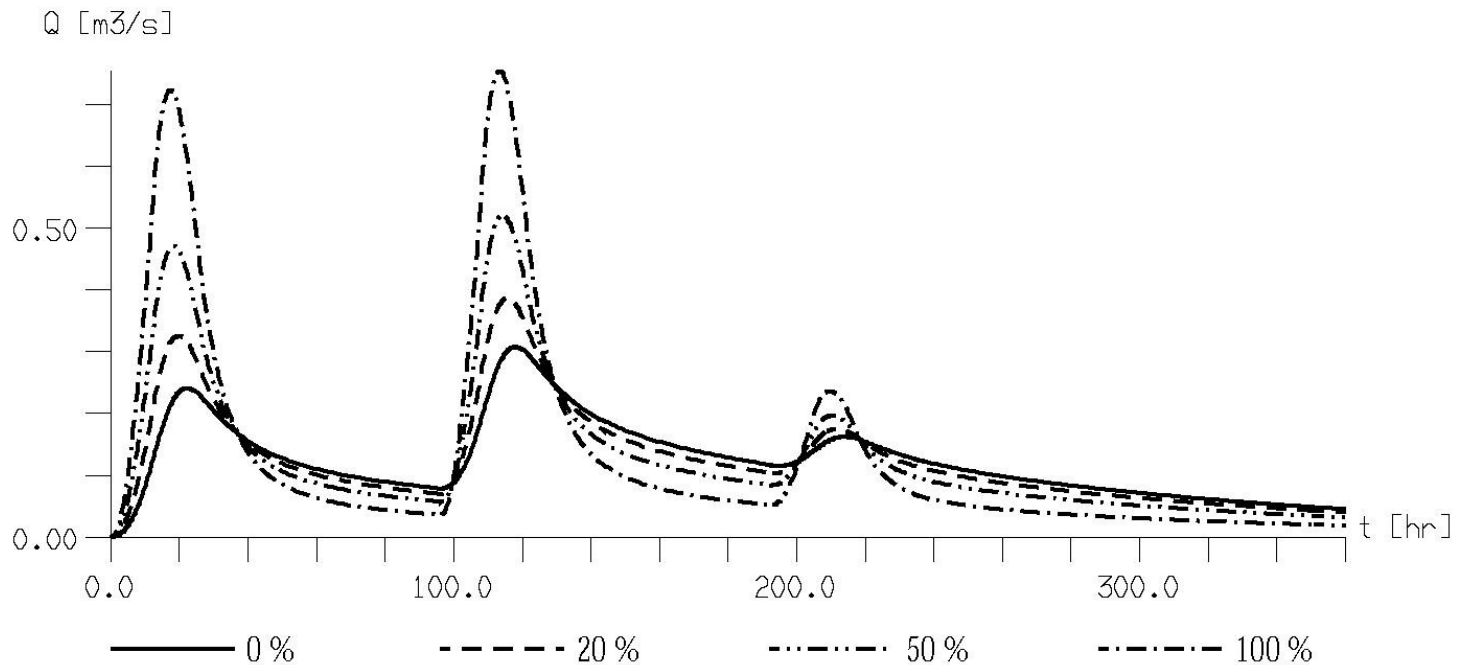
Infiltration function used in the model. The intensity is given in (mm/hr)



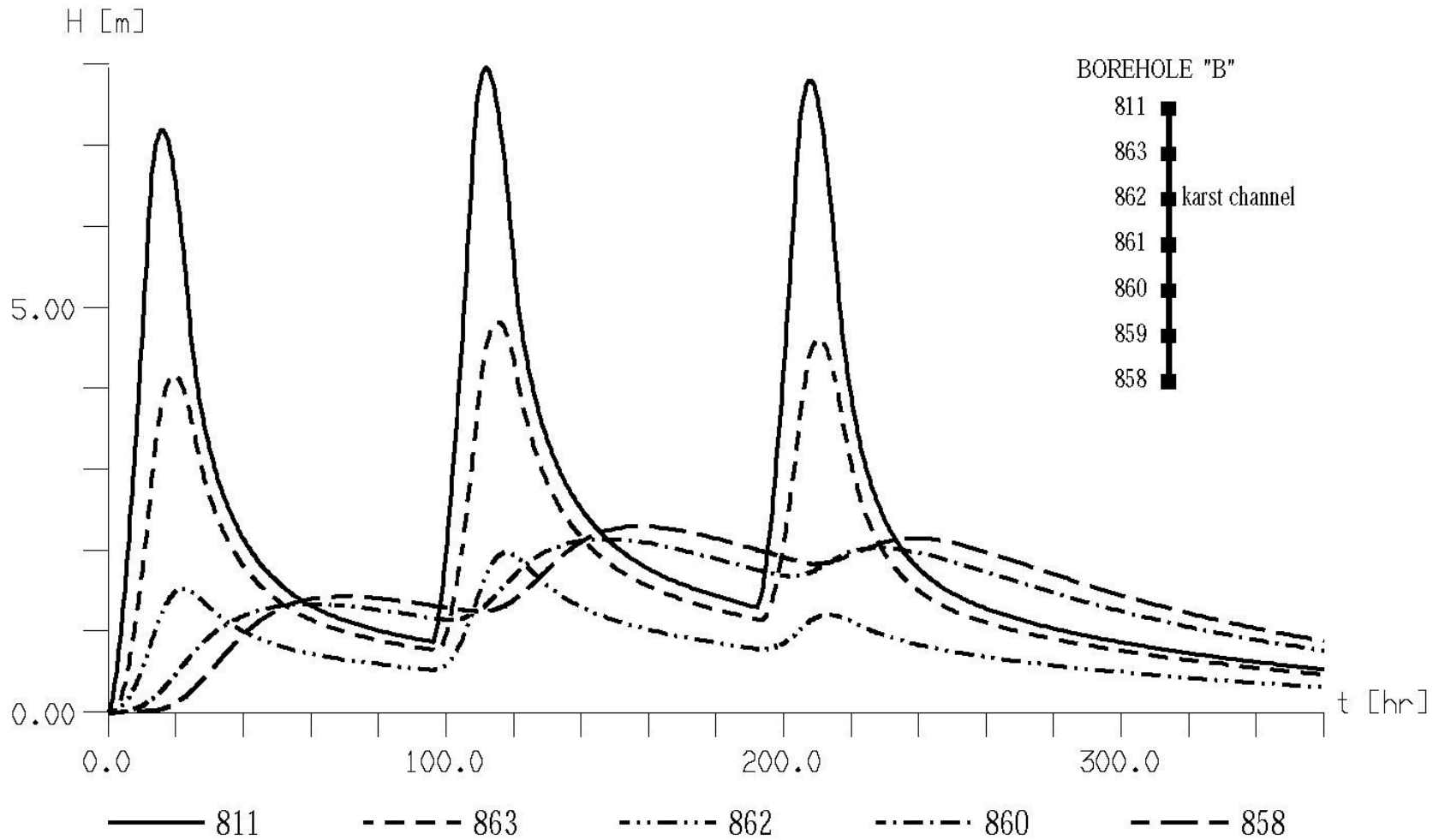
DSYN100: Infiltration in the epikarst and concentrated recharge of the channels



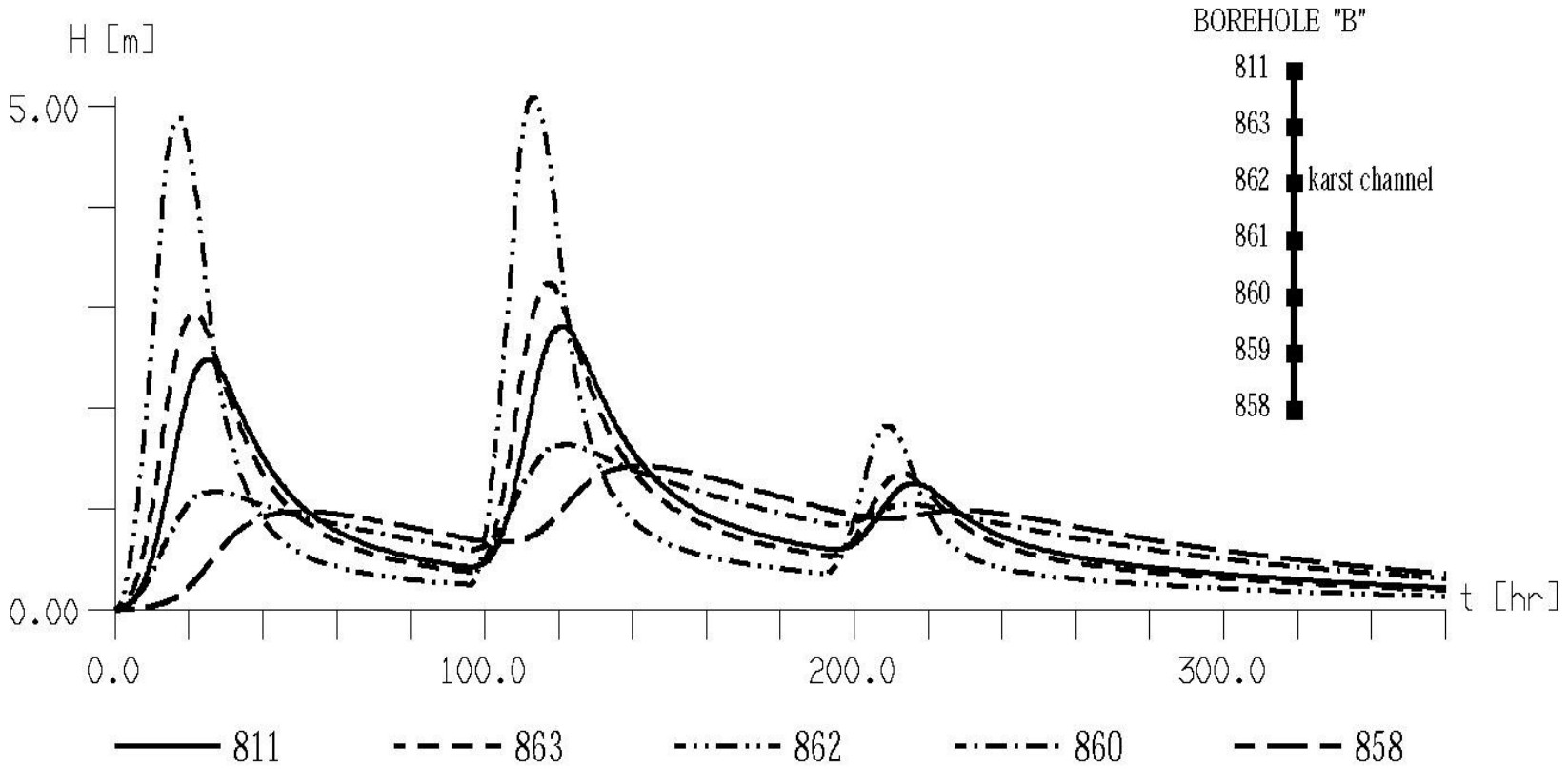
Spring discharge for different proportions of infiltration drained by the epikarst



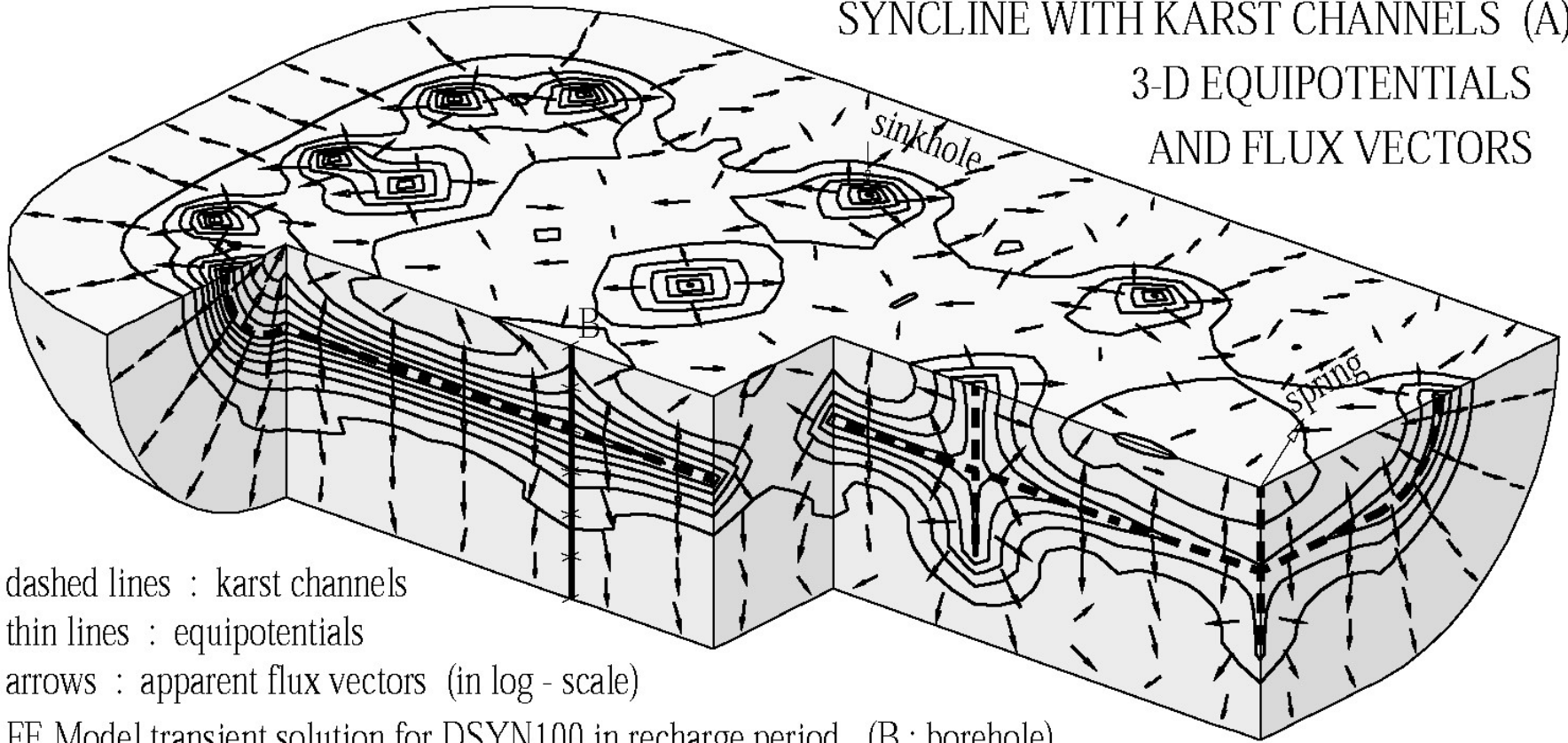
# DSYN0 without epikarst. Hydraulic heads in borehole "B".



# DSYN100 with epikarst. Hydraulic heads in borehole "B".



SYNCLINE WITH KARST CHANNELS (A)  
3-D EQUIPOTENTIALS  
AND FLUX VECTORS



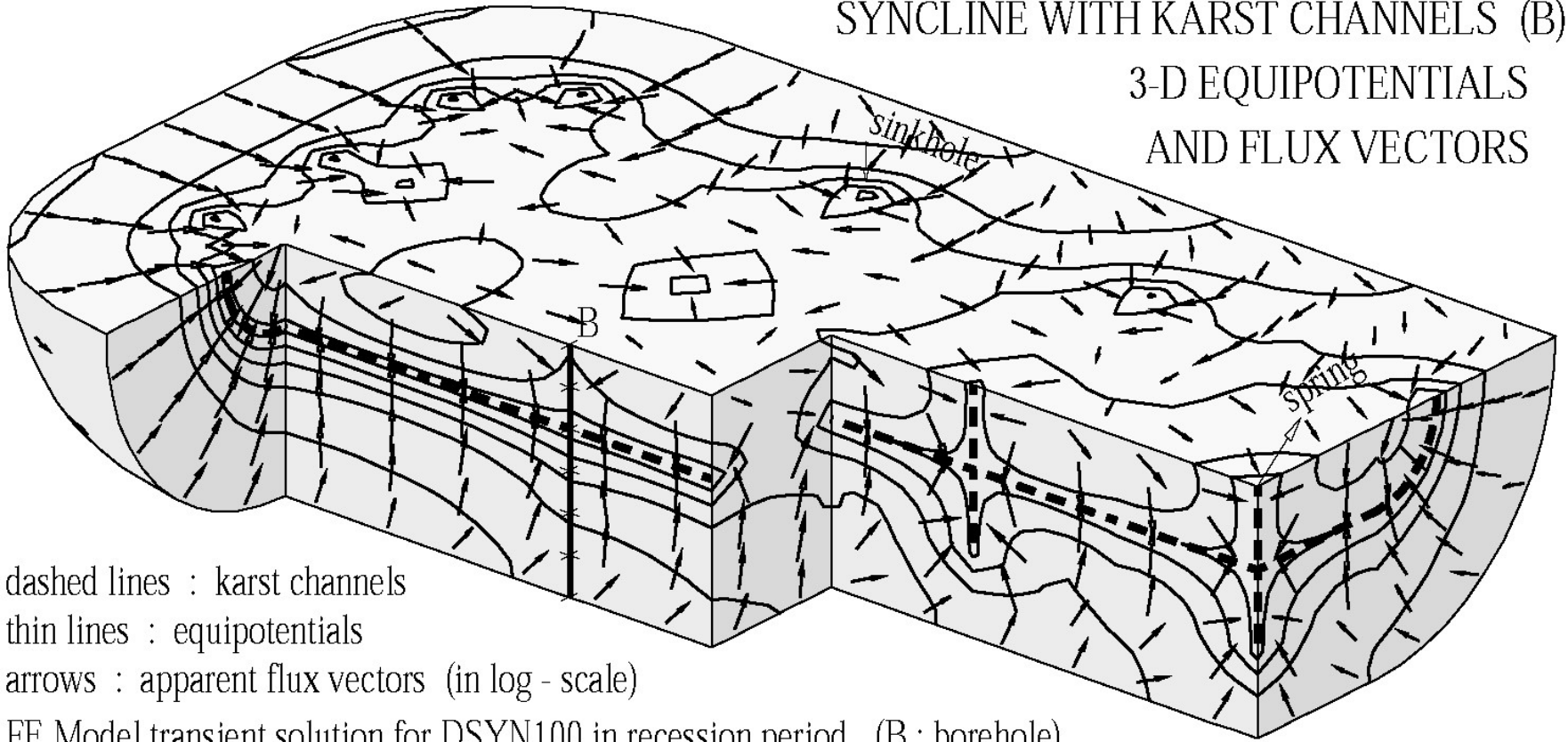
dashed lines : karst channels

thin lines : equipotentials

arrows : apparent flux vectors (in log - scale)

FE Model transient solution for DSYN100 in recharge period (B : borehole)

SYNCLINE WITH KARST CHANNELS (B)  
3-D EQUIPOTENTIALS  
AND FLUX VECTORS

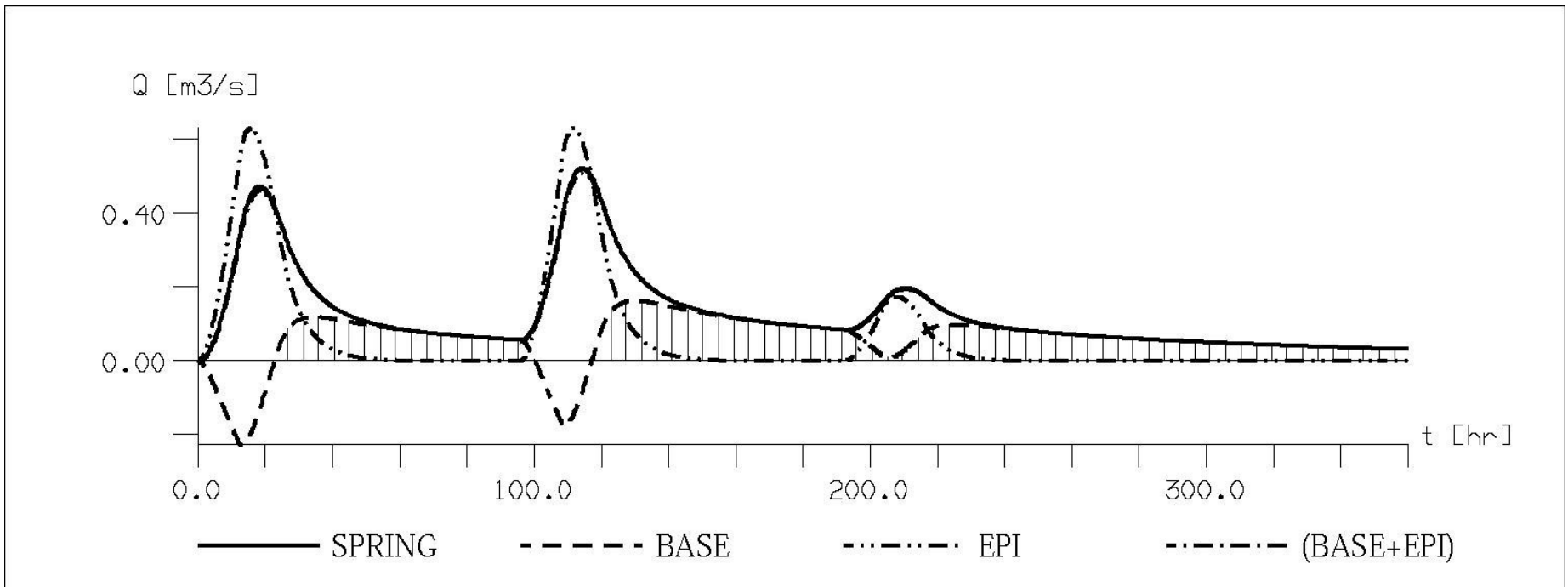
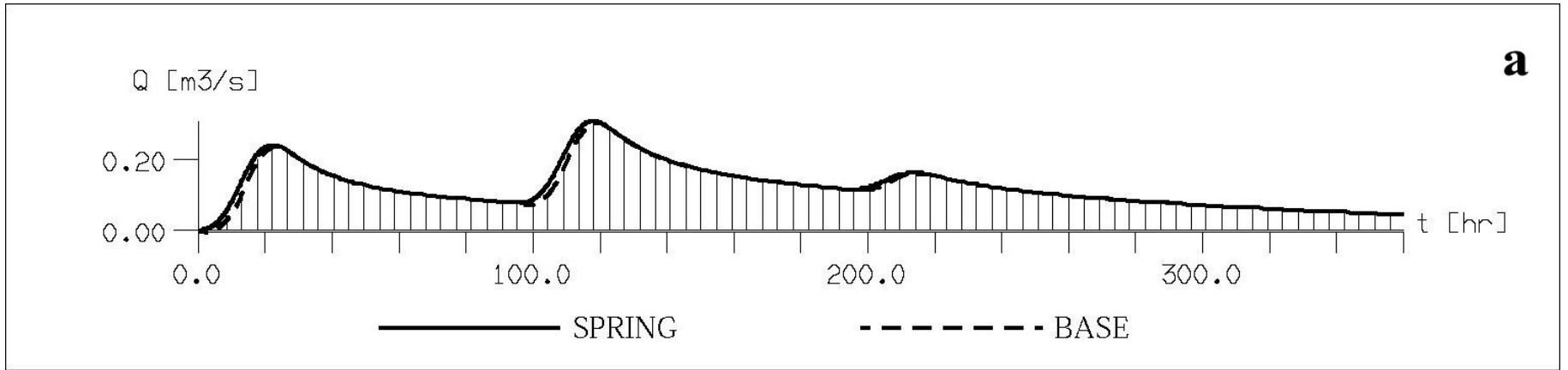


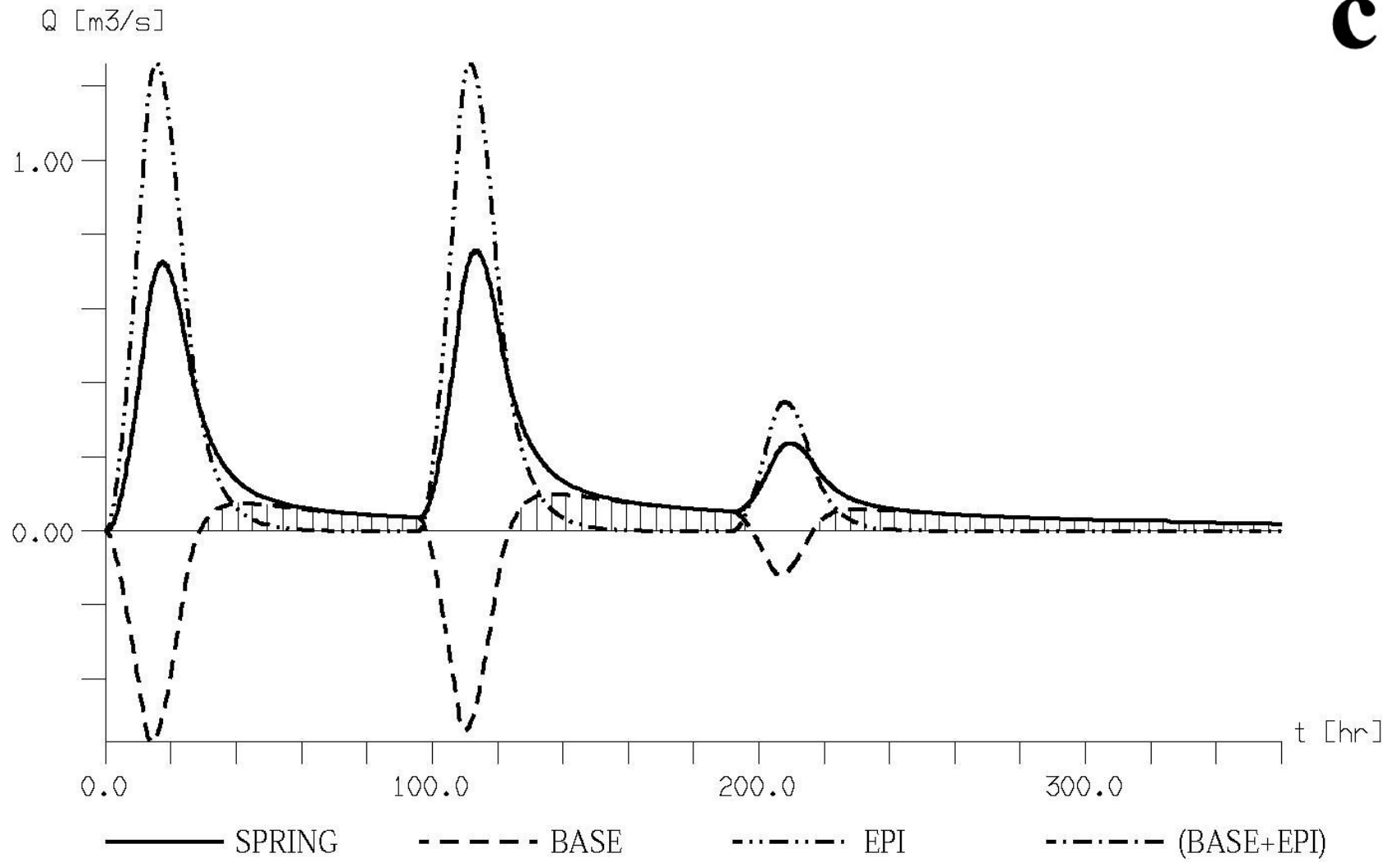
dashed lines : karst channels

thin lines : equipotentials

arrows : apparent flux vectors (in log - scale)

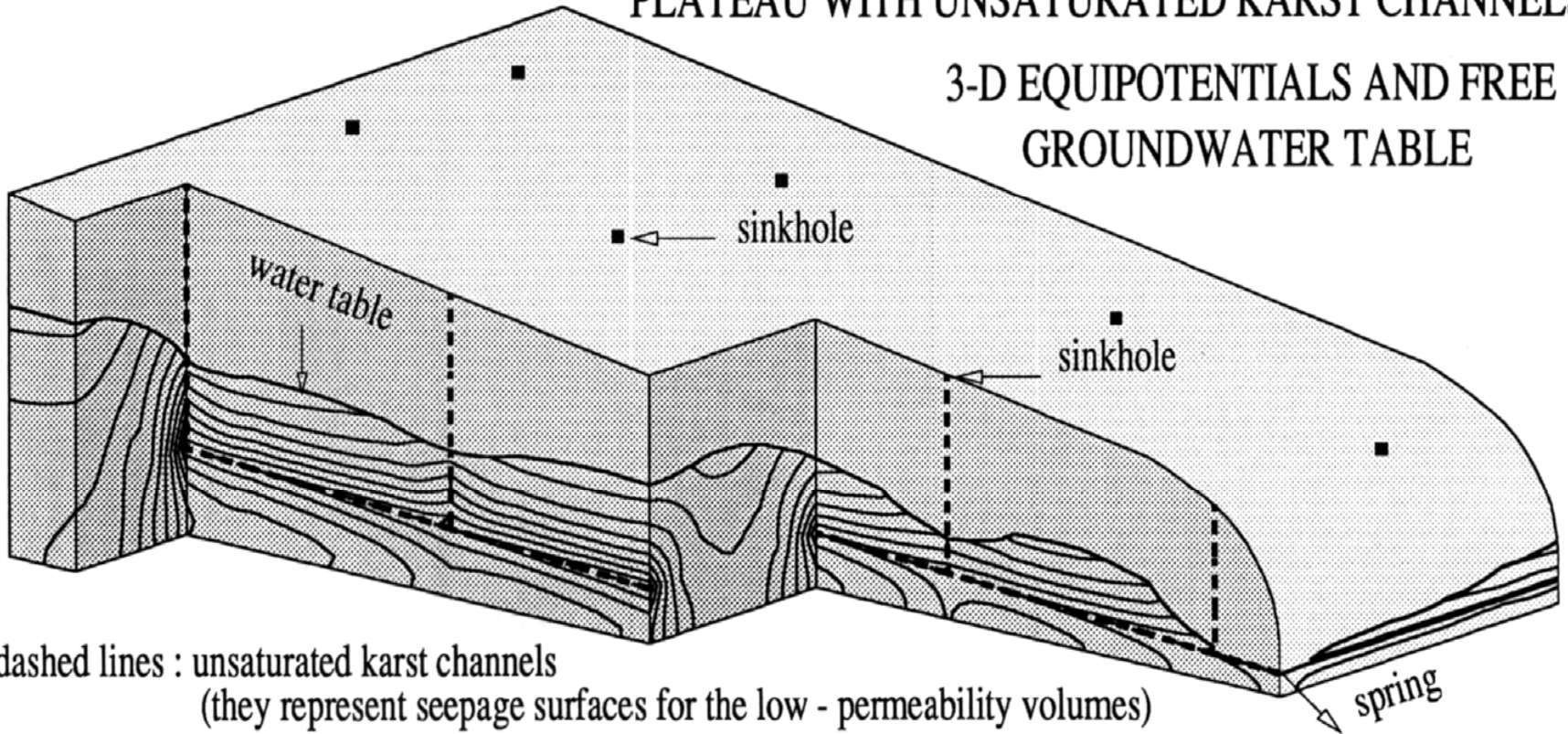
FE Model transient solution for DSYN100 in recession period (B : borehole)



**c**

# PLATEAU WITH UNSATURATED KARST CHANNELS

## 3-D EQUIPOTENTIALS AND FREE GROUNDWATER TABLE

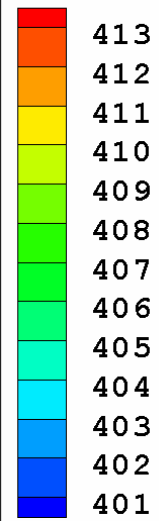


## The “Faraday-cage” effect of epikarst

The recharge mechanisms of the huge low permeability volumes may have important practical consequences on the groundwater management problems. The theoretical model studies suggest, that a well developed epikarst layer enhancing the concentrated infiltration into the high conductivity karst channel network will short-circuit the low conductivity volumes and will play the role of a Faraday-cage with respect to the main aquifer.

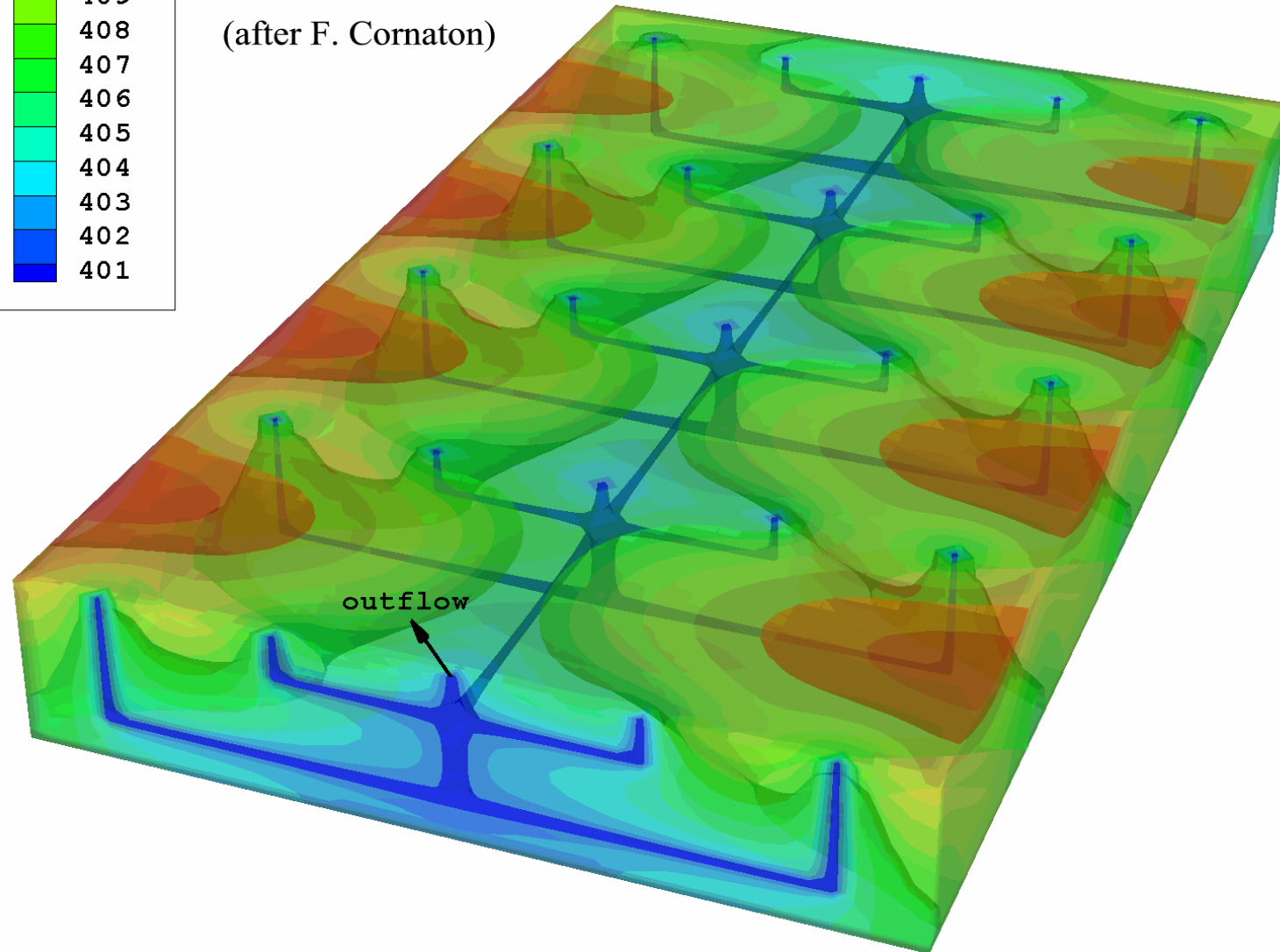
Depending on the importance of this Faraday-cage effect, the recharge of the low conductivity volumes could be much smaller than in case of pure diffuse infiltration, with important consequences on the groundwater management problems. In the deep syncline configuration the inversion of gradients will always contribute to recharging the low conductivity volumes “from the interior”, but in the shallow karst configuration the short-circuit of the low permeability volumes might be almost total.

Head [m]

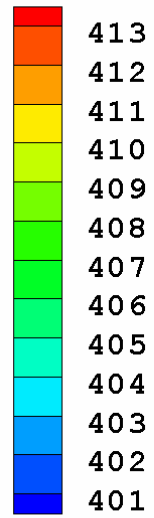


- Steady-state flow solution
- 100% of diffuse infiltration
- Manning-Strickler law in pipes
- Pipe radius = 1 m
- Friction coefficient =  $20 \text{ m}^{1/3}/\text{s}$
- Taylor's Laminar/Turbulent diffusion in pipes
- Laplace Transform Galerkin transport solution

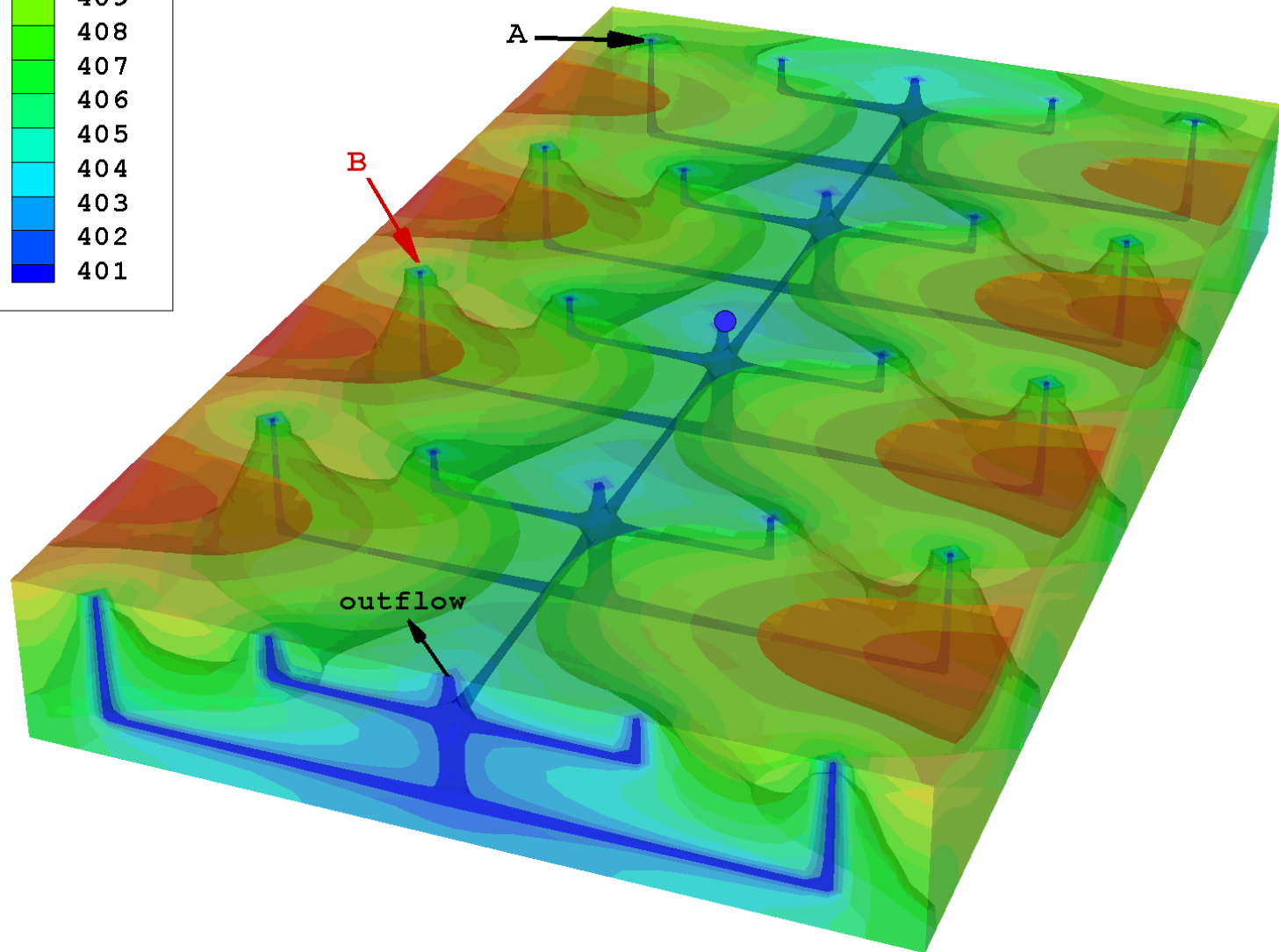
(after F. Cornaton)

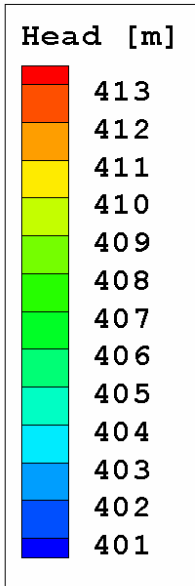


Head [m]

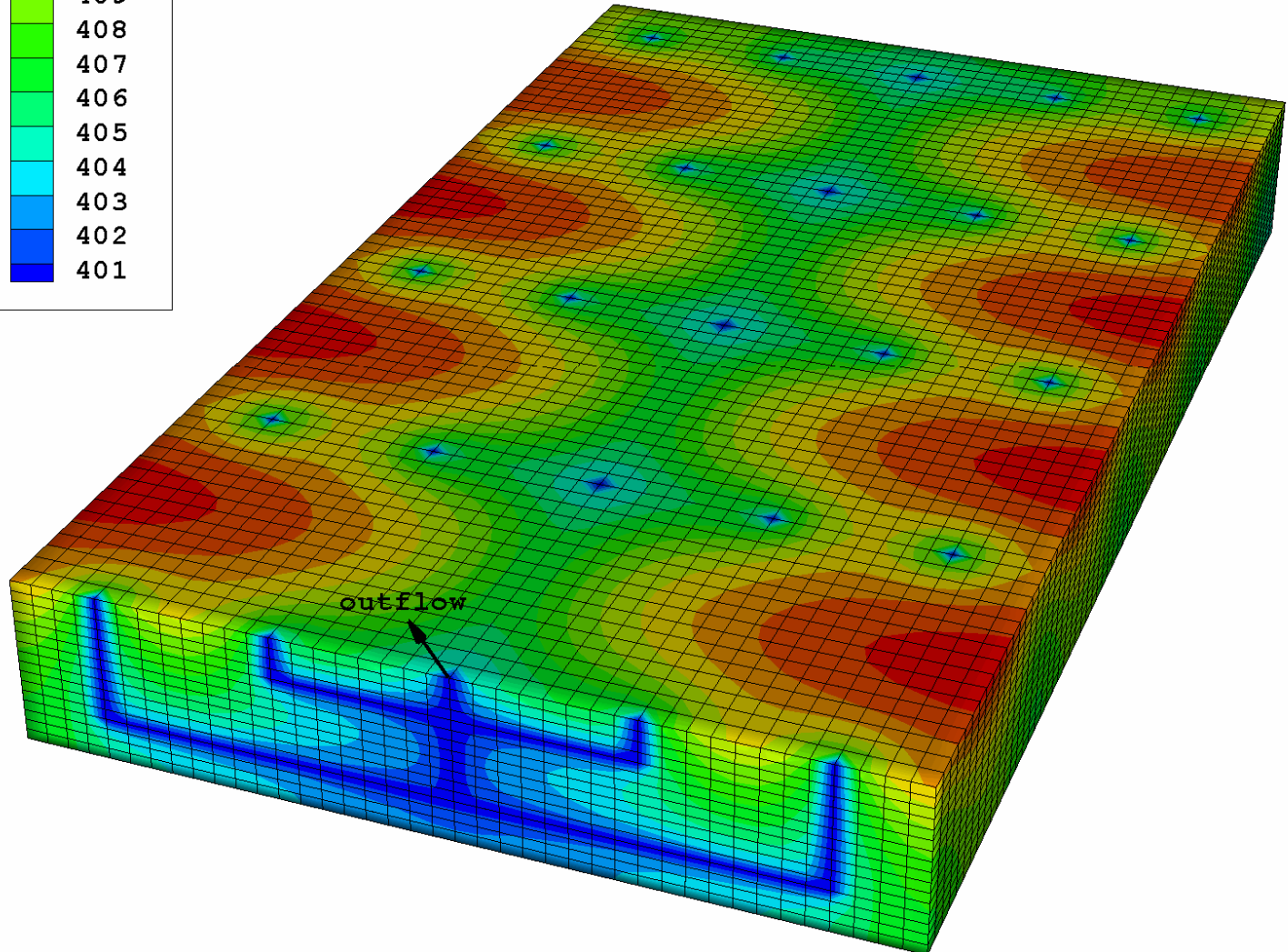


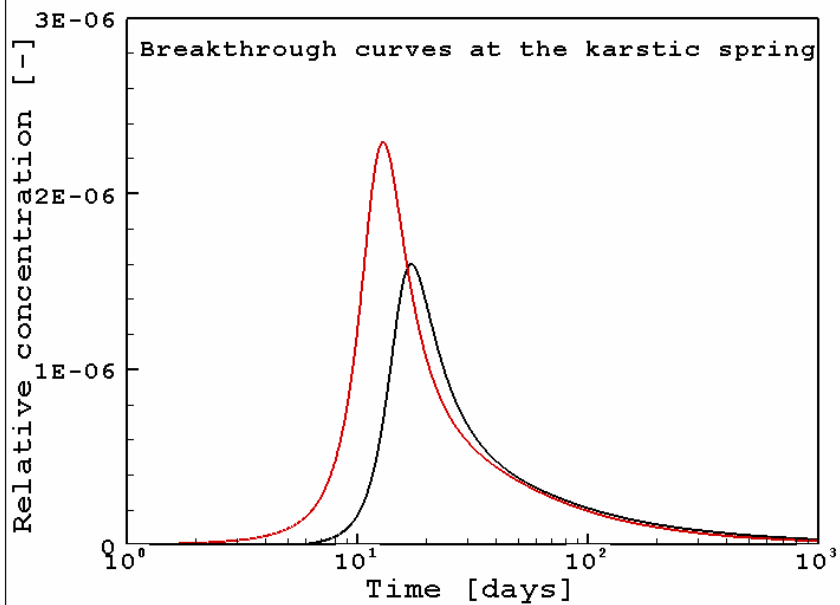
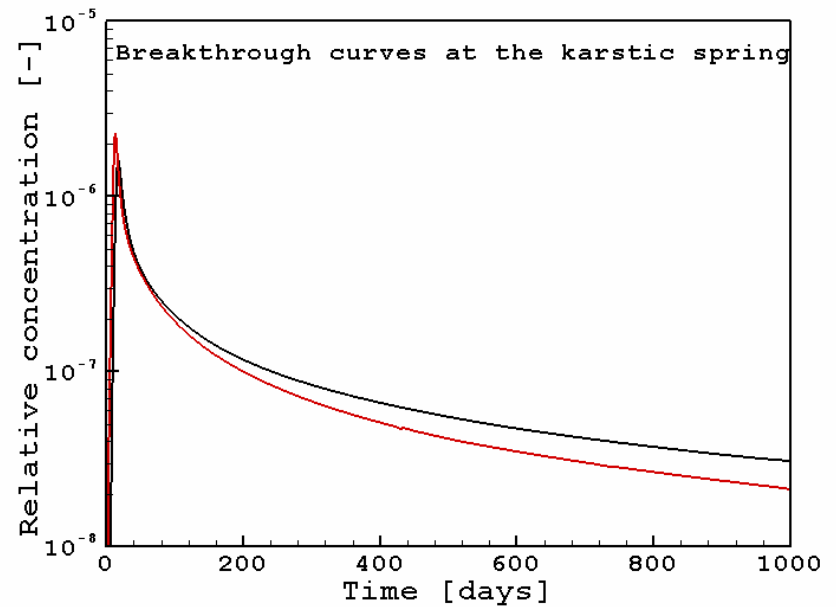
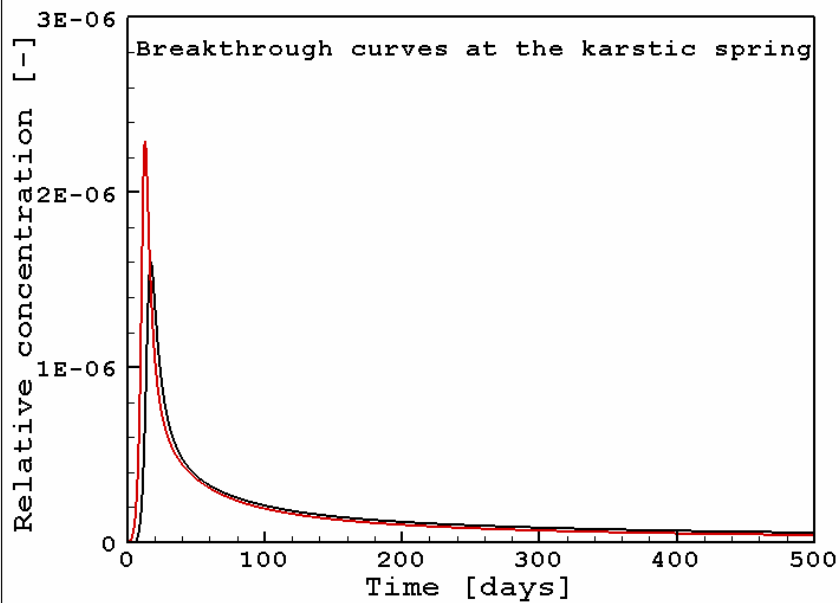
- Steady-state flow solution
- 100% of diffuse infiltration
- Manning-Strickler law in pipes
- Pipe radius = 1 m
- Friction coefficient =  $20 \text{ m}^{1/3}/\text{s}$
- Taylor's Laminar/Turbulent diffusion in pipes
- Laplace Transform Galerkin transport solution





- Steady-state flow solution
- 100% of diffuse infiltration
- Manning-Strickler law in pipes
- Pipe radius = 1 m
- Friction coefficient =  $20 \text{ m}^{1/3}/\text{s}$
- Taylor's Laminar/Turbulent diffusion in pipes
- Laplace Transform Galerkin transport solution





100 days spring capture zone:  
 Probability for the water particles  
 to reach the spring before  $t = 100$  days.  
 Iso-surfaces 0.9 (red) - 0.5 (green) - 0.1 (blue)

